PROBING THE DETAILS OF THE ALLOSTERIC INHIBITION IN PHOSPHOFRUCTOKINASE FROM *THERMUS THERMOPHILUS*

A Dissertation

by

XINXIN TIAN

Submitted to the Office of Graduate and Professional Studies of
Texas A&M University
in partial fulfillment of the requirements for the degree of

DOCTOR OF PHILOSOPHY

Chair of Committee,	Gregory Reinhart
Committee Members,	Ping He
	Frank Raushel
	James Sacchettini
Head of Department,	Gregory Reinhart

December 2016

Major Subject: Biochemistry

ABSTRACT

The enzyme, phosphofructokinase (PFK), catalyzes the phosphorylation of fructose-6-phosphate in the glycolysis pathway. Phosphoenolpyruvate (PEP) allosterically inhibits the binding of the substrate fructose-6-phosphate (Fru-6-P) in phosphofructokinase from *Thermus thermophilus* (TtPFK). The main goal of this study is to have a better understanding about how this allosteric inhibition signal is transmitted and propagated throughout the enzyme.

TtPFK is homotetramer with four active sites and four allosteric sites. There are multiple heterotropic interactions between active sites and allosteric sites. The first part of this dissertation is to isolate the four unique heterotropic inhibition interactions in wild type TtPFK. Our data shows the contribution of the four interactions are not the same, and are additive. This result suggests that the traditional two state model, either the concerted or sequential model, is not sufficient to explain the allosteric regulation in TtPFK. Also, the relative contribution of the four interactions in TtPFK is different from BsPFK and EcPFK.

The allosteric coupling between Fru-6-P and PEP in TtPFK is much weaker than BsPFK. N59D/A158T/S215H substitutions increase the coupling free energy of TtPFK similar to BsPFK. The second part of this dissertation is to isolate the four interactions in TtPFK N59D/A158T/S215H to see how the substitutions affect the coupling free energy in each of the four interactions. Our data shows that the substitutions of N59D/A158T/S215H can enhance all of the four interactions, but to different extents. 32

Å interaction exhibits the biggest increase in coupling free energy and this big increase makes it the second biggest contribution to TtPFK N59D/A158T/S215H. The coupling free energy in the isolated interactions sums to 69.5% ± 1.5% of the total coupling energy in the native tetramer. The discrepancy is likely due to the mutated residues not all interacting within a single subunit.

The third part of this dissertation is to use a fluorescence phasor to describe the four species, Apo-TtPFK, TtPFK-Fru-6-P, PEP-TtPFK, and PEP-TtPFK-Fru-6-P, involved in the allosteric coupling between Fru-6-P and PEP. TtPFK has a smaller allosteric coupling between PEP and Fru-6-P as compared to other prokaryotic PFKs, which makes it easier to form a ternary complex. Unique ternary complexes can be detected at specific positions. Our results suggest that residues F140, L313, F165 and V243 may be in an area important for the propagation and transmission of allosteric information in TtPFK. These four residues are in a region that can detect the structural conflict between Fru-6-P binding and PEP binding.

DEDICATION

To my parents and my husband

To all the people who have helped me

ACKNOWLEDGEMENTS

First, I want to thank all my committee members, Dr. He, Dr. Raushel, and Dr. Sacchettini, for their support through my PhD study.

I also want to thank Reinhart LAB members for their help and guidance in the past five years. I also want to thank Dr. Park for preventing me from giving up when I first joined the Biochemistry Department.

Finally, special thanks to my supervisor, Dr. Reinhart for everything! Thank you for recruiting me into your lab; thank you for your patience and encouragement when my experiments were not working; thank you for giving me scientific training in both kinetics and fluorescence; thank you for all the advice and support through my PhD study, not only in research, but also in life. I would not be like this today without you!

NOMENCLATURE

Abbreviations

A	Substrate or single letter code for alanine
Å	Angstroms
AC	Alternative current
ADP	Adenosine 5'-diphosphate
ATP	Adenosine 5'-triphosphate
BCA	Bicinchoninic acid
BmPFK	Phosphofructokinase from *Bacillus macquariensis*
BSA	Bovine serum albumin
BsPFK	Phosphofructokinase from *Bacillus stearothermophilus*
DC	Direct current
E	Enzyme or single letter code for glutamate
EA	Enzyme-substrate binary complex
EcPFK	Phosphofructokinase from *Escherichia coli*
EDTA	Ethylenediamine tetraacetic acid
EPPS	N-[2-Hydroxyethyl] piperazine-N'-3-propanesulfonic acid
F	Single letter code for phenylalanine
Fru-6-P	Fructose-6-phosphate
K	Single letter code for lysine
KSCN	Potassium thiocyanate
L	Single letter code for leucine

LB	Luria Bertani broth
LdPFK	Phosphofructokinase from *Lactobacillus delbrueckii*
M	Modulation
Mg	Magnesium
MOPS	3-[N-Morpholino]propanesulfonic acid
NAD^+	Nicotinamide adenine dinucleotide, oxidized form
NADH	Nicotinamide adenine dinucleotide, reduced form
NATA	N-acetyl-tryptophanamide
PAGE	Polyacrylamide gel electrophoresis
PEP	Phosphoenolpyruvate
Pi	Inorganic phosphate
R	Single letter code for arginine
S	Substrate
Tris	Tris[hyroxymethyl]aminomethane
TtPFK	Phosphofructokinase from *Thermus Thermophilus*
V	Single letter code for valine
W	Single letter code for tryptophan
X	Allosteric effector
XE	Enzyme-effector binary complex
XEA	Enzyme-substrate-effector ternary complex
Y	Allosteric inhibitor or single letter code for tyrosine

Mathematical Terms

[A]	Concentration of substrate or ligand
ΔG_{ax}	Coupling free energy between A and X
ΔG_{ay}	Coupling free energy between A and Y
$K_{1/2}$	Concentration of substrate when initial velocity is half maximal velocity
K_{ia}°	Dissociation constants for A in the absence of effector
K_{ia}^{∞}	Dissociation constants for A in the presence of saturating concentration of effector
K_{ix}°	Dissociation constant for Y in the absence of substrate
K_{ix}^{∞}	Dissociation constants for Y in the presence of saturating concentration of the substrate
M	Molar
mg	Milligram
mL	Milliliter
mM	Millimolar
n_H	Hill number
ns	Nanosecond
Qax	Coupling constant between A and X
Qay	Coupling constant between A and Y
R	Gas constant
T	Temperature

v	Initial velocity
Vmax	Maximal velocity
τ	Fluorescence lifetime
µg	Microgram
µM	Micromolar
Φ	Phase delay

TABLE OF CONTENTS

Page

LIST OF FIGURES

Page

LIST OF TABLES

Page

CHAPTER I

INTRODUCTION

Phosphofructokinase background

Phosphofructokinase (PFK) catalyzes the phosphorylation of fructose 6-phosphate in glycolysis pathway. There are two types of PFK: PFK1 and PFK2. PFK1 catalyzes the irreversible γ-phosphoryl transfer from magnesium adenosine triphosphate (MgATP) to the sugar ring of fructose-6-phosphate (Fru-6-P) producing fructose-1,6-bisphosphate and magnesium adenosine diphosphate (MgADP), which is the first committed step of glycolysis pathway and one of the three irreversible steps, making it the key regulatory enzyme in glycolysis. PFK2 is a non-homologous isozyme. The PFK in this dissertation is PFK1.

The structure and function of PFK depend on the origin. PFKs from mammals and yeast can have very complex structures and the subunit has a molecular weight of 85 kDa and 110 kDa respectively. However, the enzymes from bacteria are much smaller. Bacterial PFKs are usually tetramers and the subunit has a molecular weight between 32 kDa and 38 kDa (Evans, et al., 1981). PFK from eukaryotes is allosterically regulated by many metabolites, including citrate, ATP, AMP, fructose-1,6-bisphosphate, and fructose-2,6-bisphosphate (Bloxham and Lardy, 1973; Evans et al., 1981; Kemp and Foe, 1983; Kemp and Gunasekera, 2002). Generally PFK isolated from bacteria have a simpler allosteric regulation than that isolated from eukaryotes (Evans, et al., 1981). Bacterial PFKs are primarily regulated by two effectors: activator MgADP and inhibitor phosphoenolpyruvate (PEP). They are both K-type allosteric effectors

(Uyeda, 1979; Evans et al., 1981), which do not change the catalytic turnover of the enzyme, but change the enzyme's binding affinity for Fru-6-P. MgADP functions as activator when physiological MgATP concentration is low and increases the enzyme's affinity for Fru-6-P. PEP, the downstream product of glycolysis pathway, functions as feedback inhibitor and decreases the enzyme's affinity for Fru-6-P.

The crystal structure of phosphofructokinase from *Bacillus stearothermophilus* (BsPFK) with different ligands has been solved (Evans and Hudson, 1979; Evans, et al., 1981; Evans, et al., 1986; Schirmer and Evans, 1990; Mosser et al., 2012). Each subunit forms a strong interaction with two neighboring subunits. Bacterial PFKs are active as tetramers and are inactivated upon dissociation into monomers. Analysis of crystal structures explains why bacterial PFKs require a tetramer to be active. Fru-6-P binds to two subunits; the negatively charged phosphate group also binds with Arg162 and Arg243 from neighboring subunit (Evans, et al., 1981). So the integrity of tetramer is required for the activity of PFK. The allosteric site is also on the surface of two neighboring subunits. Hence, the allosteric effectors, MgADP and PEP, are also bound with two subunits.

PFKs from different bacterial sources have been studied (Johnson and Reinhart, 1992, 1994 a-b 1997; Tlapak-Simmons and Reinhart, 1994; Kimmel and Reinhart, 2000; Riley-Lovingshimer and Reinhart, 2001; Fenton et al., 2004; Ortigosa and Reinhart, 2004; Paricharttanakul et al., 2005; McGresham et al., 2014). EcPFK (PFK from *Escherichia coli*), BsPFK (PFK from *Bacillus stearothermophilus*), TtPFK (PFK from

Thermus thermophilus) and LdPFK (PFK from *Lactobacillus delbrueckii*) are all homotetramers with subunit molecular weight about 34kDa.

Figure 1-1 is the amino acid sequence alignment of EcPFK, BsPFK, TtPFK and LdPFK. The numbering of residues in the figure is according to the EcPFK sequence but in the text is according to the TtPFK sequence. The overall sequence is well conserved with residues in the 210s, 230s and 240s along with the C-terminus being the least conserved. EcPFK and BsPFK have 58% and 54% identity in nucleotide and amino acid sequence, respectively (French and Chang, 1987). A comparison of the crystal structure of these two enzymes indicates the overall secondary, tertiary and quaternary structures are almost identical for EcPFK and BsPFK. The binding sites residues for EcPFK and BsPFK are also nearly identical (Evans et al., 1986; Shirakihara and Evans, 1988; Schirmer and Evans, 1990). LdPFK and EcPFK have 47% identity and 66% similarity in amino acid sequence. LdPFK and BsPFK have 56% identity and 74% similarity in amino acid sequence. The overall fold of the crystal structure and the substrate binding site is conserved between EcPFK, BsPFK and LdPFK (Paricharttanakul et al., 2005).

Figure 1-2 is the amino acid sequence alignment of BsPFK and TtPFK. TtPFK and EcPFK have 46% identity and 62% similarity in amino acid sequence. TtPFK and BsPFK have 57% identity and 70% similarity in amino acid sequence.

Figure 1-3 is the crystal structure of the BsPFK tetramer. There is no crystal structure available for TtPFK, but we have no reason to expect that the three dimensional structure of TtPFK will be dramatically different from BsPFK.

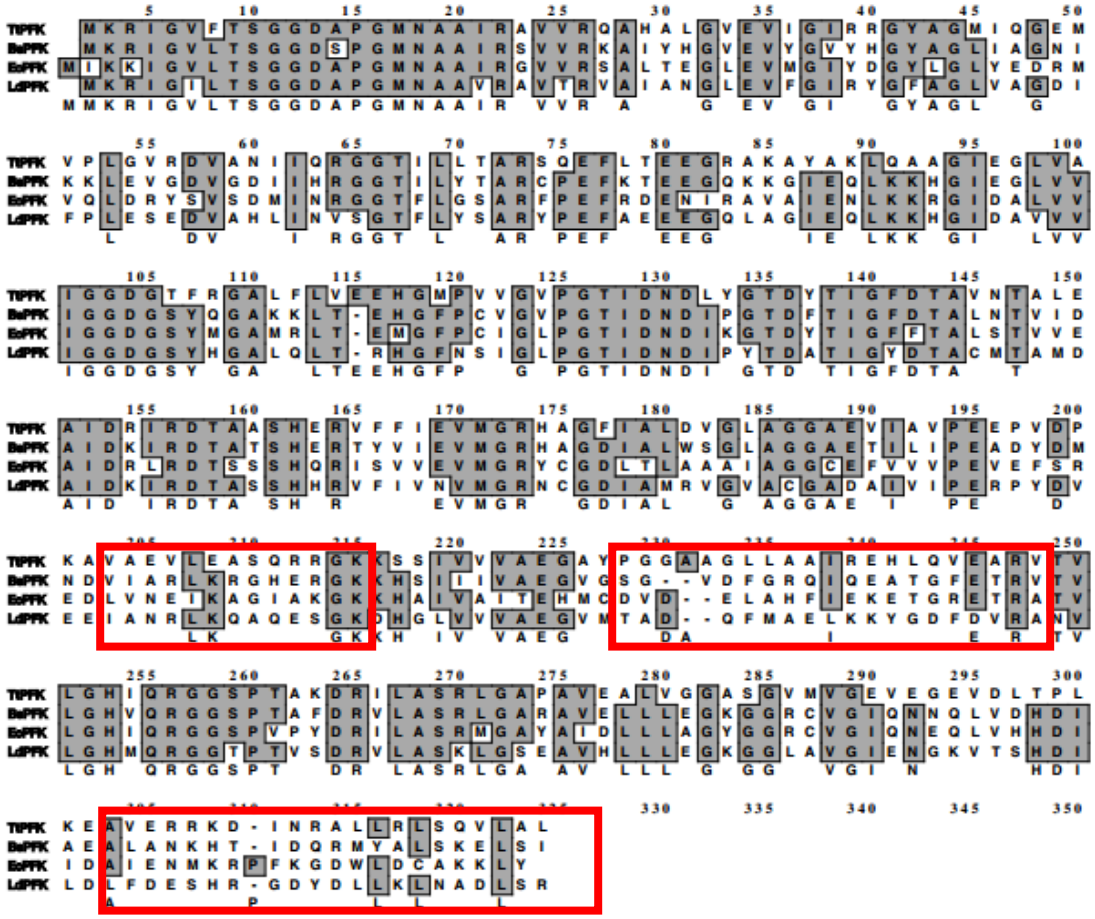

Figure 1-1. Amino acid sequence alignment of TtPFK, BsPFK, EcPFK and LdPFK. The sequences were aligned using MacVectorTM 7.0. The regions discussed within this dissertation are highlighted by red boxes. The numbering of residues is according to EcPFK sequence but in the text is according to the TtPFK sequence.

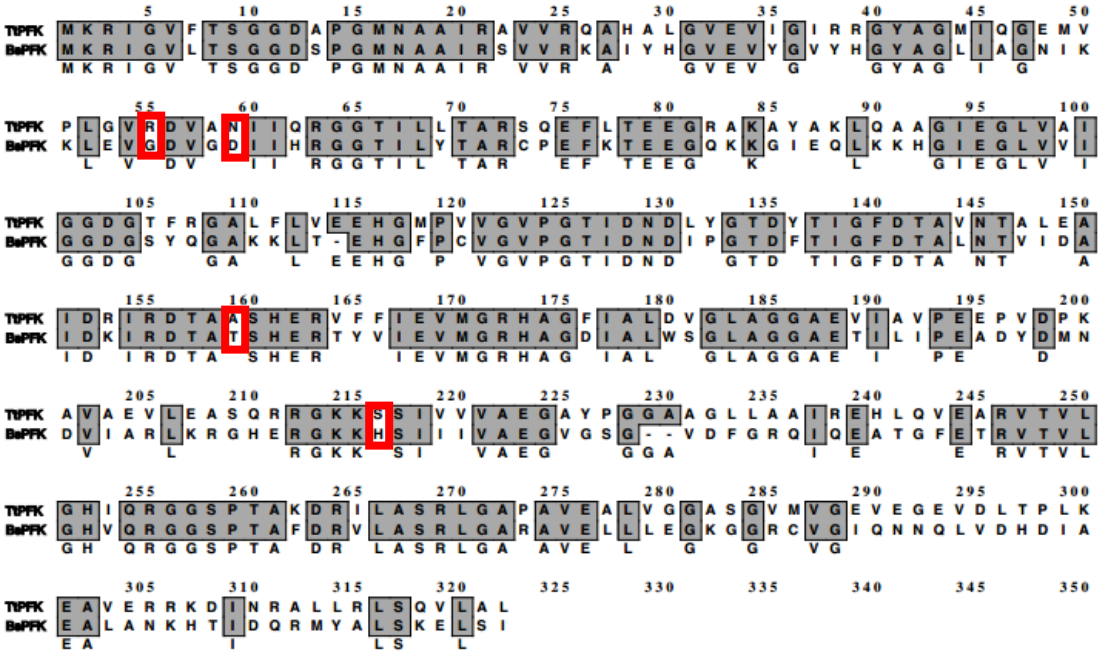

Figure 1-2. Amino acid sequence alignment of TtPFK and BsPFK. The sequences were aligned using MacVectorTM 7.0. The regions discussed within this dissertation are highlighted by red boxes. The numbering of the residues in the figure is according to the EcPFK sequence but in the text is according to the TtPFK sequence.

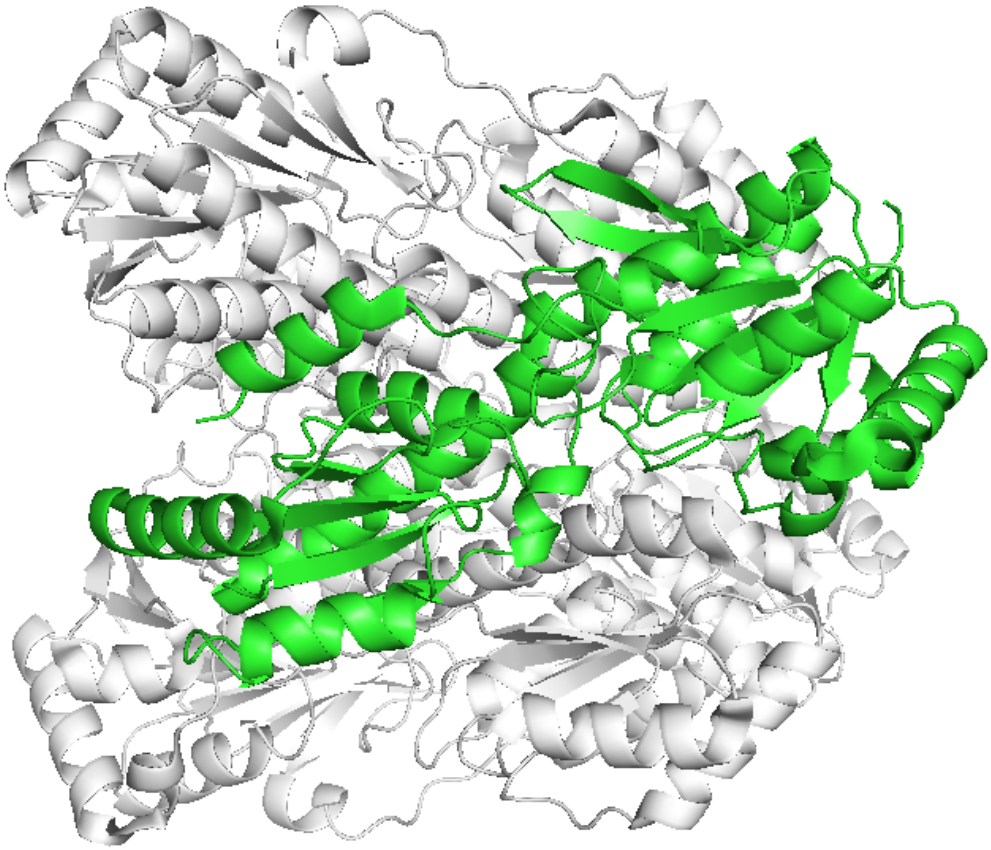

Figure 1-3. Crystal structure of BsPFK homotetramer with one subunit highlighted in green.

Models used to study allosteric regulation

Researchers have been using the concerted (MWC) model (Monod et al., 1965) and the sequential (KNF) model (Koshland et al., 1966) to study allosteric regulation. The T-state is the state capable of binding the inhibitor and binding substrate with low affinity. The R-state is the state that binds substrate or activator with high affinity. The concerted transition model was one of the first models to attempt to describe enzyme allosteric regulation. The two-state model is an oversimplification since even in the original paper it was recognized that more than two states may be involved; two-state refers to the transition of the enzyme from one state to another. In the simplest case there are only two forms: inactive T form and active R form. R form is better able to bind the ligand compared to T form. For the concerted transition, allosteric activation effects are seen as ligand stabilizing the R form; allosteric inhibition effects are seen as ligand stabilizing the T form. The concerted transition model predicts that all four allosteric sites are equally effective at influencing the binding of substrate.

The KNF model predicts that conformational changes occurs when ligand binds to one subunit of the enzyme, which then affects the conformational change of the other neighboring subunits, either positively or negatively. The conversion of states occurs sequentially. The complete conversion from one conformational state to the other occurs only when all sites are bound with ligands. The first ligand binding event seems to be the major difference between the two models. In these two models, it is not usually expected that the enzyme binds substrate and inhibitor simultaneously. They only recognize

binary complex, either substrate bound form or allosteric effector bound form, but not the ternary complex bound with both substrate and allosteric effector simultaneously.

A third model for studying allosterism is the linked-function model (Wyman, 1964, 1967; Weber, 1972, 1975). Reinhart (1983 and 1988) applied this idea to both single substrate and single modifier system (monomer) and also symmetrical dimer system. Thermodynamic linkage analysis model provides another way to describe allosteric mechanism in free energy terms without assuming the nature of structural changes caused by ligand binding. "Linkage simply refers to the phenomenon of mutual interaction of two ligands bound to the same protein at distinct sites" (quote from Reinhart, 1983). The simplest allosteric kinetic mechanism is shown figure 1-4 involving a single substrate and a single allosteric effector, where E represent free enzyme, A represent substrate, P represent product and X represent allosteric effector. The figure is cited from Reinhart, 1983. EA represent enzyme bound with substrate, XE represent enzyme bound with allosteric effector and XEA represent enzyme bound with both substrate and allosteric effector. The dissociation constants are defined as follows:

$$K_{ia}^{\circ} = [E][A]/[EA]$$

$$K_{ix}^{\circ} = [E][X]/[XE]$$

$$K_{ia}^{\infty} = [XE][A]/[XEA]$$

$$K_{ix}^{\infty} = [EA][X]/[XEA]$$

where K_{ia}° and K_{ia}^{∞} are the dissociation constants for substrate in the absence and presence of saturating concentration of effector, and K_{ix}° and K_{ix}^{∞} are the dissociation constants for the effector in the absence and presence of saturating concentration of

substrate, respectively (Cleland 1963; Reinhart 1983). The coupling constant Q_{ax} (Reinhart, 1983) is defined as the ratio of K_{ia}° and K_{ia}^{∞} or the ratio of K_{ix}° and K_{ix}^{∞}.

$$Q_{ax} = K_{ia}^{\circ} / K_{ia}^{\infty} = K_{ix}^{\circ} / K_{ix}^{\infty}$$

It describes the effect that the binding of effector has on the binding of substrate and vice versa. Q_{ax} also describes the disproportionate equilibrium constant for the following reaction:

$$XE + EA \leftrightarrow XEA + A$$

$$Q_{ax} = ([XEA]\,[E]) / ([EA]\,[XE])$$

The value of Q_{ax} describes the nature of the effect caused by X. If Q_{ax} is smaller than 1, the ligand is an inhibitor, if Q_{ax} is larger than 1, the ligand is an activator. If Q_{ax} is equal to 1, there is no allosteric effect. The common exclusive binding two-state model is a limiting case of the mechanism in fig 1-4. The essential difference lies in whether one considers the ternary complex, XEA, capable of forming.

Q_{ax} can be used to calculate the coupling free energy ΔG_{ax} (Weber, 1972, 1975; Reinhart, 1983, 1988; Reinhart. et al., 1989) between the substrate and allosteric effector based on the following equation:

$$\Delta G_{ax} = -RT \ln (Q_{ax})$$

where R is the gas constant (8.3145J/k*mol), T is the temperature in Kelvin. If $\Delta G_{ax} < 0$, it is allosteric activation; if $\Delta G_{ax} > 0$, it is allosteric inhibition; and if $\Delta G_{ax} = 0$, there is no allosteric coupling. Thermodynamic linkage model applies to activation, inhibition and no allosteric coupling.

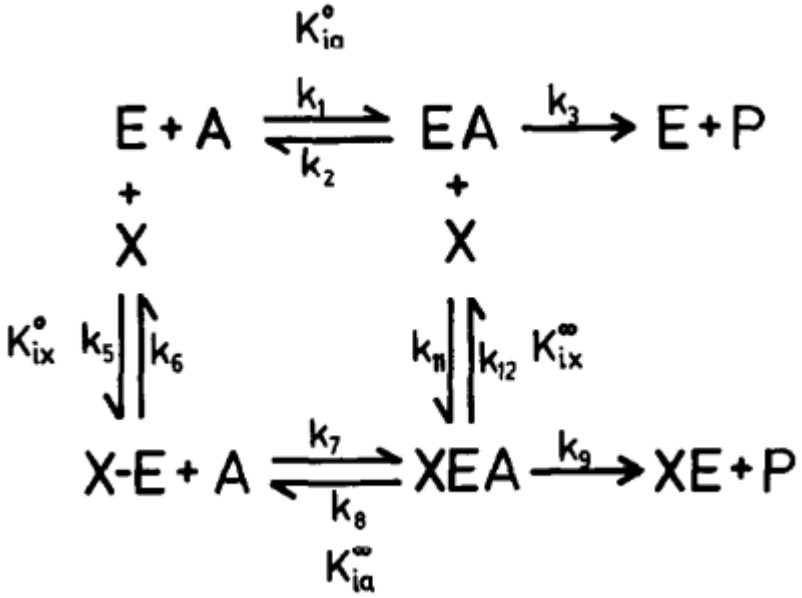

Figure 1-4. Thermodynamic linkage analysis for single substrate and single modifier. Figure is from Reinhart, 1983.

There are four different ligation states that the enzyme can adopt: E, EA or XE or XEA. Each ligation state is unique and can have different functional properties. This is in contrast to the two-state models, which only allow for the existence of either T-state or R-state, without the ternary complex because the enzyme can bind only one type of ligand, either A or X, but not both. Thermodynamic linkage analysis can not only describe the nature of the allosteric effect but also the magnitude of the effect. Several studies conducted by Reinhart (Reinhart 1983a-b, 1985, 1988; Johnson and Reinhart, 1992, 1994a-b, 1997; Braxton, et al., 1994; Tlapak-Simmons and Reinhart, 1994, 1998; Kimmel and Reinhart, 2000, 2001; Riley-Lovingshimer and Reinhart, 2001; Pham and Reinhart, 2001; Pham, et al., 2001) have employed linked-function in the analysis of allosteric regulation of EcPFK and BsPFK. The ternary complexes for both EcPFK and BsPFK have been shown to exist (Johnson and Reinhart, 1992, 1994a-b, 1997; Tlapak-Simmons and Reinhart, 1994, 1998; Kimmel and Reinhart, 2000; Riley-Lovingshimer and Reinhart, 2001). Also the crystal structures of different ligated states of both EcPFK and BsPFK have been solved (Evans and Hudson, 1979; Evans et al., 1981; Evans, et al., 1986; Shirakihara and Evans, 1988; Rypniewski and Evans, 1989; Schirmer and Evans, 1990).

Allosteric regulation in TtPFK

TtPFK has been purified and characterized (Yoshida et al., 1971; Yoshida, 1972; Xu et al., 1990; McGresham et al., 2014). Figure 1-5 is the plot of apparent dissociation constant for Fru-6-P versus increasing concentration of inhibitor PEP for TtPFK, BsPFK and EcPFK. The figure is cited from McGresham et al., 2014. TtPFK has a much higher

binding affinity for PEP and a smaller allosteric coupling between PEP and Fru-6-P compared to other prokaryotic PFKs.

Table 1-1 is the kinetic and thermodynamic coupling parameters for TtPFK, BsPFK, EcPFK and LdPFK. TtPFK, BsPFK and EcPFK data is cited from McGresham et al., 2014 and LdPFK data is cited from Paricharttanakul et al., 2005. Of the four PFKs, TtPFK exhibits the tightest binding affinity for PEP, while BsPFK exhibits the strongest inhibition by PEP. LdPFK stands out as having extremely poor PEP binding and the inhibition is only seen at very high concentrations of PEP (Paricharttanakul et al., 2005). The specific activity of TtPFK is 41 units/mg. It is much lower compared to BsPFK, EcPFK and LdPFK at 25°C, which is not surprising because the activity of enzymes from a thermophile at room temperature is expected to be lower than the activity at their native temperature (Jaenicke, 1991; Somero, 1978; Plou and Ballesterous, 1999). The dissociation constant for substrate Fru-6-P in the absence of PEP in TtPFK is close to BsPFK. The binding affinity of PEP for TtPFK is much tighter than BsPFK, but the allosteric coupling between PEP and Fru-6-P binding is much weaker, providing another example that the binding affinity is independent of the actual inhibition effect it exhibits. TtPFK and LdPFK have similar affinities for Fru-6-P, but binding affinities of LdPFK for MgADP and PEP are five orders of magnitude weaker than those for TtPFK.

For TtPFK, the allosteric inhibitor PEP decreases the enzyme's affinity for Fru-6-P but does not change the catalytic turnover of the enzyme as expected. Figure 1-6 shows the relative maximal velocity versus increasing concentration of inhibitor PEP for TtPFK. Figure 1-7 shows the hill number versus increasing concentration of inhibitor PEP for

TtPFK. There is slight positive homotropic cooperation for substrate binding. The hill number increases as PEP concentration increases, which is an example of heterotropically induced homotropic cooperativity (Reinhart 1988). Figure 1-8 shows the hill number for the binding of PEP in TtPFK. There is no PEP binding cooperativity in TtPFK.

LdPFK has extremely poor binding affinity for PEP and the inhibition is only seen at very high concentrations of PEP (Paricharttanakul et al., 2005). EcPFK, BsPFK and TtPFK are all allosterically inhibited by PEP. In EcPFK the allosteric response to the inhibitor PEP decreased as a function of temperature (Johnson and Reinhart, 1997). The van't Hoff analysis shows that the inhibition is enthalpy driven. In contrast, in BsPFK we see more inhibition by PEP at higher temperature because this process is entropy driven (Tlapak-Simmons and Reinhart, 1998). The inhibition by PEP of TtPFK is also entropy driven in (McGresham et al., 2014). The inhibition of PFK from mesophilic E. coli is enthalpy driven while the inhibition of PFKs from moderately thermophilic *Bacillus stearothermophilus* and extreme thermophilic *Thermus thermophilus* are entropy driven. It is possible that entropy driven allosteric regulation is a feature of enzymes from thermostable organisms. The other finding is that while the allosteric coupling in TtPFK is relatively weak at 25°C, it may be comparable to that of EcPFK and BsPFK at its physiological temperatures.

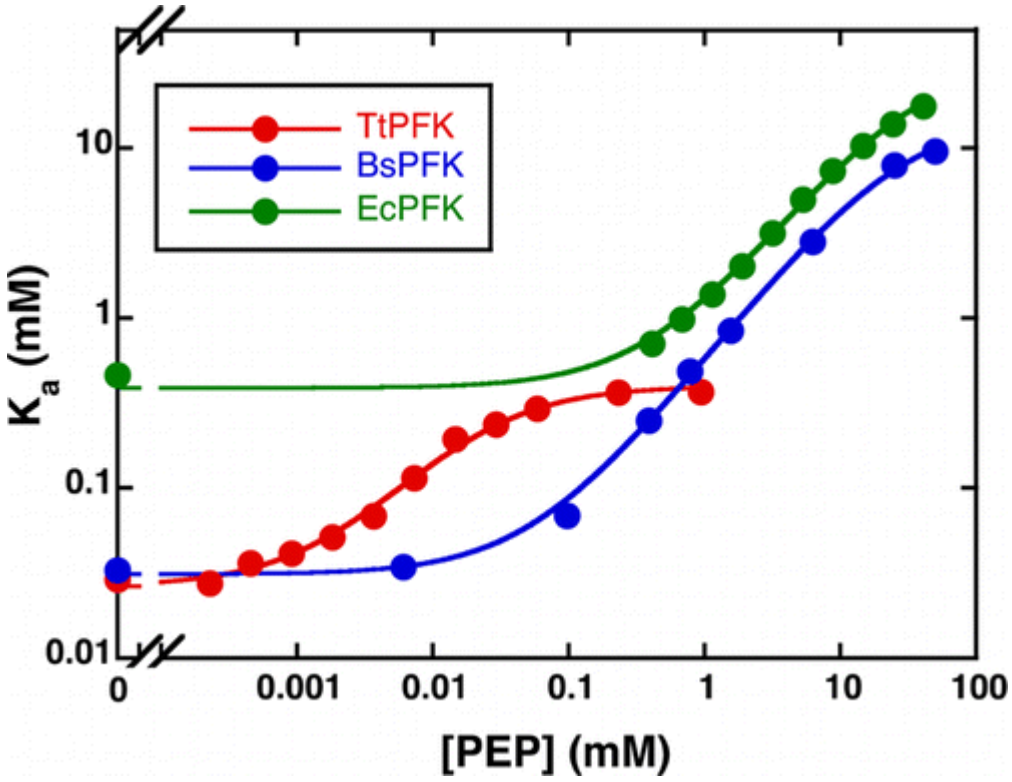

Figure 1-5. Apparent dissociation constant for Fru-6-P versus increasing concentration of inhibitor PEP for TtPFK, BsPFK and EcPFK at pH 8 and 25°C. Red is TtPFK, blue is BsPFK and green is EcPFK. Figure is from McGresham et al., 2014.

Table 1-1. Kinetic and thermodynamic coupling parameters for TtPFK, BsPFK, EcPFK and LdPFK at pH 8 and 25°C. A represent Fru-6-P, Y represent PEP and nd refers to "not determined". TtPFK, BsPFK and EcPFK data is from McGresham et al., 2014. LdPFK data is from Parichartttanakul et al., 2005.

	TtPFK	BsPFK	EcPFK	LdPFK
K_{ia}^{o} (μM)	27.0 ± 0.6	31 ± 2	300 ± 10	20 ± 5
K_{iy}^{o} (μM)	1.6 ± 0.1	93 ± 6	300 ± 10	24000 ± 2000
Q_{ay}	0.067 ± 0.002	0.0021±0.0003	0.0080 ± 0.0003	nd
ΔG_{ay} (kcal/mol)	1.60 ± 0.02	3.67 ± 0.1	2.7 ± 0.1	nd
SA (unit/mg)	41	163	240	240
k_{cat} (s^{-1})	23	91	136	136

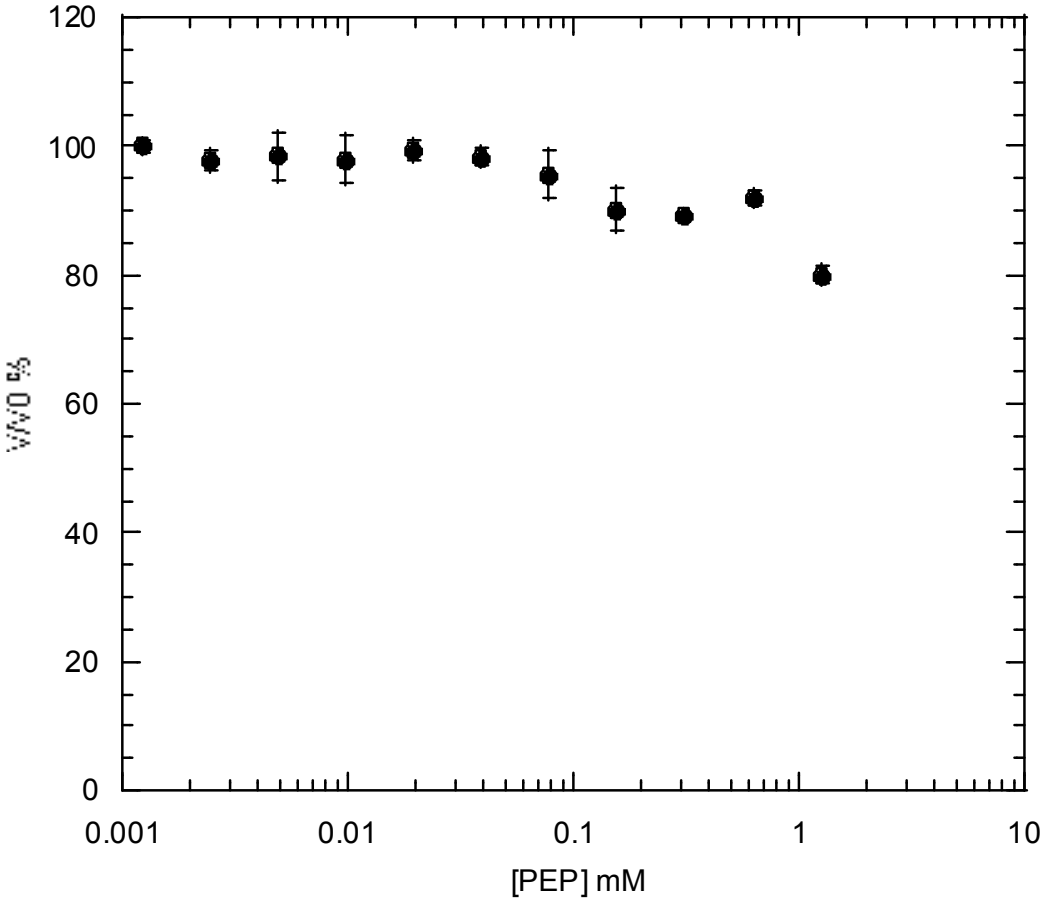

Figure 1-6. Relative maximal velocity versus increasing concentration of inhibitor PEP for TtPFK at pH 8 and 25°C.

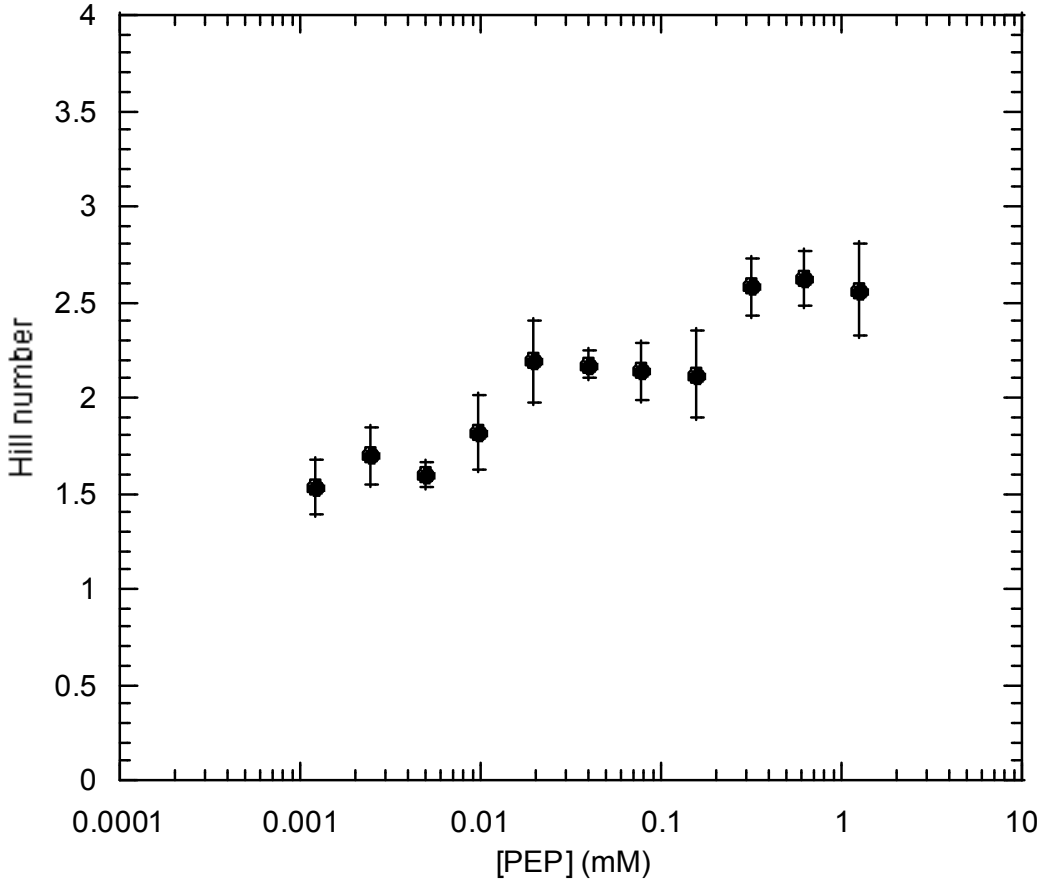

Figure 1-7. Hill number versus increasing concentration of inhibitor PEP for TtPFK at pH 8 and 25°C.

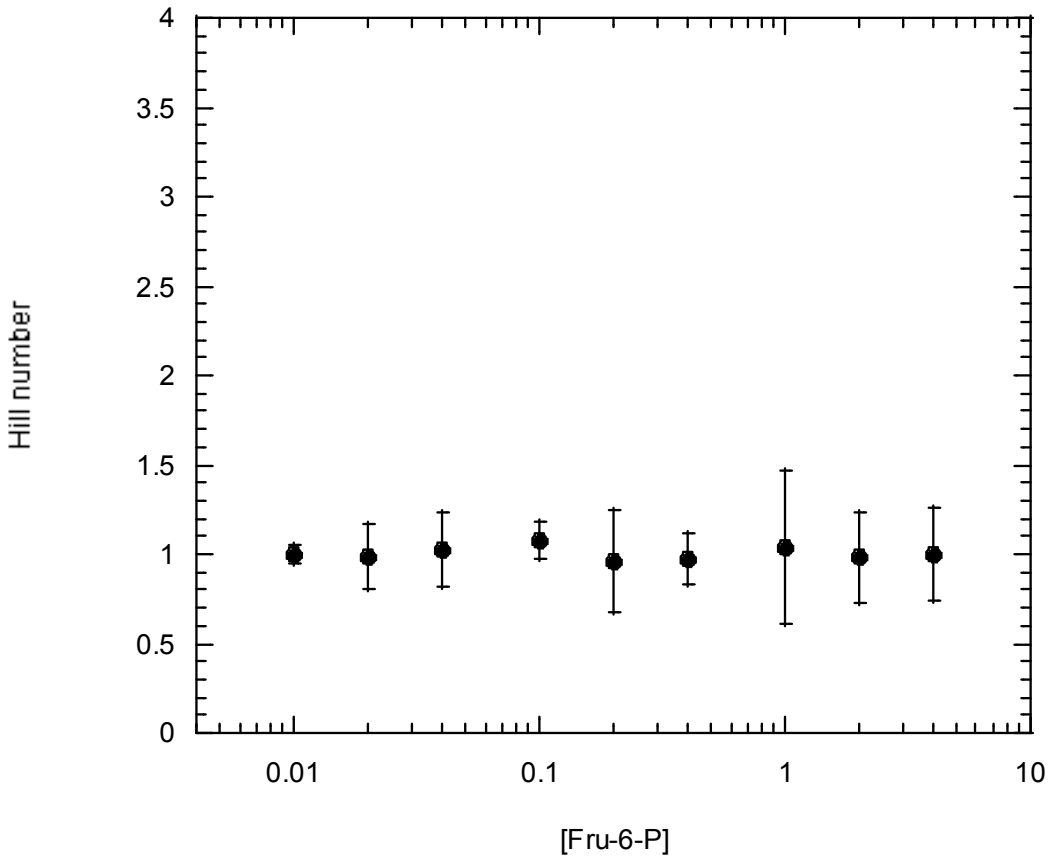

Figure 1-8. Hill number for the binding of PEP as function of Fru-6-P in TtPFK.

When studying allosteric regulation in PFK, we need to consider all four species of the enzyme, including the ternary complex. The ternary complex with both substrate and activator bound is easy to achieve because positive cooperativity of the binding of these two ligands. However, the ternary complex with both substrate and inhibitor is more difficult to achieve because of the antagonism of the binding of these two ligands. The tight binding for PEP and weaker coupling between Fru-6-P and PEP in TtPFK suggests that the ternary complex with both Fru-6-P and PEP is easier to form compared to PFK from other organisms, which can be taken advantage of when studying allosteric regulation mechanisms.

McGresham and Reinhart (2015) have identified three non-conserved residues N59, A158 and S125 (circled in figure 1-2), which contribute to the weaker coupling between Fru-6-P and PEP in TtPFK. In BsPFK, the side chains of the corresponding residues D59, T158 are H215 are involved in the interaction network, which is missing in TtPFK. They were able to increase the coupling free energy by 2.4 kcal/mol by introducing the N59D/A158T/S215H mutations. Also, each single mutation contributes approximately equally to the total the increase. The strong binding affinity of TtPFK for its allosteric inhibitor is particularly interesting considering the extremely weak binding of PEP in LdPFK. McGresham and Reinhart have shown that the non-conserved R55 (circled in figure 1-2) is important residue for the tight binding of PEP in TtPFK (Maria S. McGresham unpublished data). It is possible that the positioning of the PEP molecule in the allosteric binding cavity is different from that of BsPFK and other PFKs due to the presence of arginine at position 55. This possibility is also supported by the fact that

E55R LdPFK did not show any enhancement in the binding affinity of PEP (Paricharttanakul et al., 2005).

Hybrid study in EcPFK and BsPFK

Allosteric regulation and how allosteric information is transmitted through the enzyme has been extensively studied in the past decades. Different methods have been use to address this question. For example, site-directed mutagenesis to study allosteric regulation (Lau et al., 1987; Lau and Fersht, 1987 and 1989; Wang and Kemp, 1999; Kimmel and Reinhart, 2000; Pham et al., 2001); determination of the crystal structure of enzymes in different ligated states to study allosteric regulation (Schirmer and Evans, 1990); the use of hybrid enzymes to isolate specific allosteric interactions and characterize their function (Ackers et al. 1992; Kimmel and Reinhart, 2001; Fenton and Reinhart, 2002; Fenton et al., 2004; Ortigosa et al., 2004; Fenton and Reinhart, 2009); and the use of a genetic approach to make chimeric proteins and study their allosteric properties (Byrnes et al. 1995; Eroglu and Powers-Lee, 2002; Pawlyk and Pettigrew, 2002).

It is difficult to determine the allosteric pathways because most allosteric enzymes are oligomeric. There are multiple possible interactions. For example, tetrameric PFK has four active sites and four allosteric sites total. For allosteric interaction between Fru-6-P and PEP, there are a total of 28 interactions within the homotetramer: six homotropic interactions between the four active sites; six homotropic interactions between the four allosteric sites; and sixteen heterotropic interactions between the four active sites and the four allosteric sites. Homotropic refers to interaction between identical ligands and

heterotropic refers to interaction between different ligands. Due to the symmetry of the enzyme, only four heterotropic interactions between the active sites and the allosteric sites are unique.

Hybrid enzymes have been used to study the propagation of allosteric information in several systems. The hybrid strategy was adapted for phosphofructokinase by Kimmel and Reinhart (2001). The binding sites of PFK lie across subunit interfaces, as part of its oligomeric character. The active sites are aligned along one dimer-dimer interface, and the allosteric sites are aligned along the other dimer-dimer interface. The residues contributing to the active site and allosteric site are different. In BsPFK, the active site includes R162 and R243 from one subunit and R252, R72 and H249 from the other subunit. The allosteric binding site includes R211, K213 and R154 from one subunit and R25 and R21 from the other subunit. Mutations to only one side of a binding site can decrease ligand affinity dramatically. Each of the above mentioned residues has been mutated to glutamate to achieve the desired decrease in ligand affinity. Combination of specific active and allosteric site mutations with a method of reconstructing the enzyme allowed for the isolation of a heterotetramer of BsPFK which contained only one allosteric interaction. Four different heterotetrameric BsPFK molecules each of which contain a single unique heterotropic allosteric interaction can be created. Four heterotropic interactions, 22 Å interaction, 30 Å interaction, 32 Å interaction and 45 Å interaction, are labeled as the distance in angstroms between the ligands in the reference crystal structure. These distances do not imply the length of the pathway which allosteric signal must travel through, but rather, is a simple way of identifying which interaction is

being described. For EcPFK, the four heterotropic interactions are 23 Å interaction, 30 Å interaction, 33 Å interaction and 45 Å interaction.

Hybrid enzymes have been used to study the propagation of allosteric inhibition information in BsPFK (Ortigosa et al., 2004). Figure 1-9 shows the sum of coupling free energy measured for the isolated interactions for BsPFK compared to the total coupling free energy measured for the 4|1 control hybrid. The figure is cited from Ortigosa et al., 2004. The 4|1 control hybrid was used to eliminate PEP binding cooperativity. The overall inhibition pattern with pH is consistent with wild type BsPFK, the coupling free energy increases with pH. At pH 6, the coupling free energy of the isolated interactions sum to 75% of the total coupling free energy, "but the relative errors are large enough to make this discrepancy of questionable significance" (quote from Ortigosa et al., 2004). At pH 7 and 8, the sum of the isolated interactions is close to the total. At pH 8, the 22 Å interaction contributes 50%, the 30 Å interaction contributes 16.5%, the 32 Å interaction contributes 27.7%, and the 45 Å interaction contributes 5.7% to the total coupling free energy.

Hybrid enzymes have also been used to study the propagation of allosteric inhibition information in EcPFK (Fenton and Reinhart, 2009). Figure 1-10 shows the sum of coupling free energy measured for the isolated interactions for EcPFK compared to the total coupling free energy measured for the 1|4 control hybrid. The figure is cited from Fenton and Reinhart, 2009. 1|4 control hybrid was used to eliminate Fru-6-P binding cooperativity. For EcPFK, 23 Å interaction contributes 42% ± 3%, 30 Å interaction contributes 31% ± 2%, 33 Å interaction contributes -8% ± 2% (actually a

small activation), and 45 Å interaction contributes 25% ± 1% to the total coupling free energy. The coupling free energy of the three isolated inhibition interactions sum to 97% ± 4% of the total coupling free energy. After including the small activation of 33 Å interaction, the coupling free energy of the four interactions sum to 89% ± 4% of the total, suggesting that "this contribution might be inconsequential within the context of the overall tetramer" (quote from Fenton and Reinhart, 2009).

In both EcPFK and BsPFK, the shortest interaction, 22 Å interaction is the dominant contributor, but the percentage is higher in BsPFK than EcPFK. The most dramatic difference is the 33 Å (32 Å) interaction. In BsPFK 32 Å interaction is the second largest contributor, while in EcPFK it actually has a small activation effect. In EcPFK, 30 Å interaction and 45 Å interaction contributes 1/3 and 1/4 respectively. While in BsPFK, 30 Å interaction only contributes 16.5% and 45 Å interaction only contributes 5.7%. The relative contributions of the interactions are different for these two highly homologous isoforms. This suggests that these two enzymes use two different pathways for the transmission of inhibitory information.

Hybrid enzymes have also been used to study the propagation of allosteric activation information in EcPFK. The relative contribution of the four interactions for MgADP activation is dramatically different from that for PEP inhibition in EcPFK (Fenton and Reinhart, 2009). Although MgADP and PEP bind to the same allosteric site, but the propagation and transmission of allosteric information for activation and inhibition are different.

It will be very useful to employ the hybrid method to study the propagation of allosteric inhibition information in TtPFK and know how the relative contribution of the four unique heterotropic interactions in TtPFK compares to that of BsPFK and EcPFK.

Fluorescence phasor

Fluorescence spectroscopic properties of intrinsic fluorophore of tryptophan are very sensitive to local environment within the protein. Tryptophan has been used as fluorescence probe to detect the conformation change of allosteric regulation. Luminescence results when photons are emitted from electronically excited states, including fluorescence and phosphorescence. As shown in the Jablonski diagram (figure 1-11), the ground state is labeled as S_0 and the first and second electron states are labeled as S_1 and S_2. The figure is cited from http://www.shsu.edu. There are three vibrational energy levels in each of these energy levels. At room temperature, the majority of electrons exist in the lowest energy level, S_0. When light is absorbed electrons may gain enough energy to occupy some of the higher vibrational energy levels, S_1 or S_2. The excited electron can transit to the lowest vibrational level S_1 through internal conversion, which takes about 10^{-12} second and is complete before light is emitted. Fluorescence occurs during the process of an electron falling from the lowest vibrational level S_1 to the ground state S_0 and losing its energy as light. The time for this process is on the order of 10^{-8} second. It is possible for electrons in S_1 to transit to the triplet state T_1 through intersystem crossing. The emission from T_1 is called phosphorescence.

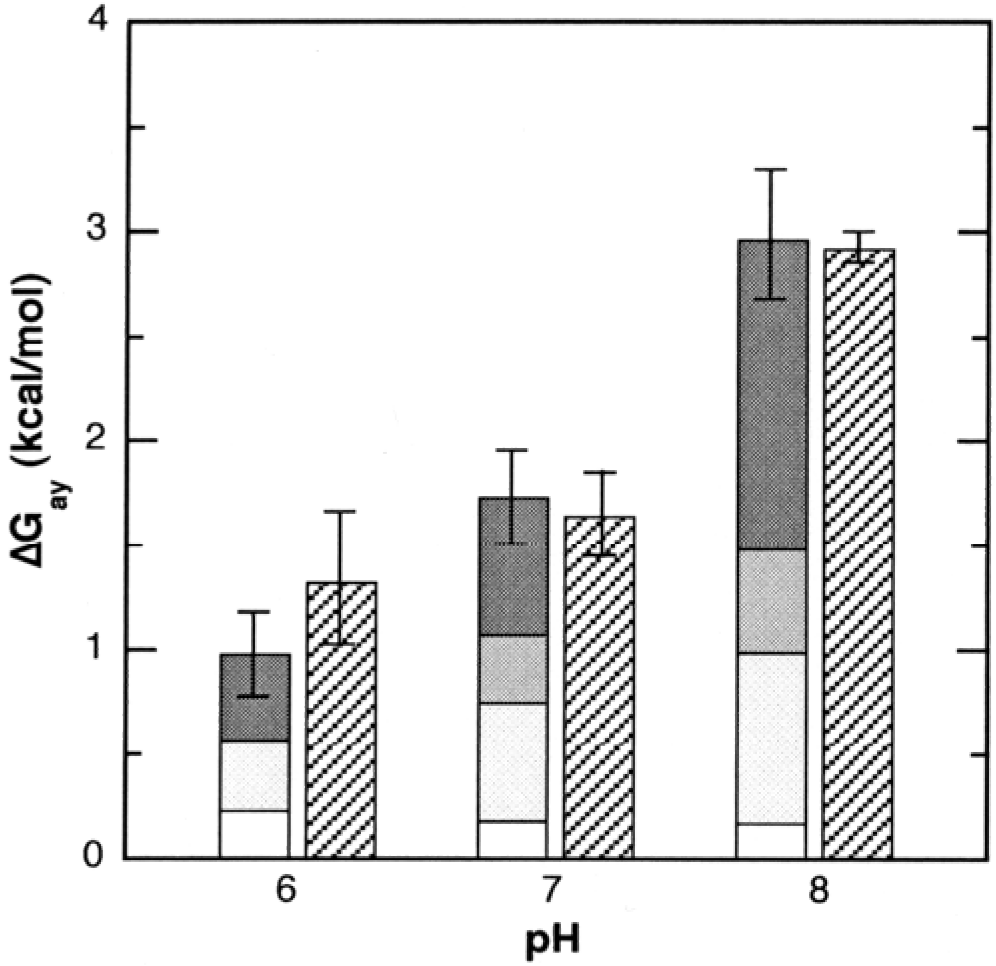

Figure 1-9. The sum of coupling free energy measured for the isolated interactions for BsPFK compared to the total coupling free energy measured for the 4|1 control hybrid at 25°C, pH 6.0, 7.0 and 8.0. Black is 22 Å interaction, dark gray is 30 Å interaction, light gray is 32 Å interaction, and white is 45 Å interaction. Figure is from Ortigosa et al., 2004.

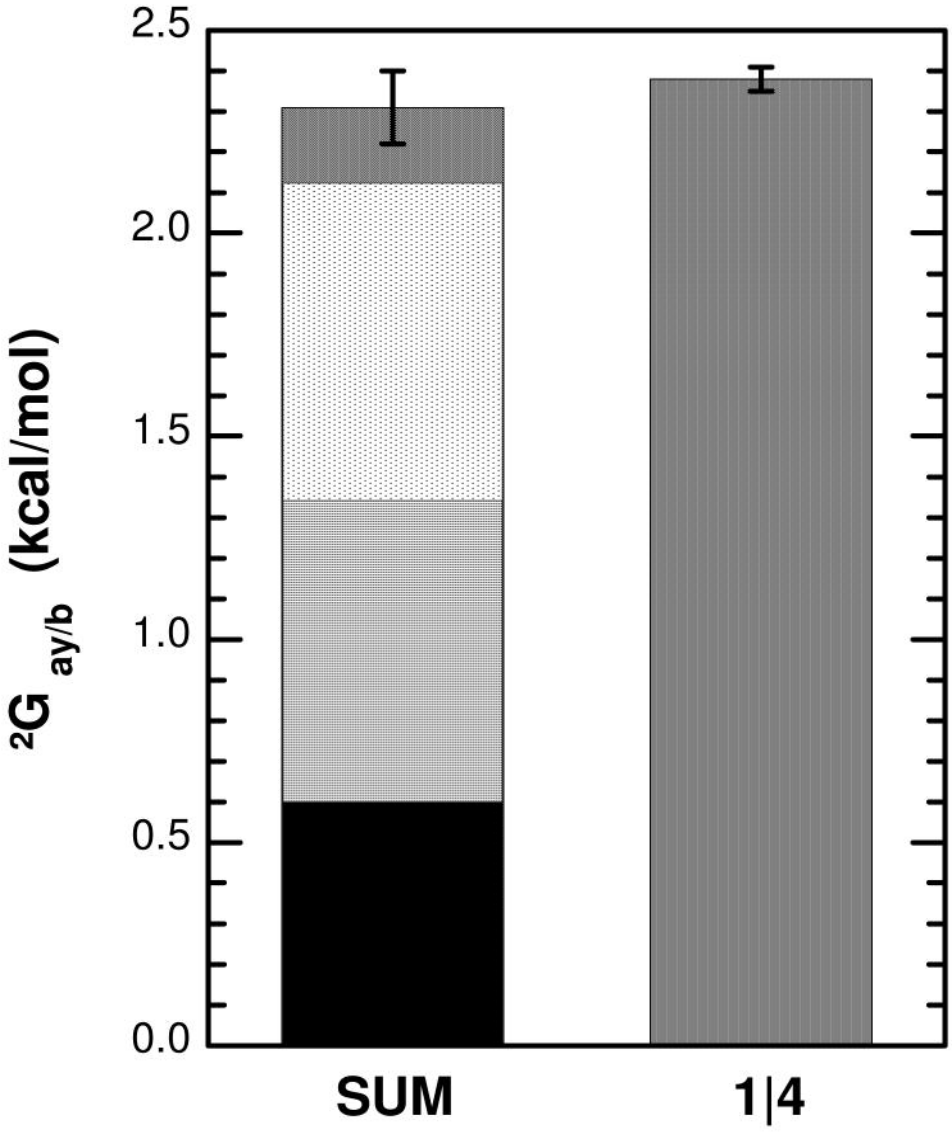

Figure 1-10. The sum of coupling free energy measured for the isolated interactions for EcPFK compared to the total coupling free energy measured for the 1|4 control hybrid at 8.5°C and pH 8. Black is 45 Å interaction, dark gray is 33 Å interaction, light gray is 30 Å interaction, and white is 23 Å interaction. Figure is from Fenton and Reinhart, 2009.

Fluorescence measurement can be categorized into two types: steady-state and time-resolved. In steady-state measurement, the sample is directly excited to a higher energy level with continuous light, and the emission spectra or intensity is recorded. In order to determine explicitly fluorescence decay rates, time-resolved techniques must be used. There are generally two methods employed in time-resolved work: the time-domain measurement and the frequency domain measurement, which is used in this dissertation and will be discussed in detail.

In the time-domain fluorescence measurement, the sample is directly excited to a higher energy level with an instantaneous short pulse of light, and the intensity decrease over time is recorded. In frequency-domain fluorescence measurement, the continuous excitation light is intensity modulated. The modulated emission of the fluorophores will have a phase delay relative to the excitation light. Figure 1-12 shows modulation and phase shift of the emission relative to excitation. The figure is cited from Spencer and Weber, 1969. The modulation factor M is defined as follows, $M= (AC_{em}/DC_{em})/(AC_{ex}/DC_{ex})$, where AC is the alternative current and DC is direct current of the excitation light detected at the photo detector from a scatter in sample compartment. The modulation of the emission is defined similarly, except using the current of the emission of the fluorescence sample. Φ is the phase delay between the excitation and emission. Figure 1-13 is the experimental phase and modulation of Ethidium Bromide free and in presence of DNA. The phase angle shifts and relative modulation values increase and decrease respectively, with higher frequencies of modulated excitation.

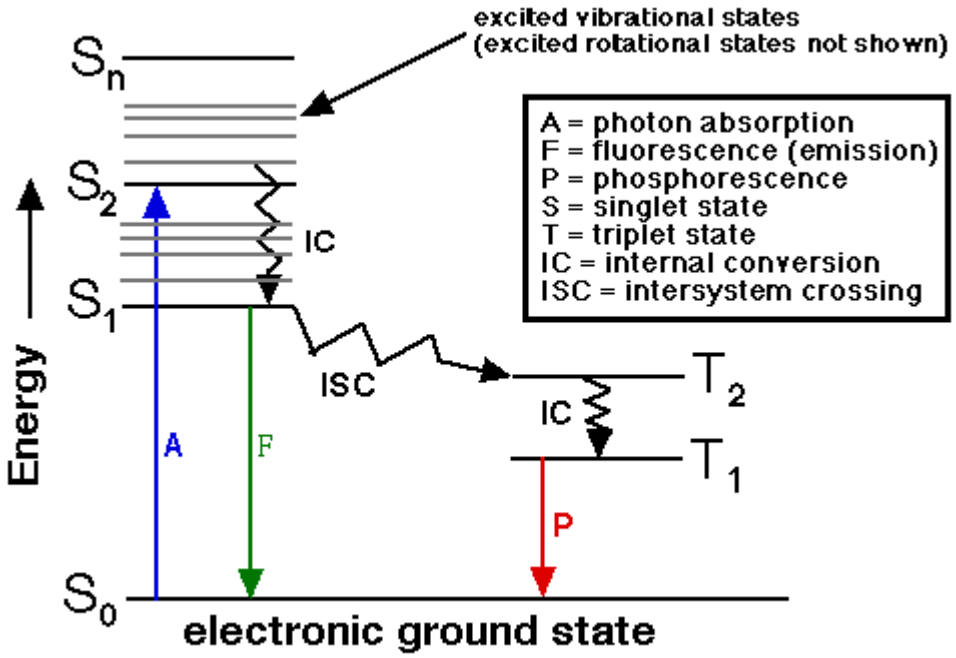

Figure 1-11. Jablonski diagram. Figure is from http://www.shsu.edu.

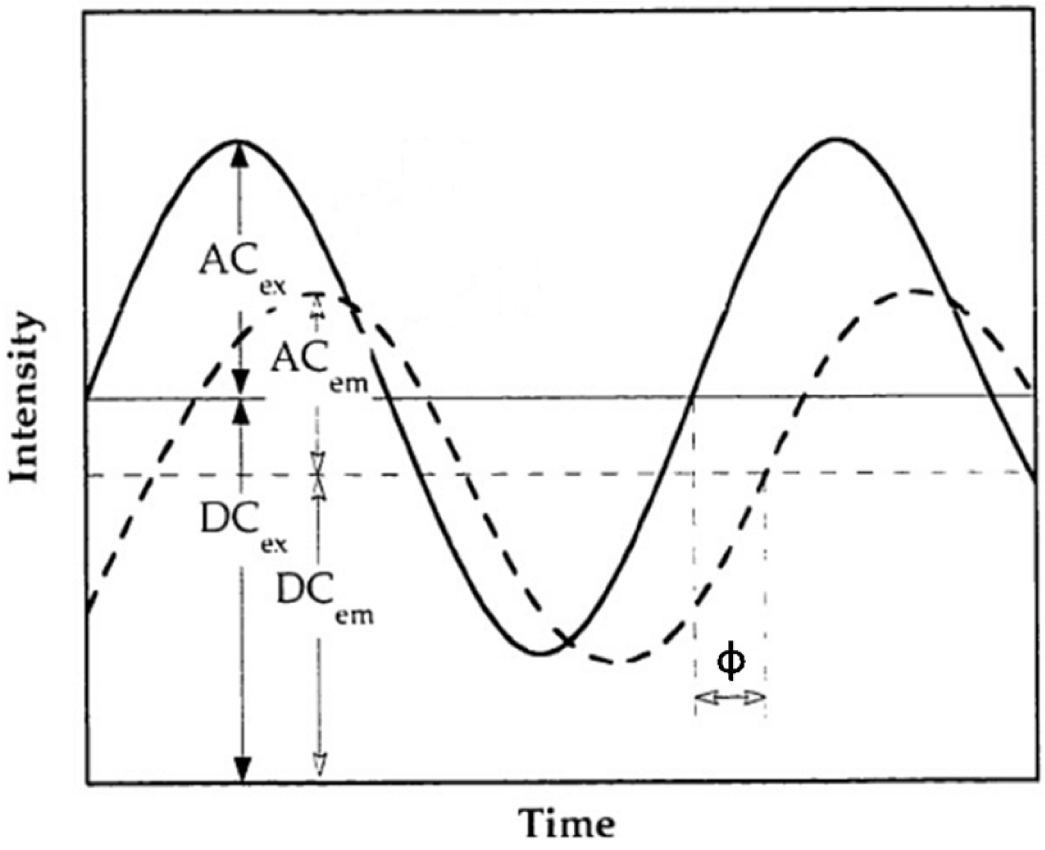

Figure 1-12. Fluorescence modulation and phase shift of the emission relative to excitation. Figure adapted from Spencer and Weber, 1969.

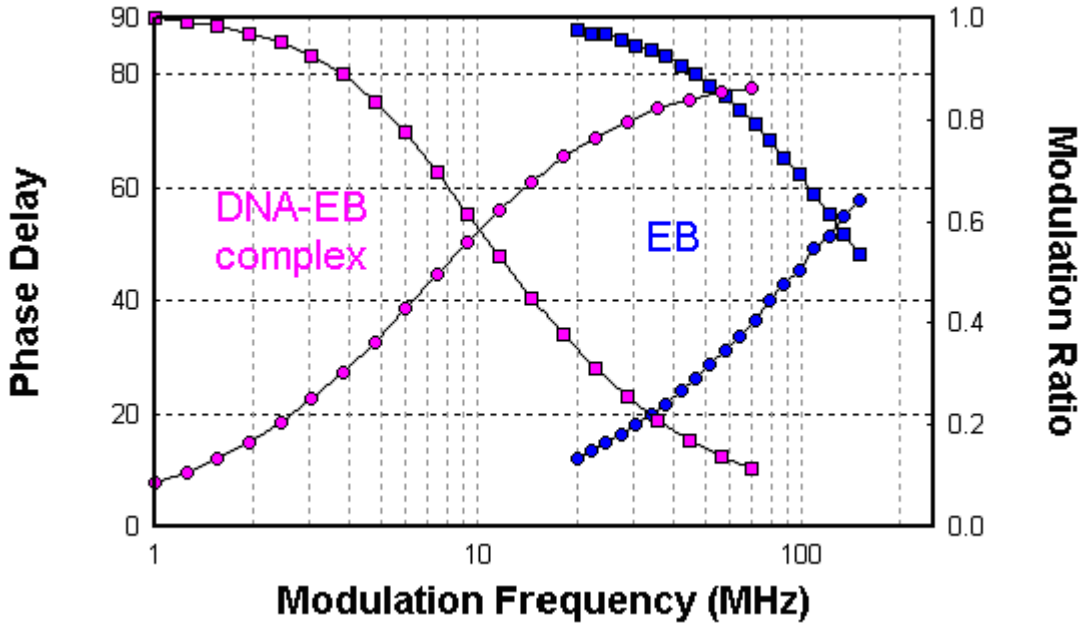

Figure 1-13. Phase and modulation of Ethidium Bromide free and in presence of DNA. Figure is from www.iss.com.

The two main parameters, phase angle and modulation, determined in frequency-domain fluorescence measurements, can be acquired with high precision. Unfortunately, when analyzing systems with complex decay mechanism, error is often introduced by the imperfect modeling. The phasor approach (Jameson et al. 1985) allows a description of the system utilizing only the raw phase angle and modulation data. The phase delay (Φ) and the modulation (M) are used to calculate G and S: $G = M \cos \Phi$, $S = M \sin \Phi$. Then these G and S are used as coordinates in the phase plot as shown in figure 1-14. The figure is cited from Stefl et al., 2011. Since G and S vary with frequency, plotting G and S as a function of frequency will form a curve, known as "universal circle". The phasor point of fluorphore with single lifetime will fall on this universal circle. The exact location of the point will depend upon the lifetime of the fluorophore and the light modulation frequency. In figure 1-14-B, there are two fluorphores with single lifetime t1 and t2 at a single frequency. If we have a mixture of these two fluorphores, the phasor point of this mixture will be on the line between the two individual phasor points weighted by the intensity of each component and produce the phasor point inside the universal circle. Consequently, for samples containing more than one fluorescence components, the phasor point of each component is inside the semicircle, the phasor point of this mixture will still be on the line between the two individual samples weighted by the intensity of each component.

Phasor provide a useful way to study complex decays. For example, even single tryptophan protein exhibits very complex decays, if we consider a protein containing more than one tryptophan residues, it is often more difficult to analyze the lifetime and it

will be more challenging to study the effects of ligand binding. With the phasor plot there will be only one phasor point at a given frequency no matter how many tryptophans contribute to the emission. If ligand binding affects one or more emitting residues, the phasor point will move. So movement of the phasor point can be an indication of a conformational change of the protein. Fluorescence phasor is an easy and fast method to evaluate data obtained from frequency-domain measurement without the assumption of any exponential decay model. As discussed earlier, there are four species, Apo-TtPFK, TtPFK-Fru-6-P, PEP-TtPFK, and PEP-TtPFK-Fru-6-P, involved in the allosteric coupling between Fru-6-P and PEP in TtPFK. In chapter IV, we will employ fluorescence phasor method to the system of TtPFK. If the ternary complex is a mixture of two binary complexes, the phasor point of the ternary complex will be on the line between the two binary complexes. If the ternary complex is a unique conformation, the phasor point of the ternary complex will be off the line between the two binary complexes.

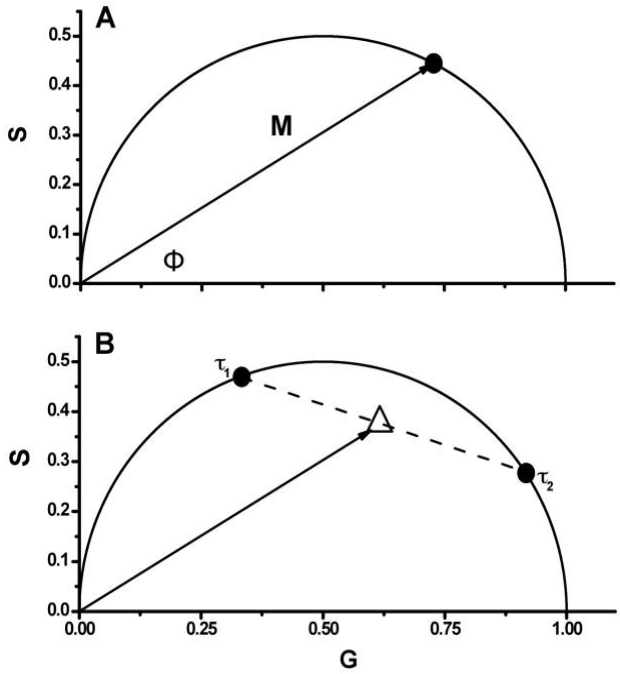

Figure 1-14. Schematic illustration of phasor plot. A. Schematic illustration of phasor plot. M is the modulation, Φ is the phase delay. B. Schematic illustration of phasor plot of mixture of two different fluorophores with lifetime τ_1 and τ_2. The dashed line is their hypothetical mixtures. Triangle is where the fluorescence contributions from two fluorophores are equal. Figure is from Stefl et al., 2011.

Chapter objective

The general objective is to improve the understanding on how allosteric regulation occurs, and more specifically how inhibition by PEP occurs in TtPFK, in other words, how the inhibition signal is transmitted and propagated throughout the enzyme.

The general objective of chapter II is to isolate the four unique heterotropic allosteric interactions in TtPFK using hybrid strategy and determine the contribution of each interaction to the total coupling free energy. Also we want to know how the relative contribution of each interaction in TtPFK compares to that of EcPFK and BsPFK.

N59D/A158T/S215H substitutions increase the coupling free energy of TtPFK similar to BsPFK. The general objective of chapter III is to employ the hybrid strategy discussed in chapter II to TtPFK N59D/A158T/S215H and isolate the four unique heterotropic interactions in TtPFK N59D/A158T/S215H. We want to know how the substitutions of N59D/A158T/S215H affect the coupling free energy in each of the four individual heterotropic interactions.

Ternary complex (enzyme bound with both substrate and effector) is not anticipated by the traditional two-state allosteric regulation model. The general objective of chapter IV is to identify unique conformations of ternary complex using fluorescence phasor. And then we want to identify residues and areas may be important for the transmission of allosteric inhibition information in TtPFK.

Chapter V summarizes the results of discussed in chapter II, chapter III and chapter IV, and discusses the possible future study direction.

CHAPTER II

ISOLATION OF INDIVIDUAL INHIBITION ALLOSTERIC INTERACTION IN PHOSPHOFRUCTOKINASE FROM *THERMUS THERMOPHILUS*

Introduction

Phosphofructokinase from *Thermus thermophilus* (TtPFK*)* is a homotetramer and the subunit has a molecular weight of 34kDa. The enzyme displays slight positive homotropic cooperation for substrate binding with hill coefficient about 1.6. It is allosterically inhibited by PEP, which does not change the catalytic turnover of the enzyme, but changees the enzyme's binding affinity for the substrate Fru-6-P. TtPFK has four active sites and four allosteric sites. It is difficult to determine the allosteric pathways since there are multiple possible interactions. For the allosteric interaction between Fru-6-P and PEP, there are sixteen heterotropic interactions between the four active sites and the four allosteric sites. But only four heterotropic interactions between the active sites and the allosteric sites are unique due to the symmetry of the enzyme.

A hybrid strategy has been developed to study the single heterotropic allosteric interaction in PFK. The binding sites of PFK lie across subunit interfaces. The active sites are aligned along one dimer-dimer interface, and the allosteric sites are aligned along the other dimer-dimer interface. The residues contributing to the active site and allosteric site are different. Mutations to only one side of a binding site can decrease ligand affinity dramatically. So mutations were made at the active site and allosteric site to block both Fru-6-P binding and PEP binding and charge tag mutations were added to the surface of the mutant subunit to increase the charge difference, facilitating the

separation of different hybrids species. Hybrids were constructed between the wild-type enzyme and the triple mutant enzyme (active site mutation, allosteric site mutation and surface charge mutation). Combination of specific active and allosteric site mutations allowed for the isolation of a functional heterotetramer of PFK which contained only one allosteric interaction. This heterotetramer has no homotropic interaction and has only one heterotropic interaction.

There are four unique heterotropic interactions in BsPFK (PFK from *Bacillus stearothermophilus*): 22 Å interaction, 30 Å interaction, 32 Å interaction and 45 Å interaction (Ortigosa et al., 2004), which are labeled as the distance in angstroms between the ligands in the BsPFK crystal structure. In EcPFK (PFK from *Escherichia coli*) the four interactions are 23 Å interaction, 30 Å interaction, 33 Å interaction and 45 Å interaction (Fenton and Reinhart, 2009). These distances do not imply the length of the pathway which allosteric signal must travel through, but rather, is a simple way of identifying which interaction is being described.

Four specific heterotropic interactions have been successfully isolated in BsPFK (Ortigosa et al., 2004) and EcPFK (Fenton and Reinhart, 2009). In both EcPFK and BsPFK, the shortest interaction, 22 Å interaction (23 Å interaction in EcPFK) is the dominant contributor, but the percentage is higher in BsPFK than EcPFK. The most dramatic difference is the 32 Å interaction (33 Å interaction in EcPFK). In BsPFK 32 Å interaction is the second largest contributor, while in EcPFK it actually has a small activation effect. In EcPFK, 30 Å interaction and 45 Å interaction contributes 1/3 and 1/4 respectively. While in BsPFK, 30 Å interaction only contributes 16.5% and 45 Å

interaction only contributes 5.7%. The relative contributions of the four unique heterotropic interactions are different for these two highly homologous isoforms; this suggests that the inhibition communications are different.

In this chapter we employ the hybrid strategy to the system of TtPFK. The aim is to isolate the four unique heterotropic interactions in TtPFK and quantitatively measure the contribution of each interaction to the total coupling free energy. Also, the inhibition in mesophile EcPFK is enthalpy driven (Johnson and Reinhart, 1997) while the inhibition in thermophile BsPFK and extreme thermophile TtPFK are entropy driven (Tlapak-Simmons and Reinhart, 1998, McGresham et al., 2014). We want to know the relative contributions of the four unique heterotropic interactions in TtPFK and how the pattern compares to EcPFK and BsPFK.

As discussed earlier in chapter I, the overall secondary, tertiary and quaternary structures are almost identical for EcPFK and BsPFK. The binding sites residues for EcPFK and BsPFK are also nearly identical (Evans et al., 1986; Shirakihara and Evans, 1988; Schirmer and Evans, 1990). TtPFK and BsPFK have 57% identity and 70% similarity in amino acid sequence. There is no crystal structure information available for TtPFK, but we have no reason to expect that the three dimensional structure of TtPFK will be dramatically different from BsPFK. So BsPFK crystal structure was used as a reference to determine the active sites and allosteric sites based on the amino acid sequence alignment of TtPFK and BsPFK. To block the binding of Fru-6-P in BsPFK, two active site mutants were made: arginine 162 to glutamate and arginine 252 to glutamate. And the corresponding residues are arginine 163 and arginine 255 in TtPFK.

To block the binding of PEP in BsPFK, two allosteric site mutants were made: arginine 25 to glutamate and arginine 211 to glutamate / lysine 213 to glutamate. And the corresponding residues are arginine 25 and arginine 212 and lysine 214 in TtPFK. The names of the four heterotropic interactions (22 Å interaction, 30 Å interaction, 32 Å interaction and 45 Å interaction) also follow BsPFK (Ortigosa et al., 2004).

Materials and methods

Materials

All reagents were of analytical grade. Glycerol-3-phosphate dehydrogenase and creatine kinase were purchased from Roche (Indianapolis, IN). Phosphocreatine, Fru-6-P, PEP, aldolase, triose phosphate isomerase, and ATP were purchased from Sigma-Aldrich (St. Louis, MO). The coupling enzymes (glycerol-3-phosphate dehydrogenase, aldolase and triose phosphate isomerase) were in ammonium sulfate suspensions. They were dialyzed with three exchanges of 50 mM MOPS pH 8.0 buffer, which contains 100 mM KCl, 5 mM $MgCl_2$ and 0.1 mM EDTA before use. The mono Q anion exchange column used for fast performance liquid chromatography (FPLC) was purchased from GE Lifescience (Charlottesville, VA). Site-directed mutagenesis follows the instruction manual from Stratagene (La Jolla, CA). The template was pALTER-1 (Promega) with wild type TtPFK gene. Oligonucleotides for quikchange site-directed mutagenesis were purchased from Integrated DNA Technologies Inc (Coralville, IA). Plasmid purification kit was purchased from Qiagen (Hilden, Germany). XL1Blue cells used for transformation were purchase from Stratagene (La Jolla, CA). Plasmid sequencing to

confirm the mutation introduced by quikchange site-directed mutagenesis is done with the BigDye kit of ABI (Foster City, CA) and Eton Bioscience (San Diego, CA).

Hybrid nomenclature

In order to differentiate different kinds of hybrids species formed in this study, two kinds of notations were introduced. The first one introduced by Kimmel and Reinhart (2000) is to use colon punctuation to separate the two numbers that define the number of subunits that each of the two parental tetramer enzyme contributes to the hybrid enzyme. The number on the left side of the colon punctuation is the number of subunit coming from one parental tetramer and the number on the right side of the colon punctuation is the number of subunit coming from the other parental tetramer. For example, notation 1:3 refers to that in the hybrid tetramer enzyme, one subunit comes from one parental tetramer enzyme and three subunits come from the other parental tetramer enzyme.

The second kind of notation introduce by Fenton and Reinhart (2002) use vertical bar to separate the two numbers that define the number of native active sites and the native allosteric sites in the hybrid tetramer enzyme, respectively. The number on the left side of the vertical bar is the number of native active sites and the number on the right side of the vertical bar is the number of native allosteric sites. For example, 1|4 refers to one native active site and four native allosteric sites.

Site-directed mutagenesis

Site-directed mutagenesis follows the instruction manual from Stratagene. Figure 2-1 is the overview of the quikchange site-directed mutagenesis method. The figure is cited from stratagene quikchange site-directed mutagenesis kit instruction manual. The

template used for all the mutagenesis was pALTER-1 plasmid with wild type TtPFK gene and tetracycline resistance. A pair of complementary primers was used to construct mutation in the wild type TtPFK gene in the plasmid. Table 2-1 lists all the oligonucleotides used in this chapter. Mutant strand synthesis reaction (thermal cycling) follows the instruction manual of quikchange site-directed mutagenesis system from Stratagene. After the PCR reaction the plasmids were transformed into competent XL1-Blue cells, colonies with tetracycline resistance were selected, and the plasmid was purified using a Qiagen kit and then sent to sequencing to confirm the mutated DNA bases.

Protein expression and purification

RL257 is a PFK-1 and PFK-2 deficient strain (Lovingshimer et al., 2006) was grown at 37°C in LB (Luria-Bertani) media which contains 10 g/L tryptone, 5 g/L yeast extract, and 10 g/L sodium chloride with 15 μg/mL tetracycline until OD_{600} is 0.6. Then the cells were induced with 0.5mM IPTG and grow at 18°C for 24 hours. The cells are centrifuged in Beckman J6 centrifuge at 4,550 x g for 30 minutes at 4°C. The cell was stored in -80°C freezer for later use.

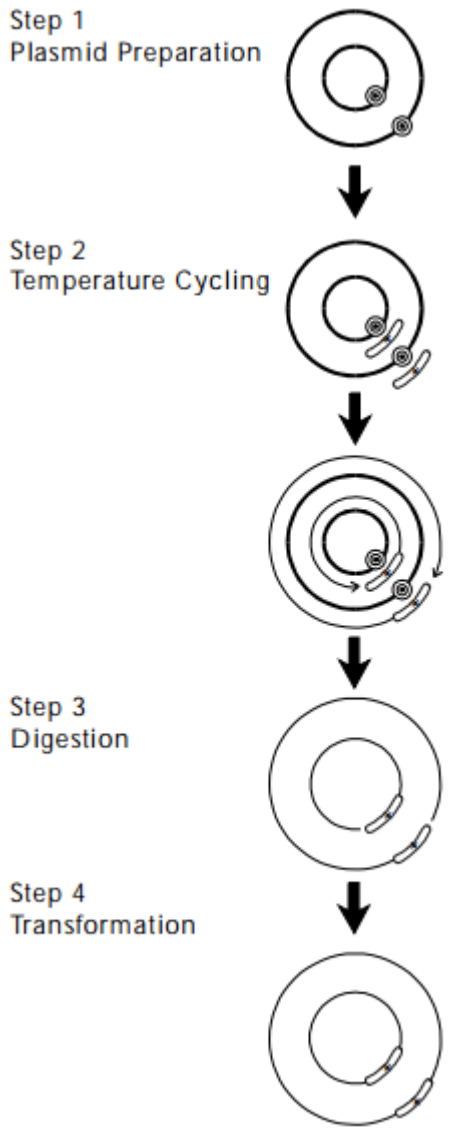

Figure 2-1. Overview of the quikchange site-directed mutagenesis method. Figure is from stratagene quikchange site-directed mutagenesis kit instruction manual.

Table 2-1. Oligonucleotides used in the quikchange site-directed mutagenesis.

	Oligonucleotides sequence
R306E	5’GGAGGCGGTGGAGGAAAGGAAGGACATCAACCGGG3’
R163E	5’CGCGGCGAGCCACGAGGAAGTCTTCTTCATAGAGG3’
R212E&K214E	5’GAGGCCTCCCAGAGGGAAGGGAAGGAAAGCTCCATC GTGGTG3’
R25E	5’CCGGGCGGTGGTGGAACAGGCCCACGCCC3’
R255E	5’GGGGCACATCCAGGAAGGCGGGAGCCCCAC3’

The cell was resuspended in 20 mM pH 8 Tris-HCl buffer with 0.5 mM EDTA. The cells were lysed using Sonic Dismembrator Model 550 (Fisher Scientific).The program is 15 second sonication and 45 second delay to cool down and the total sonication time is 8 minutes. The lysate was centrifuged in Beckman J2-21 centrifuge at 22,500 x g for 30 min at 4°C. The supernatant was heated at a 70°C water bath for 15 minutes, cool on ice for 10 min and then centrifuged at 22,500 x g for 30 min at 4°C. The supernatant was applied to 35% ammonium sulfate precipitation and then centrifuged at 22,500 x g for another 30 min at 4°C. The protein pellet was resuspended in purification buffer A and then dialyzed to get rid of any residual ammonium sulfate in the protein solution with two each exchange of buffer, each 1 hour. The protein was then applied to 10/10 mono Q anion exchange column. SDS-PAGE with 4% polyacrylamide stacking gel and 10% polyacrylamide resolving gel was used to check the purity of the protein. If there are multiple bands on the gel, proteins will be applied to another anion exchange column. Protein concentration was measured by pierce BCA assay (Smith et al., 1985).

Hybrid formation and separation

Hybrid formation and separation follow the method developed by Kimmel and Reinhart (2001) generally. TtPFK are active as tetramers and are inactivated upon dissociation into monomers by potassium thiocyanate (KSCN), a mild denaturant. They can rehybridize to tetramer given enough time of dialysis. R306E mutation was introduced to the surface of the mutant subunit to increase charge difference, facilitating the separation of hybrids through anion exchange chromatography. Wild type TtPFK enzyme and mutant TtPFK enzyme were incubated with 5M KSCN for 30 minutes to

dissociate the tetramer to monomers. Protein concentration is 2M and volume is 5-10 mL. Mixture of wild type enzyme monomers and mutant enzyme monomers were dialyzed together against purification buffer A for total 4.5 hours with 3 exchange of buffer, each 1.5 hours. The hybrid mixture was then applied to Mono-Q FPLC anion-exchange column to separate the different hybrid species. Purification buffer B was used to elute different hybrid species from the column. The absorbance at 280 nm was monitored. In figure 2-2, the elution profile shows the isolation of five different hybrid species: from left to right are 4:0 (wild type enzyme), 3:1, 2:2, 1:3 and 0:4 (mutant enzyme). Fractions were run on native PAGE gel to identify all the five hybrid species. Figure 2-3 is the identification of five hybrid species using 7.5% native PAGE gel. Lane 1 is all the five species before separation. Lane 2 is 4:0 hybrid (wild type enzyme); Lane 3 is 3:1 hybrid; Lane 4 is 2:2 hybrid; Lane 5 is 1:3 hybrid; Lane 6 is 0:4 hybrid (mutant enzyme). Hybrid of interest was dialyzed against 20mM Tris-HCl (pH 8) and stored at 4°C. No re-hybridization is observed after at least four weeks and confirmed by native PAGE.

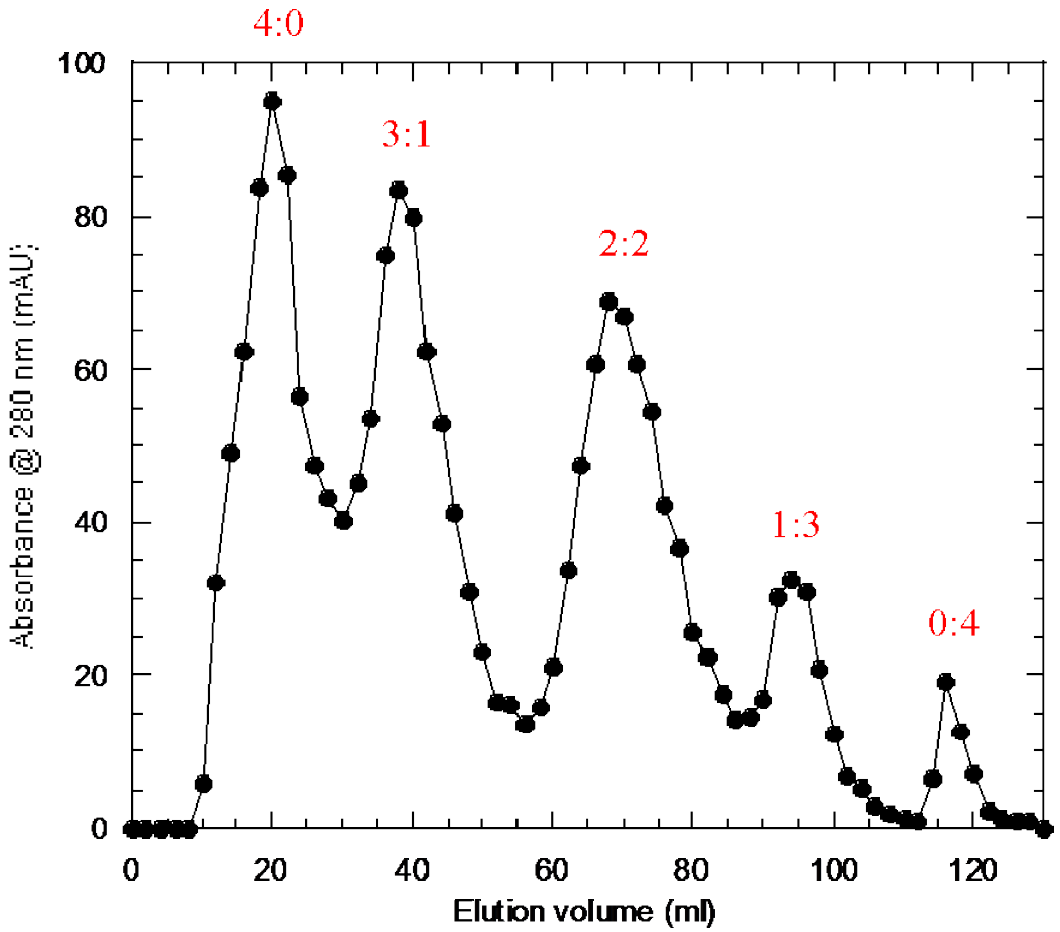

Figure 2-2. Elution profile of the isolation of hybrids between wild type TtPFK and combined mutant of TtPFK containing R163E, R212E/K214E and R306E mutations. Y axis is absorbance at 280nm and X axis is elution volume with increasing concentration of NaCl.

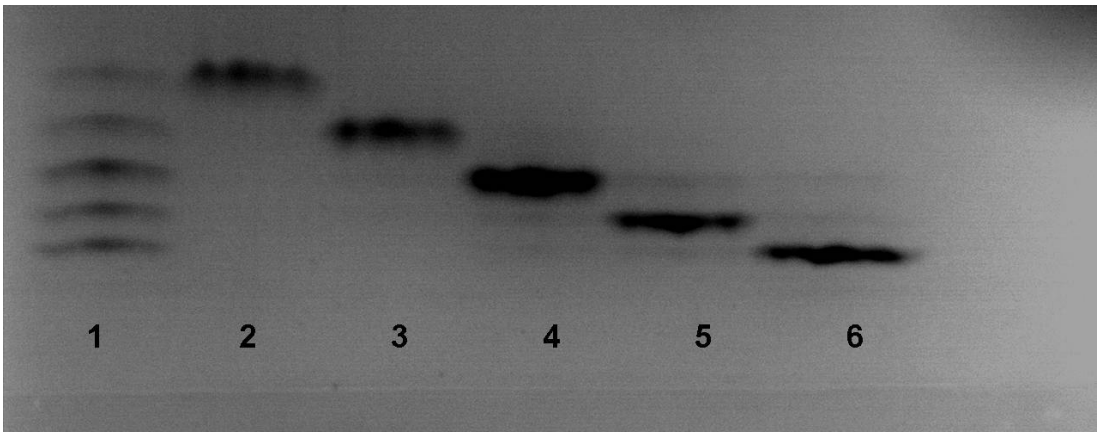

Figure 2-3. Identification of hybrids between wild type TtPFK and combined mutant of TtPFK containing R163E, R212E/K214E and R306E mutations using 7.5% native PAGE gel. Lane 1 is all the five species before separation. Lane 2 is 4:0 hybrid (wild type enzyme); Lane 3 is 3:1 hybrid; Lane 4 is 2:2 hybrid; Lane 5 is 1:3 hybrid; Lane 6 is 0:4 hybrid (mutant enzyme).

Enzymatic activity assay

The activity of TtPFK enzyme was measured at 600 µL of EPPS-KOH buffer (pH 8, 50 mM EPPS, 100 mM KCl, 5 mM MgCl2, 0.1 mM EDTA, 2 mM dithiothreitol), with 0.2 mM NADH, coupling enzymes (250 µg of aldolase, 50 µg of glycerol-3-phosphate dehydrogenase, 5 µg of triose phosphate isomerase) and 0.5mM MgATP. For maximal velocity assay, 3mM Fru-6-P was used. To measure the coupling between Fru-6-P and PEP, various concentration of Fru-6-P and PEP were used. All enzyme activity assays were measured by Beckman Series 600 spectrophotometer. The decrease in absorbance at 340nm was converted to enzyme rate. Figure 2-4 shows the coupling system for measuring TtPFK enzyme activity (Babul, 1978; Kolartz and Buc, 1982).

Data analysis

All data were fit using Kaleidagraph software (Synergy). The initial velocity data were fit to Hill equation (Hill, 1910):

$$v = \frac{V_{max}[A]^{n_H}}{K_{1/2}^{n_H} + [A]^{n_H}} \qquad (2\text{-}1)$$

where v is the initial velocity, [A] is the concentration of substrate Fru-6-P, V_{max} is the maximal velocity, n_H is the hill coefficient, and $K_{1/2}$ is the concentration of Fru-6-P when initial velocity is half maximal velocity.

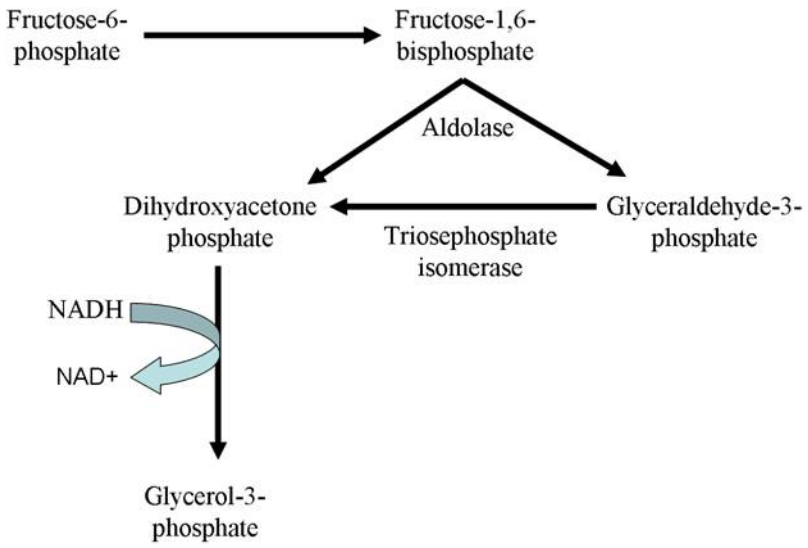

Figure 2-4. Coupling system for measuring TtPFK enzyme activity.

Since $K_{1/2}$ increase with the increasing concentration of PEP, the $K_{1/2}$ data versus increasing concentration of PEP were fit to the following equation (Reinhart, 1983):

$$K_{1/2} = K_{ia}^{0}\left(\frac{K_{iy}^{0} + [Y]}{K_{iy}^{0} + Q_{ay}[Y]}\right) \tag{2-2}$$

where $K_{ia}{}^{0}$ is the dissociation constant for Fru-6-P in the absence of PEP, $K_{iy}{}^{0}$ is the dissociation constant for PEP in the absence of Fru-6-P, [Y] is the PEP concentration, Q_{ay} is the coupling constant between of PEP and Fru-6-P.

For hybrid data which has two binding affinities for Fru-6-P and two maximal velocities, initial velocity were fit to the following equation:

$$v = \frac{V_{max}[A]}{K_{1/2} + [A]} + \frac{V'_{max}[A]}{K'_{1/2} + [A]} \tag{2-3}$$

where V_{max} is the maximal velocity for the high binding affinity site, $K_{1/2}$ is the concentration of Fru-6-P when initial velocity is half maximal velocity for the high binding affinity site, V'_{max} is the maximal velocity for the low binding affinity site, $K'_{1/2}$ is the concentration of Fru-6-P when initial velocity is half maximal velocity for the low binding affinity site, [A] is concentration of Fru-6-P.

The coupling free energy can be calculated from the following equation (Reinhart, 1983):

$$\Delta G_{ay} = -RT \ln Q_{ay} \tag{2-4}$$

where ΔG_{ay} is the coupling free energy between Fru-6-P and PEP, R is the gas constant, T is the temperature in Kelvin.

Results

Strategy

TtPFK is homotetramer with four active sites and four allosteric sites. The active sites lie along one dimer-dimer interface and the allosteric sites lie along the other dimer-dimer interface. The residues contributing to the active site and allosteric site are different. In figure 2-5, figure A is schematic illustration of one subunit of TtPFK, active sites R163 and R255 are labeled as a and b, and mutation at either a side or b side decreases the binding of Fru-6-P dramatically. The figure is cited from Ortigosa et al., 2004. Allosteric sites R212/K214 and R25 are labeled as α and β, and mutations at either α side or β side decreases the binding of PEP dramatically. Figure B is schematic representation of TtPFK tetramer. Four heterotropic interactions, 22 Å interaction, 30 Å interaction, 32 Å interaction and 45 Å interaction, are labeled as the distance in angstrom between the ligands in the reference BsPFK crystal structure.

The strategy is to construct a hybrid that has one subunit from wild type enzyme and three subunits from triple mutant enzyme, which has both active site and allosteric site mutations to block the binding of substrate and allosteric inhibitor to isolate each of the four heterotropic interactions. Figure 2-6 is schematic illustration of the four heterotropic interactions isolated in TtPFK. The figure is cited from Ortigosa et al., 2004. Shaded shape refers to the mutated active residues or allosteric residues. Open shape refers to the native active residues or allosteric residues. Combination of specific active and allosteric site mutations allowed for the isolation of a functional heterotetramer of

PFK which contained only one allosteric interaction. Table 2-2 is the summary of mutations used in each of the four heterotropic interactions.

TtPFK is active as tetramers and is dissociated into monomers by high concentration KSCN. Incubation of monomer mixture of wild type TtPFK and mutant TtPFK form five different combinations (4:0, 3:1, 2:2, 1:3 and 0:4). R306E mutation was introduced to the surface of the mutant subunit to increase the charge difference, facilitating the separation of hybrids through anion exchange chromatography.

The active site and allosteric site mutations

To block the binding of Fru-6-P, two active site mutants were made: arginine 163 to glutamate and arginine 255 to glutamate. Enzyme activities versus increasing concentration of Fru-6-P in the absence of PEP was measured and fitted to equation 2-1. Figure 2-7 is Fru-6-P saturation profile for wild type TtPFK and two active site mutants. After incorporating R163E mutation in the substrate binding site, the $K_{1/2}$ for Fru-6-P increases significantly compared to wild type (about 400-fold). After incorporating R255E mutation in the substrate binding site, the $K_{1/2}$ for Fru-6-P also increases significantly compared to wild type (about 40-fold).

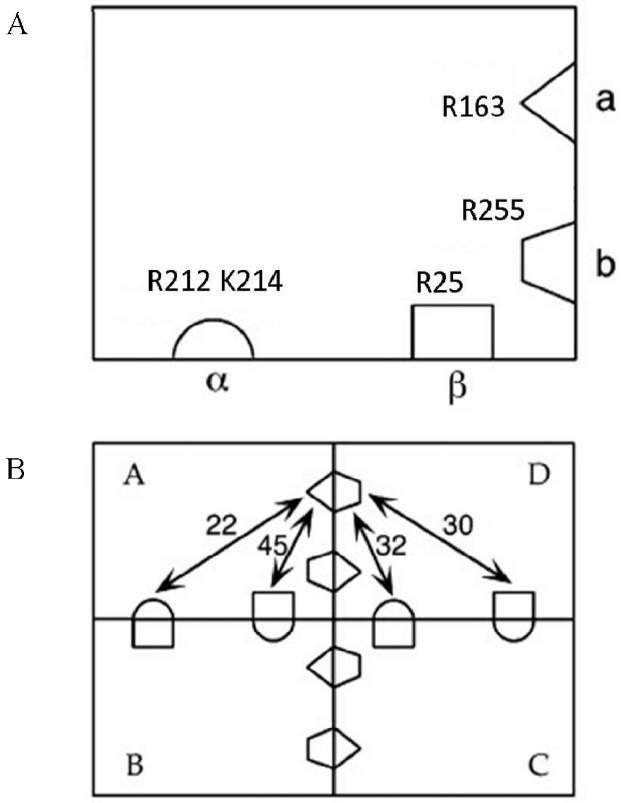

Figure 2-5. Schematic illustration of one subunit of TtPFK and TtPFK tetramer. A. Schematic illustration of one subunit of TtPFK. Active sites R163 and R255 are labeled as a and b; allosteric sites R212/K214 and R25 are labeled as α and β. B. Schematic representation of TtPFK tetramer. Four heterotropic interactions are labeled as the distance between the interacting ligands in angstrom. Figure adapted from Ortigosa et al., 2004.

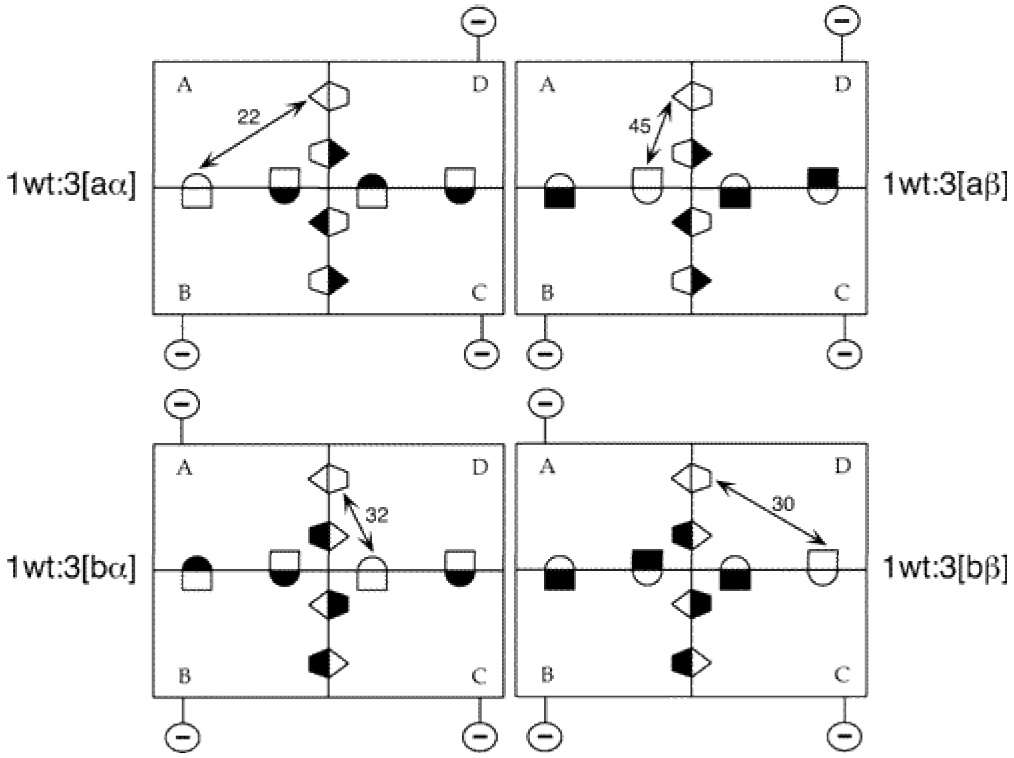

Figure 2-6. Schematic illustration of the four heterotropic interactions isolated in TtPFK. R306E mutation was introduced to the surface of the mutant subunit to increase charge difference, facilitating the separation of hybrids through anion exchange chromatography. Shaded shape refers to the mutated active residues or allosteric residues that substantially diminish binding to that site, as described in figure 2-5A and table 2-2. Figure is from Ortigosa et al., 2004.

Table 2-2. Mutations used in each of the four heterotropic interactions.

Heterotropic interaction	Active site	Allosteric site
22Å	R163E	R212E/K214E
30Å	R255E	R25E
32Å	R255E	R212E/K214E
45Å	R163E	R25E

To block the binding of PEP, two allosteric site mutants were made: arginine 25 to glutamate and arginine 212 to glutamate / lysine 214 to glutamate. Enzyme activities versus increasing concentration of Fru-6-P at different PEP concentration was measured and fitted to equation 2-1. Then the $K_{1/2}$ data versus increasing concentration of PEP were fit to equation 2-2. Figure 2-8 is the plot of apparent dissociation constant for Fru-6-P versus increasing concentration of PEP for wild type TtPFK and two allosteric site mutants. After incorporating R25E mutation in the allosteric site, it requires three orders of magnitude more PEP to see increase in $K_{1/2}$ for Fru-6-P. After incorporating R212E/K214E mutations in the allosteric site, it requires three orders of magnitude more PEP to see increase in $K_{1/2}$ for Fru-6-P. All of the four active site and allosteric site mutants are stable throughout the whole purification and kinetic characterization process.

Table 2-3 is the summary of kinetics parameters for wild type TtPFK, two active site mutants and two allosteric site mutants. The specific activity of two active site mutants decreased about 25% compared to wild type. While the specific activity of two allosteric site mutants are not affected significantly. The $K_{1/2}$ for Fru-6-P of two allosteric site mutants increases about 2-fold compared wild type. The hill coefficients are not affected for all four mutants.

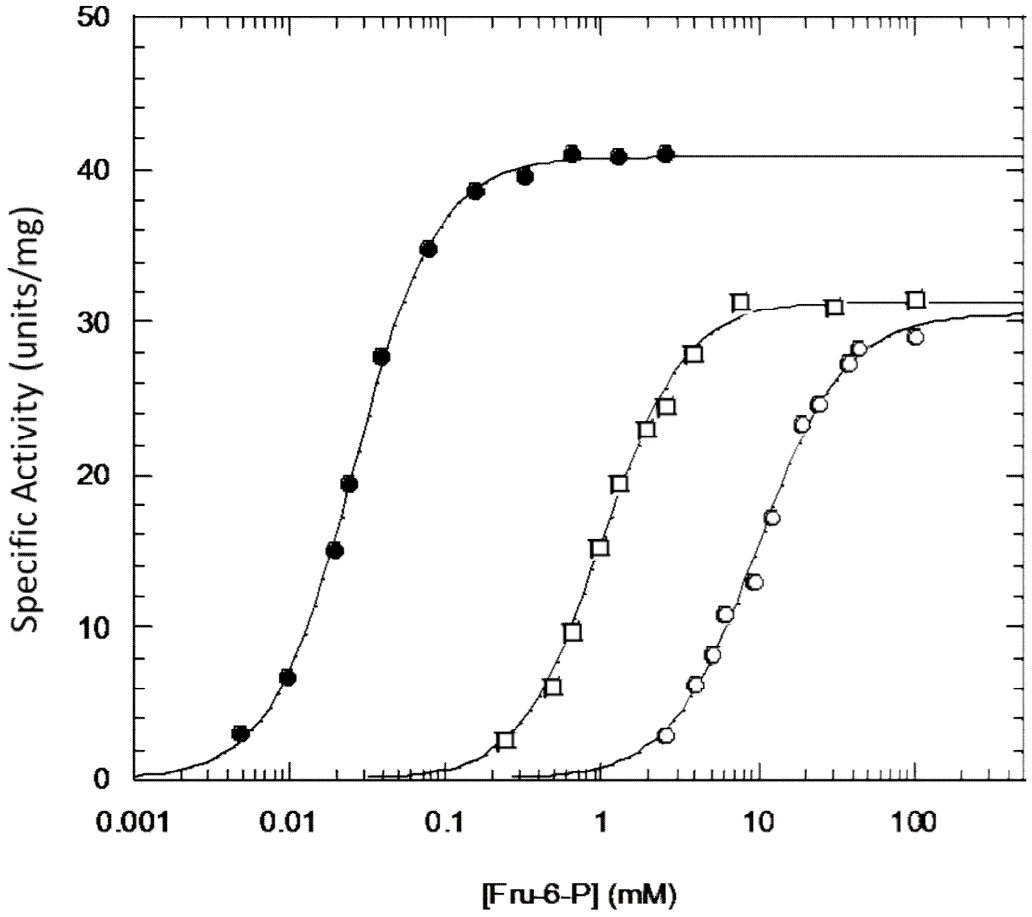

Figure 2-7. Fru-6-P saturation profile for wild type TtPFK and two active site mutants at pH 8 and 25°C. Closed circle is wild type TtPFK, open circle is R163E TtPFK and open square is R255E TtPFK.

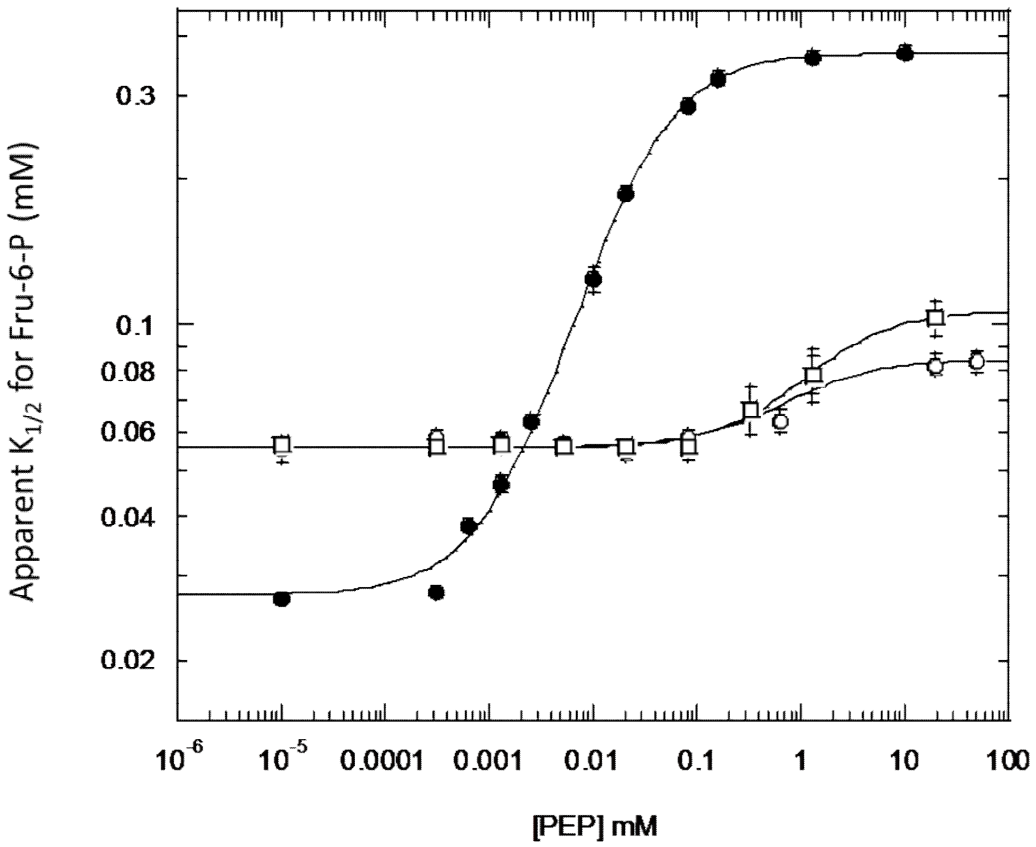

Figure 2-8. Apparent dissociation constant for Fru-6-P versus increasing concentration of PEP for wild type TtPFK and two allosteric site mutants at pH 8 and 25°C. Closed circle is wild type TtPFK, open circle is R25E TtPFK and open square is R212E/K214E TtPFK.

Table 2-3. Kinetics parameters for wild type TtPFK, two active site mutants and two allosteric site mutants at pH 8 and 25°C with [MgATP]=0.5 mM.

Enzyme	Vmax(units/mg)	$K_{1/2}$ (mM) for Fru-6-P	n_H
Wild type	41±0.2	0.027±0.002	1.63±0.05
R163E	30±0.9	9.8±0.6	1.56±0.12
R255E	31±0.5	1.0±0.1	1.65±0.09
R25E	35±0.9	0.055±0.003	1.60±0.09
R211E/K214E	36±0.8	0.057±0.003	1.50±0.11

Control hybrid

The isolated 1:3 hybrid tetramer with only one native active site has no homotropic cooperativity for Fru-6-P binding. So the inhibition coupling free energy cannot be compared to wild type which has four native active sites. 1|4 control was made to eliminate substrate Fru-6-P binding cooperativity. As shown in figure 2-9, the R163E mutation was introduced to block Fru-6-P binding in the 1|4 control.

The isolated 1:3 hybrid tetramer has one native allosteric site and three mutated allosteric sites. To eliminate the contribution of these mutated sites to the apparent inhibition effect exhibited in the hybrid, two 1|0 hybrids were made, $1|0_{25}$ control and $1|0_{211/214}$ control, as shown in figure 2-9. The R25E mutation was introduced to block PEP binding in the $1|0_{25}$ control. $1|0_{25}$ control is the 1:3 hybrid with one subunit from TtPFK R25E and three subunits from TtPFK R25E/R163E. $1|0_{25}$ serves as control for 30 Å interaction and 45 Å interaction, which have R25E mutation in the allosteric site. The K211E/K214E mutation was introduced to block PEP binding in the $1|0_{211/214}$ control. $1|0_{211/214}$ control is the 1:3 hybrid with one subunit from TtPFK R212E/K214E and three subunits from TtPFK R212E/K214E/R255E. $1|0_{211/214}$ serves as control for 22 Å interaction and 32 Å interaction, which have R212E/K214E mutation in the allosteric site. The $K_{1/2}$ for each of the 1|1 hybrid was corrected by $K_{1/2}$ of the corresponding 1|0 control hybrid using this equation:

$$K_{1/2}(\text{corrected}) = \frac{K_{1/2}(1|1)}{K_{1/2}(1|0)} \qquad (2\text{-}5)$$

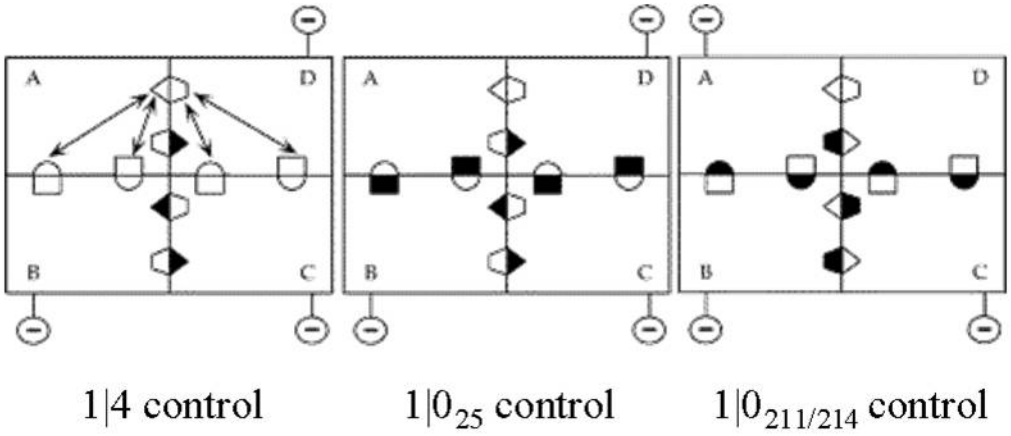

Figure 2-9. Schematic illustration of the controls used in this study. Figure adapted from Fenton et al., 2004.

Isolating the four unique heterotropic interactions

Specific active site mutation and allosteric site mutation are combined with the charge tag mutation to make triple mutant enzyme. Hybrids between wild type enzyme and triple mutant enzyme were made, separated and confirmed as described in methods. The 1:3 hybrid has both high binding affinity site for Fru-6-P, exhibited by the subunit from wild type enzyme and low binding affinity site for Fru-6-P, exhibited by the subunit from triple mutant enzyme. The initial velocity data were fit to equation 2-3, which has two $K_{1/2}$ and two V_{max}. Table 2-4 is the summary of kinetics parameters for wild type TtPFK and the isolated interactions. As expected, the $K_{1/2}$ for the high affinity site is similar to wild type, the $K_{1/2}$ for the low affinity site is close to the corresponding active site mutant. And the specific activity of the high affinity site is about 1/4 of wild type.

The $K_{1/2}$ data for the high affinity site is corrected by equation 2-5 and fitted to equation 2-2. Figure 2-10 is apparent dissociation constant for Fru-6-P versus increasing concentration of PEP for the isolated interactions in TtPFK. The allosteric coupling of 22 Å interaction is the strongest of the four while 45 Å interaction only has a very small coupling. Table 2-5 is the summary of thermodynamic coupling parameters for wild type TtPFK and the isolated interactions. Q_{ay} increased and ΔG_{ay} decreased compared to wild type by different extent.

Table 2-4. Kinetics parameters for wild type TtPFK and the isolated interactions at pH 8 and 25°C with [MgATP]=0.5 mM, and [PEP]=0 mM.

	High affinity site		Low affinity site	
Enzyme	V_{max}(units/mg)	$K_{1/2}$ (mM)	V_{max}(units/mg)	$K_{1/2}$ (mM)
Wild type	41.0±0.2	0.027±0.002	n/a	n/a
22Å	11.2±0.6	0.028±0.004	19.4±0.8	2.3±0.2
30Å	10.2±0.7	0.062±0.010	20.4±0.9	2.8±0.3
32Å	10.4±0.7	0.069±0.010	20.2±0.9	2.8±0.3
45Å	10.3±0.7	0.022±0.004	20.6±1.1	1.1±0.1

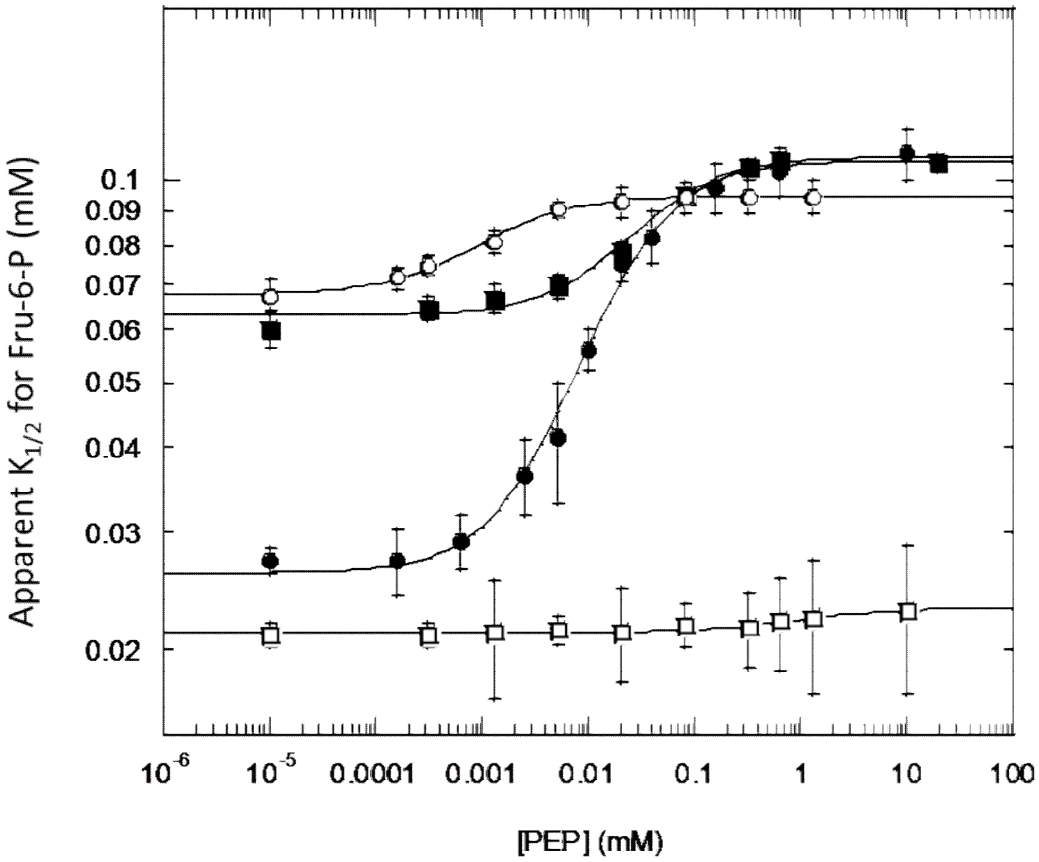

Figure 2-10. Apparent dissociation constant for Fru-6-P versus increasing concentration of PEP for the isolated interactions (22 Å, 30 Å, 32 Å and 45 Å) in TtPFK at pH 8 and 25°C. Closed circle is 22 Å interaction, closed square is 30 Å interaction, open circle is 32 Å interaction and open square is 45 Å interaction.

Table 2-5. Thermodynamic coupling parameters for wild type TtPFK and the isolated interactions at pH 8 and 25°C with [MgATP]=0.5 mM.

Enzyme	K°_{ia} (mM)	K°_{iy} (mM)	Q_{ay}	ΔG_{ay} (kcal/mol)
Wild type	0.027±0.002	0.0016±0.0002	0.07±0.005	1.46±0.04
22Å interaction	0.026±0.001	0.004±0.001	0.24±0.014	0.84±0.03
30Å interaction	0.063±0.001	0.019±0.004	0.58±0.012	0.32±0.01
32Å interaction	0.068±0.001	0.0008±0.0001	0.72±0.007	0.19±0.01
45Å interaction	0.021±0.001	0.79±0.36	0.92±0.010	0.05±0.01

Figure 2-11 is coupling free energy for the isolated interactions in TtPFK. 22Å interaction is the dominant contributor, 30Å interaction is the second biggest contributor, 32Å interaction is the third and 45Å interaction only has a very small contribution. Figure 2-12 is the sum of coupling free energy measured for the isolated interactions for TtPFK compared to the total coupling free energy measured for the control hybrid. 22Å interaction contributes 57.5% ± 2.5%, 30Å interaction contributes 21.9% ± 0.9%, 32Å interaction contributes 13.0% ± 0.5%, and 45Å interaction contributes 3.4% ± 0.4% with respect to the total coupling free energy. The free energies of the isolated interactions sum to 95.8% ± 2.7% of the total.

Discussion

To separate each of the four unique heterotropic interactions in TtPFK, the first step is to introduce a charge tag mutation to the surface of the protein without altering the kinetic and thermodynamic coupling parameters dramatically. R306E is the only mutant that meets these criteria of the ten mutants we constructed. The second step is to construct active site mutants and allosteric site mutants to block the binding of Fru-6-P and PEP, respectively. The specific activity of the two active site mutants does not decrease dramatically compared to wild-type and the specific activity of the two allosteric site mutants are very close to wild-type as shown in table 2-3. Also, only one amino acid mutation or two amino acid mutations in the active site and allosteric site can decrease Fru-6-P binding affinity and PEP binding affinity dramatically.

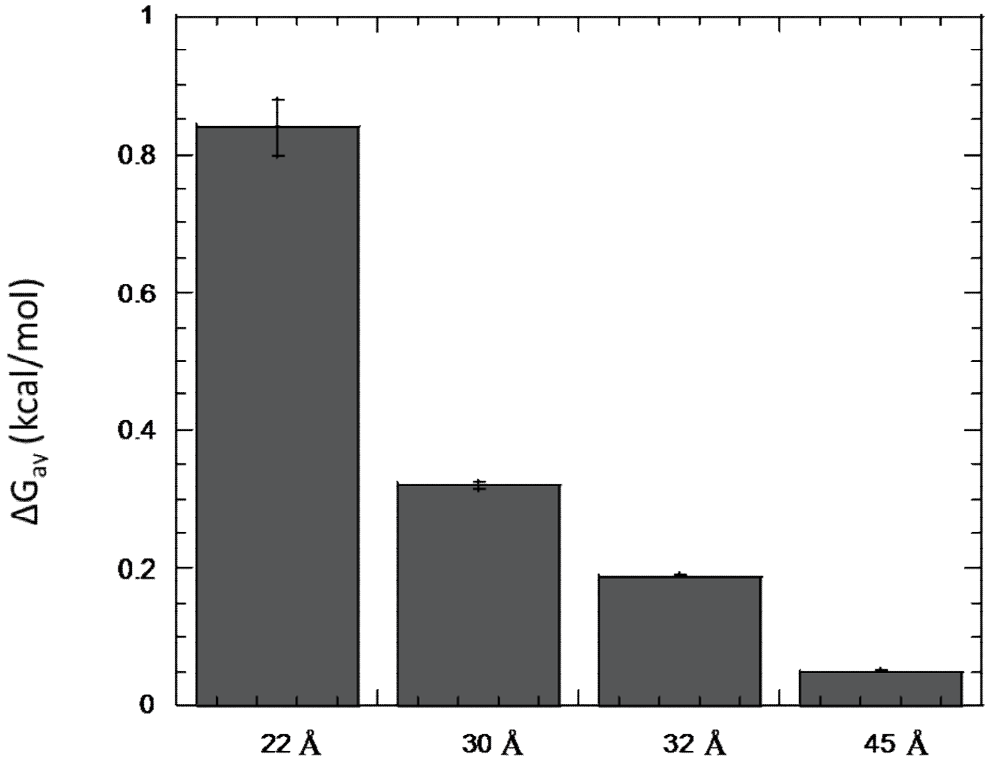

Figure 2-11. Coupling free energy for the isolated interactions in TtPFK.

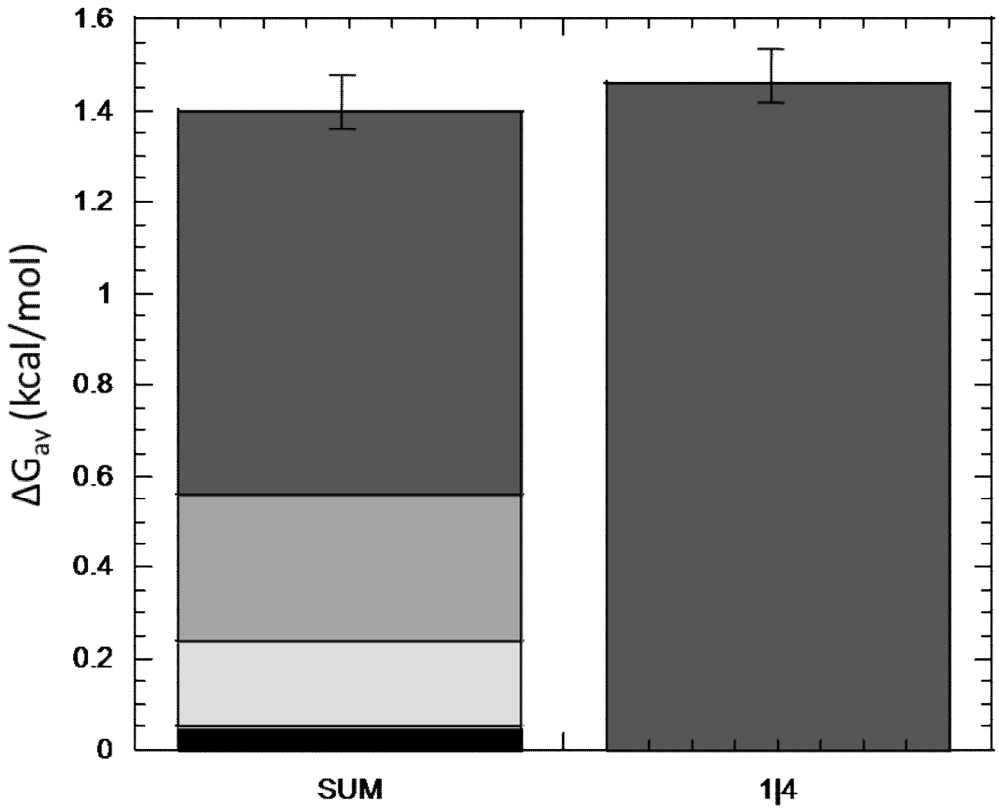

Figure 2-12. The sum of coupling free energy measured for the isolated interactions for TtPFK compared to the total coupling free energy measured for the 1|4 control hybrid at 25°C and pH 8. Dark grey is 22 Å interaction, grey is 30 Å interaction, white is 32 Å interaction and black is 45 Å interaction.

All of the four mutants are stable, so we can combine them with the charge tag mutation to make triple mutant enzyme, which can be used construct 1:3 hybrid containing only one heterotropic interaction. The dissociation constant for Fru-6-P in the absence of PEP (K^{o}_{ia}) of 22 Å interaction and 45 Å interaction are very close to wild-type as shown in table 2-5. The dissociation constant for Fru-6-P in the absence of PEP of 30 Å interaction and 32 Å interaction increases by about 3-fold when compared to wild-type, which suggests decreased binding affinity. The dissociation constant for PEP in the absence of Fru-6-P (K^{o}_{iy}) of all the interactions increases to different extent except for 32 Å interaction.

For EcPFK, the dissociation of tetramer to monomer can be achieved at only 0.4M KSCN (Deville-Bonne et al., 1989; Johnson et al., 2001), while BsPFK requires 2M KSCN (Fenton and Reinhart, 2002; Kimmel and Reinhart, 2001) and TtPFK requires 5M KSCN to achieve the same results. It is reasonable that BsPFK is more stable than EcPFK and TtPFK is more stable than BsPFK at room temperature. Because optimal growth temperature for *Bacillus stearothermophilus* is about 50°C and for *Thermus thermophilus* is above 70°C.

TtPFK has slight positive cooperativity for Fru-6-P binding. The isolated 1:3 hybrid tetramer with only one native active site has no homotropic cooperativity for Fru-6-P binding. So the coupling free energy cannot be compared to wild-type which has four native active sites. 1|4 control was made to eliminate Fru-6-P binding cooperativity. TtPFK has no cooperativity for PEP binding, so 4|1 control is not required. While in

BsPFK, 4|1 control is required to eliminate PEP binding cooperativity. And in EcPFK, 1|4 control is required to eliminate Fru-6-P binding cooperativity.

Table 2-6 is the summary of coupling free energy for the isolated interactions in EcPFK, BsPFK and TtPFK. EcPFK data is cited from Fenton and Reinhart 2009 and BsPFK data is cited from Ortigosa et al., 2004. 22Å interaction is the dominant contributor for all of the three. 30 Å interaction and 45 Å interaction make much smaller contribution in BsPFK and TtPFK than EcPFK. 32 Å interaction is the second biggest contributor and 30 Å interaction is the third contributor in BsPFK, while in TtPFK, 30 Å interaction and 32 Å interaction switch their positions.

The good agreement of the sum of the coupling free energy measured for the isolated interactions compared to the total coupling free energy suggest that we can relate the coupling we observed in the isolated individual interactions to their corresponding interactions in the native tetramer.

Each of the isolated interactions contribution to inhibition is unique and is additive, which agrees with the EcPFK and BsPFK. This suggests that the traditional two state model, either concerted model or sequential model is not sufficient to explain the allosteric regulation in TtPFK. The sequential model predicts that one of the four interactions will inhibit to a significant extent, not the other three. The concerted model predicts that each single interaction will fulfill all of the allosteric effect, while in TtPFK all four interactions are required to produce total allosteric effect.

Table 2-6. Coupling free energy for the isolated interactions in EcPFK, BsPFK and TtPFK and the corresponding control hybrids. EcPFK data is from Fenton and Reinhart 2009. BsPFK data is from Ortigosa et al., 2004.

Enzyme	EcPFK ΔG_{ay} (kcal/mol)	BsPFK ΔG_{ay} (kcal/mol)	TtPFK ΔG_{ay} (kcal/mol)
1|4 or 4|1 control	2.38±0.03	2.92±0.08	1.46±0.04
22/23 Å	0.99±0.07	1.48±0.15	0.84±0.03
30 Å	0.73±0.04	0.49±0.11	0.32±0.01
32/33 Å	- 0.19±0.04	0.82±0.12	0.19±0.01
45 Å	0.59±0.02	0.17±0.20	0.05±0.01

The use of hybrid enzymes provides an important experimental approach to study the allosteric regulation in oligomeric proteins because it can reduce the number of homotropic interaction to zero and reduce the number of heterotropic interactions to only one. Other than this, hybrid enzyme has also been used to study mechanism of substrate inhibition in EcPFK (Fenton and Reinhart, 2003).

TtPFK is a very good model to study allosteric regulation in prokaryotes system. First, the high native growth temperature can be taken advantage during the protein purification process. We express TtPFK in RL257, so heating the cell lysate at 70°C can denature most of the protein from E.*coli* while TtPFK is not affected, which is the most efficient purification step. Second, the binding affinity of PEP for TtPFK is 60-fold tighter than BsPFK, but the allosteric coupling between PEP and Fru-6-P binding is 30-fold weaker. It is easier to achieve PEP saturation when measuring the allosteric coupling between Fru-6-P and PEP without extrapolation. It will be very hard to employ hybrid to LdPFK (PFK from *Lactobacillus delbrueckii*) because LdPFK has extremely poor binding affinity for PEP and the inhibition is only seen at very high concentrations of PEP (Paricharttanakul et al., 2005). Last, the 1:3 hybrids that we use to measure the allosteric coupling of individual interactions are very stable at 4°C and no rehybridization is observed after four weeks, which is especially important when using hybrid to study allosteric regulation.

Hybrid has also been used to study the propagation of allosteric activation information in EcPFK. The relative contribution of the four interactions for MgADP activation is dramatically different from that for PEP inhibition in EcPFK (Fenton and

Reinhart, 2009). Although MgADP and PEP bind to the same allosteric site, but the propagation and transmission of allosteric information for activation and inhibition are different. Further study can isolate the four individual activation interactions in TtPFK and see how the relative contribution of the four activation interactions compares to that of inhibition interactions.

CHAPTER III

STUDY OF THE ALLOSTERIC INHIBITION IN PHOSPHOFRUCTOKINASE N59D/A158T/S215H FROM *THERMUS THERMOPHILUS*

Introduction

The allosteric coupling between Fru-6-P and PEP in phosphofructokinase from the extreme thermophile *Thermus thermophilus* is much weaker compared to phosphofructokinase from the moderate thermophile *Bacillus stearothermophilus*. McGresham and Reinhart (2015) have identified three non-conserved residues N59, A158 and S125 (circled in figure 1-2), which contribute to the weaker coupling between Fru-6-P and PEP in TtPFK. In BsPFK, the side chains of the corresponding residues aspartate 59, threonine 158 are histidine 215 are involved in the interaction network, which is missing in TtPFK due to the nature of the amino acid residues. They were able to increase the coupling free energy by about 2.4 kcal/mol by introducing the N59D/A158T/S215H mutations. And each of the substitution can increase the coupling free energy by about 0.8 kcal/mol. Due to the difference in the numbering of TtPFK and BsPFK primary sequence, the actual residue in TtPFK corresponding to BsPFK N59, A158 and S125 are N59, A159 and S216, respectively. We still use the numbering of BsPFK when referring to TtPFK in this chapter.

Table 3-1 summarizes the kinetic and thermodynamic coupling parameters for TtPFK, TtPFK N59D/A158T/S215H and BsPFK. BsPFK data is cited from McGresham et al., 2014. The binding for Fu-6-P of TtPFK N59D/A158T/S215H is slightly tighter compared to wild type TtPFK, which resulted from the substitution of A158T. And the

binding affinity for PEP of TtPFK N59D/A158T/S215H dramatically decreased compared to wild type TtPFK, which resulted from the substitution of N59D. N59D substitution decrease PEP binding affinity by about 50-fold but has no dramatic effect on Fru-6-P binding. A158T substitution increase Fru-6-P binding slightly and decrease PEP binding slightly. S215H has no dramatic effect on PEP binding and Fru-6-P binding (McGresham and Reinhart, 2015). N59D/A158T/S215H substitutions increase the coupling free energy by 2.4 kcal/mol. The coupling free energy in TtPFK N59D/A158T/S215H is 4.00 kcal/mol, which is even slightly higher than the coupling free energy of BsPFK (3.67 kcal/mol). The hill number for Fru-6-P binding is about 1.0 for this triple variant of TtPFK, which suggests there is no substrate binding cooperativity in TtPFK N59D/A158T/S215H. From the prospective of total coupling free energy and PEP binding affinity, TtPFK N59D/A158T/S215H behaves more like BsPFK than TtPFK.

In chapter II, we have isolated the four unique heterotropic interactions in wild type TtPFK and quantitatively measure the coupling free energy of each interaction. In this chapter we employ the hybrid strategy discussed in chapter II to TtPFK N59D/A158T/S215H and isolate the four interactions in TtPFK N59D/A158T/S215H. We want to know how the substitutions affect the coupling free energy in each of the four interactions. One possibility is that substitutions of N59D/A158T/S215H can only enhance the coupling in some of the four unique interactions; the other possibility is that substitutions of N59D/A158T/S215H can enhance all of the four unique interactions, either to the same extent or to different extent. Also since the total coupling free energy

in TtPFK N59D/A158T/S215H is very close to BsPFK, we want to know how the relative contribution of the four interactions in TtPFK N59D/A158T/S215H compares to BsPFK.

Materials and methods

Refer to materials and methods in chapter II.

Results

Strategy

The strategy is to construct hybrid that has one subunit from TtPFK N59D/A158T/S215H enzyme and three subunits from mutant enzyme, which has mutations at active site and allosteric site. The three subunits from mutant enzyme do not have N59D/A158T/S215H substitution. Figure 3-1 is schematic illustration of the four heterotropic interactions isolated in TtPFK. The figure is cited from Ortigosa et al., 2004. Shaded shape refers to the mutated active residues or allosteric residues. Open shape refers to the native active residues or allosteric residues. Subunit with R163E and R212E/K214E mutations are [aα]; subunit with R163E and R25E mutations are [aβ]; subunit with R255E and R212E/K214E mutations are [bα]; subunit with R255E and R25E [bβ].

Table 3-1. Kinetic and thermodynamic coupling parameters for wild type TtPFK, TtPFK N59D/A158T/S215H and BsPFK at pH 8 and 25°C. A represent Fru-6-P, Y represent PEP. BsPFK data is from McGresham et al., 2014.

Enzyme	Wild Type TtPFK	TtPFK N59D/A158T/S215H	BsPFK
K_{ia}^{o} (μM)	27.0 ± 0.6	13.0 ± 0.4	31± 2
K_{iy}^{o} (μM)	1.6 ± 0.1	83 ± 3	93±6
Q_{ay}	0.067 ± 0.002	0.0011 ± 0.0008	0.0021±0.0003
ΔG_{ay} (kcal/mol)	1.60 ± 0.02	4.00 ± 0.04	3.67±0.1
SA (unit/mg)	41	45	163
k_{cat} (s^{-1})	23	25	91
Hill number	1.5 ± 0.1	1.0 ± 0.1	1.30±0.09

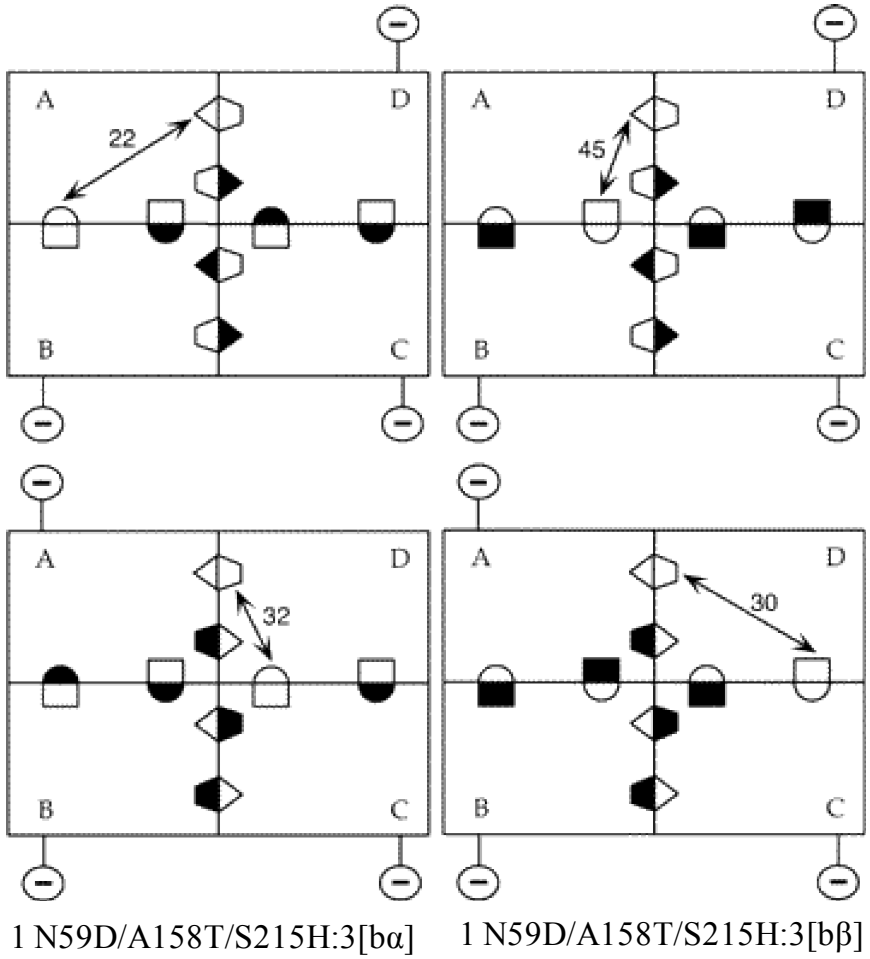

Figure 3-1. Schematic illustration of the four heterotropic interactions isolated in TtPFK N59D/A158T/S215H. Circle with negative sign refers to charge mutation. R306E mutation was introduced to the surface of the mutant subunit to increase charge difference, facilitating the separation of hybrids through anion exchange chromatography. Shaded shape refers to the mutated active residues or allosteric residues. Figure adapted from Ortigosa et al., 2004.

Isolating the four individual heterotropic interactions

Hybrids between enzyme TtPFK N59D/A158T/S215H and triple mutant enzyme (same as the mutant enzyme in chapter II) which has active site mutation, allosteric mutations and charge tag mutation were made, separated and confirmed as described in methods. The initial velocity data were fit to equation 2-3, which has two $K_{1/2}$ and two V_{max}. Table 3-2 is the summary of kinetics parameters for TtPFK N59D/A158T/S215H and the isolated interactions. As expected, the $K_{1/2}$ for the high affinity binding site is close to the $K_{1/2}$ of TtPFK N59D/A158T/S215H: 22 Å interaction and 45 Å interaction agrees very well while 30 Å interaction and 32 Å interaction shows slightly decreased Fru-6-P binding affinity. The $K_{1/2}$ for the low affinity binding site is comparable to the corresponding active site mutant. The specific activity of the high affinity binding site is about 1/4 of the specific activity of TtPFK N59D/A158T/S215H and the specific activity of the high affinity binding site is about 3/4 of the specific activity of the corresponding mutant tetramer.

Figure 3-2 is the comparison of apparent dissociation constant for Fru-6-P versus increasing concentration of PEP for the isolated interactions in wild type TtPFK and TtPFK N59D/A158T/S215H. For all of the isolated interactions, the coupling between Fu-6-P and PEP is enhanced, but to different extent. Also, the dissociation constant for Fu-6-P in the absence of PEP is smaller in TtPFK N59D/A158T/S215H than wild type, which resulted from the substitution of A158T (McGresham and Reinhart, 2015).

Table 3-2. Kinetics parameters for TtPFK N59D/A158T/S215H and the isolated interactions at pH 8 and 25°C with [MgATP]=0.5 mM, and [PEP]=0 mM.

	High affinity site		Low affinity site	
Enzyme	V_{max}(units/mg)	$K_{1/2}$(mM)	V_{max}(units/mg)	$K_{1/2}$(mM)
TtPFK N59D/A158T/S215H	45±0.5	0.013±0.004	n/a	n/a
22Å	11.7±0.5	0.014±0.002	19.4±0.7	2.3±0.2
30Å	11.1±0.5	0.027±0.004	19.3±0.7	2.3±0.2
32Å	11.6±0.6	0.027±0.004	19.5±0.8	2.3±0.2
45Å	11.8±0.6	0.015±0.002	21.5±1.0	1.1±0.1

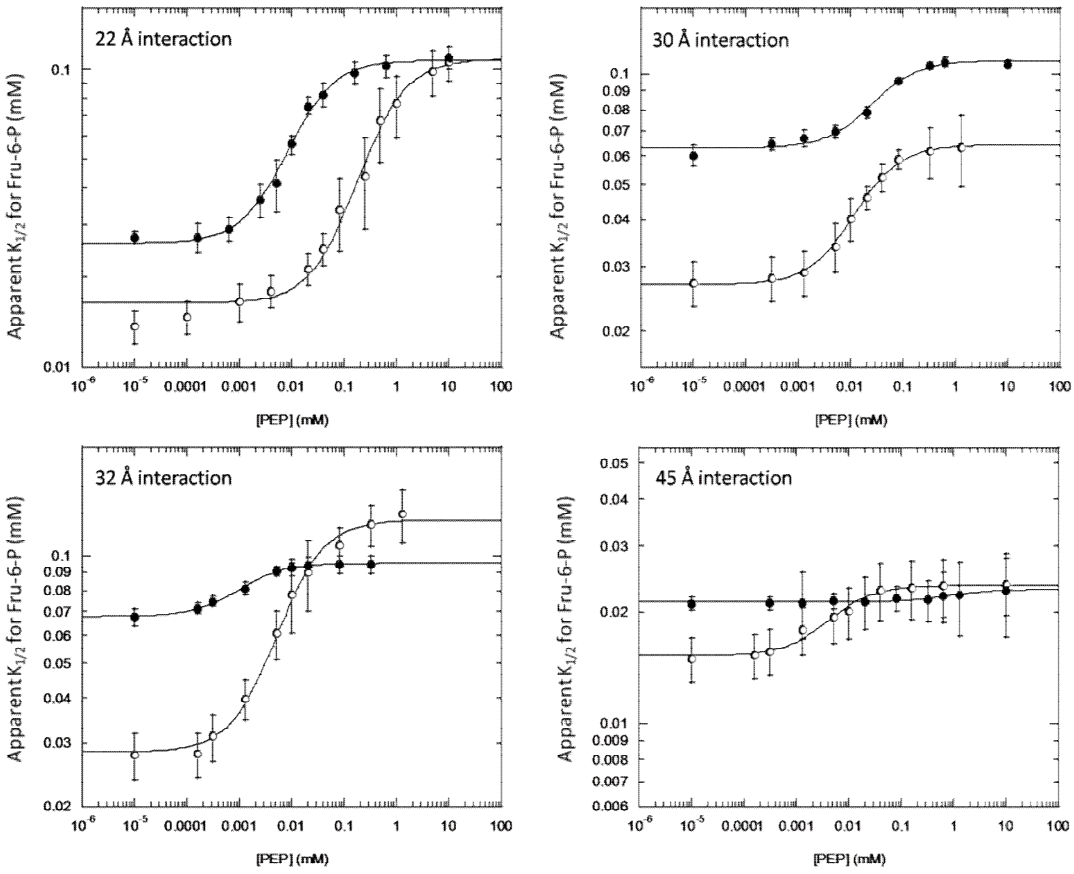

Figure 3-2. Apparent dissociation constant for Fru-6-P versus increasing concentration of PEP for the isolated interactions in wild type TtPFK and TtPFK N59D/A158T/S215H at pH 8 and 25°C. Figure A is the comparison of 22 Å interaction. Open circle is 22 Å interaction with TtPFK N59D/A158T/S215H, and closed circle is 22 Å interaction with wild type TtPFK. Figure B is the comparison of 30 Å interaction. Open circle is 30 Å interaction with TtPFK N59D/A158T/S215H, and closed circle is 30 Å interaction with wild type TtPFK. Figure C is the comparison of 32 Å interaction. Open circle is 32 Å interaction with TtPFK N59D/A158T/S215H, and closed circle is 32 Å interaction with wild type TtPFK. Figure A is the comparison of 45 Å interaction. Open circle is 45 Å interaction with TtPFK N59D/A158T/S215H, and closed circle is 45 Å interaction with wild type TtPFK.

Figure 3-3 is the apparent dissociation constant for Fru-6-P versus increasing concentration of PEP for the isolated interactions in TtPFK N59D/A158T/S215H. Table 3-3 is the summary of thermodynamic coupling parameters for TtPFK N59D/A158T/S215H and four isolated interactions. ΔG_{ay} of the individual interaction decreased to different extent compared to TtPFK N59D/A158T/S215H as Q_{ay} increased.

Figure 3-4 is the coupling free energy for the isolated interactions in wild type TtPFK and TtPFK N59D/A158T/S215H. In wild type TtPFK, 22Å interaction is the dominant contributor, 32Å interaction is the second biggest contributor, 30Å interaction is the third and 45Å interaction only has a very small contribution. In TtPFK N59D/A158T/S215H, 22Å interaction is still the dominant contributor and 45Å interaction still has relatively small contribution. The most dramatic difference is that 30Å interaction becomes the second biggest contributor and 32Å interaction becomes the third contributor, which is same as the relative inhibition pattern in BsPFK.

A shown in figure 3-5, there is no PEP binding cooperativity in TtPFK N59D/A158T/S215H, no control hybrid is required. Figure 3-6 is the sum of coupling free energy measured for the isolated interactions for TtPFK N59D/A158T/S215H compared to the total coupling free energy measured for the TtPFK N59D/A158T/S215H tetramer. 22Å interaction contributes 28.0% ± 1.0%, 30Å interaction contributes 13.0% ± 0.3%, 32Å interaction contributes 22.0% ± 1.0%, and 45Å interaction contributes 6.5% ± 0.3% with respect to the total coupling free energy. The free energies of the isolated interactions sum to 69.5% ± 1.5% of the total. But previous hybrid study in EcPFK (Fenton et al., 2004, Fenton and Reinhart, 2009),

BsPFK (Ortigosa et al., 2004) and wild type TtPFK (chapter II) all showed good agreement of the sum of the coupling free energy measured for the isolated interactions compared to the total coupling free energy measured for the control hybrid. One possible reason for this non-agreement is that the three mutant subunits we use to create 1:3 hybrid does not have N59D/A158T/S215H substitution.

Discussion

From the prospective of total coupling free energy, entropy and enthalpy of inhibition and PEP binding affinity, TtPFK N59D/A158T/S215H behaves more like BsPFK than TtPFK. Table 3-4 is the summary of coupling free energy for the isolated interactions in wild type TtPFK, TtPFK N59D/A158T/S215H and BsPFK. By introducing the substitutions, the coupling free energy for the 22 Å interaction increases by about 0.28 kcal/mol; 30 Å interaction increases by about 0.20 kcal/mol; 32 Å interaction increases by about 0.69 kcal/mol; and 45 Å interaction increases by about 0.21 kcal/mol. The substitutions of N59D/A158T/S215H can enhance all of the four interactions, but to different extent. 32 Å interaction exhibits the biggest increase in coupling free energy and this big increase makes 32 Å interaction become the second biggest contributor to the total coupling free energy in TtPFK N59D/A158T/S215H. The coupling free energy of the 30 Å and 32 Å interactions in this triple variant is very close to BsPFK. But But the free energies of the isolated interactions in TtPFK triple variant sum to 69.5% of the total. One possible reason for this large discrepancy is that the three mutant subunits we use to create 1:3 hybrid does not have these three substitutions.

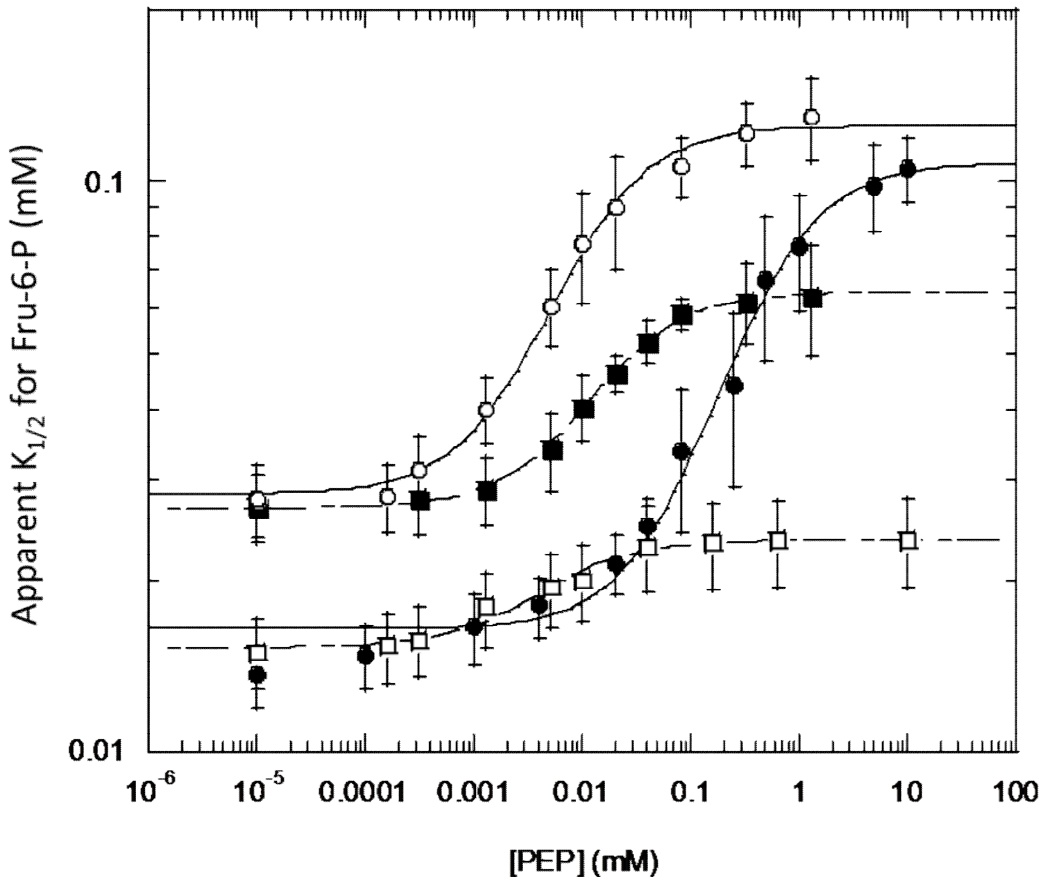

Figure 3-3. Apparent dissociation constant for Fru-6-P versus increasing concentration of PEP for the isolated interactions in TtPFK N59D/A158T/S215H at pH 8 and 25°C. Closed circle is 22 Å interaction, closed square is 30 Å interaction, open circle is 32 Å interaction and open square is 45 Å interaction.

Table 3-3. Thermodynamic coupling parameters for TtPFK N59D/A158T/S215H and the isolated interactions at pH 8 and 25°C with [MgATP]=0.5 mM.

Enzyme	K°_{ia} (mM)	K°_{iy} (mM)	Q_{ay}	ΔG_{ay} (kcal/mol)
TtPFK N59D/A158T/S215H	0.013±0.004	0.083±0.003	0.0011±0.0008	4.00±0.04
22Å interaction	0.016±0.001	0.070±0.01	0.15±0.011	1.12±0.04
30Å interaction	0.027±0.004	0.008±0.0005	0.42±0.007	0.52±0.01
32Å interaction	0.028±0.002	0.002±0.0004	0.23±0.017	0.88±0.04
45Å interaction	0.015±0.003	0.003±0.0007	0.65±0.014	0.26±0.01

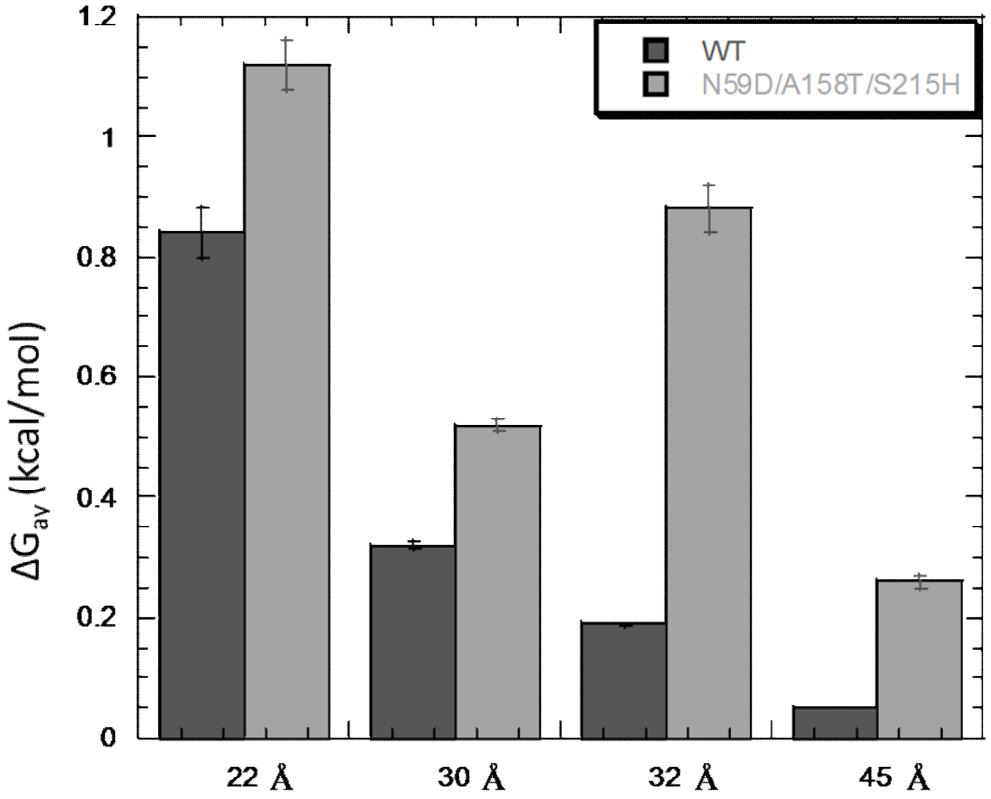

Figure 3-4. Coupling free energy for the isolated interactions in wild type TtPFK and TtPFK N59D/A158T/S215H. Black bar is the isolated interactions in wild type TtPFK and grey bar is isolated interactions in TtPFK N59D/A158T/S215H.

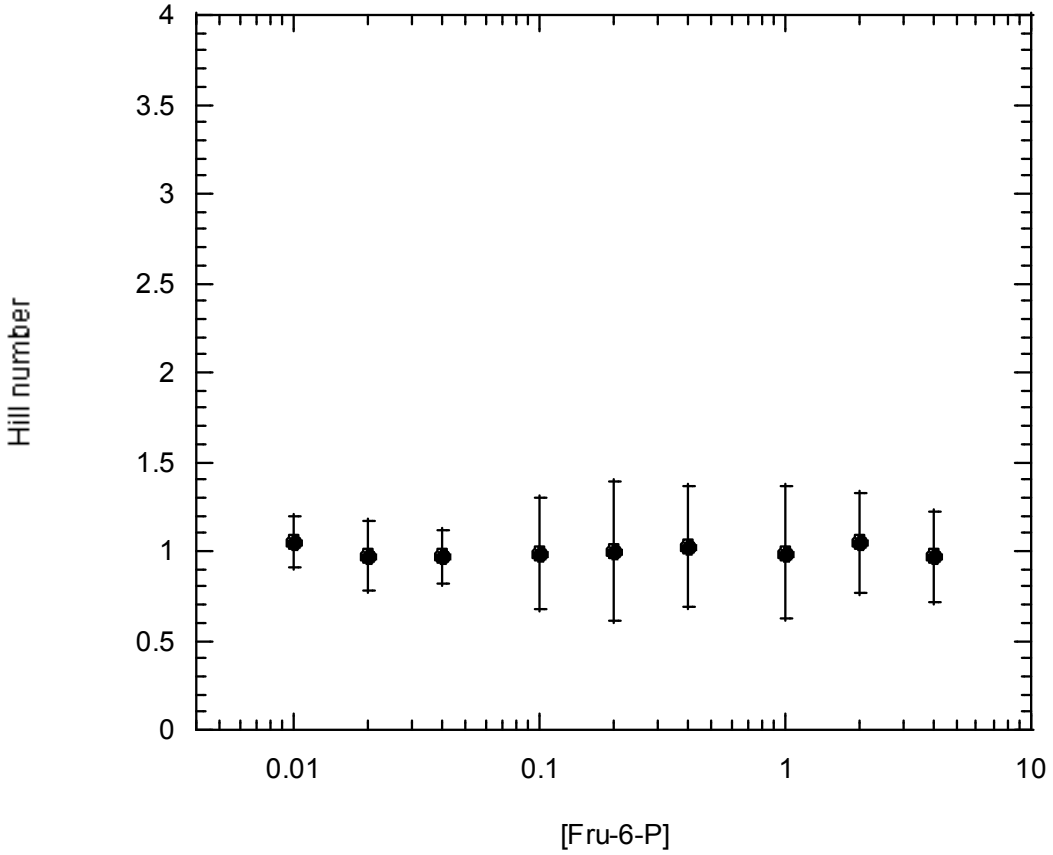

Figure 3-5. Hill number for the binding of PEP as function of Fru-6-P in TtPFK N59D/A158T/S215H.

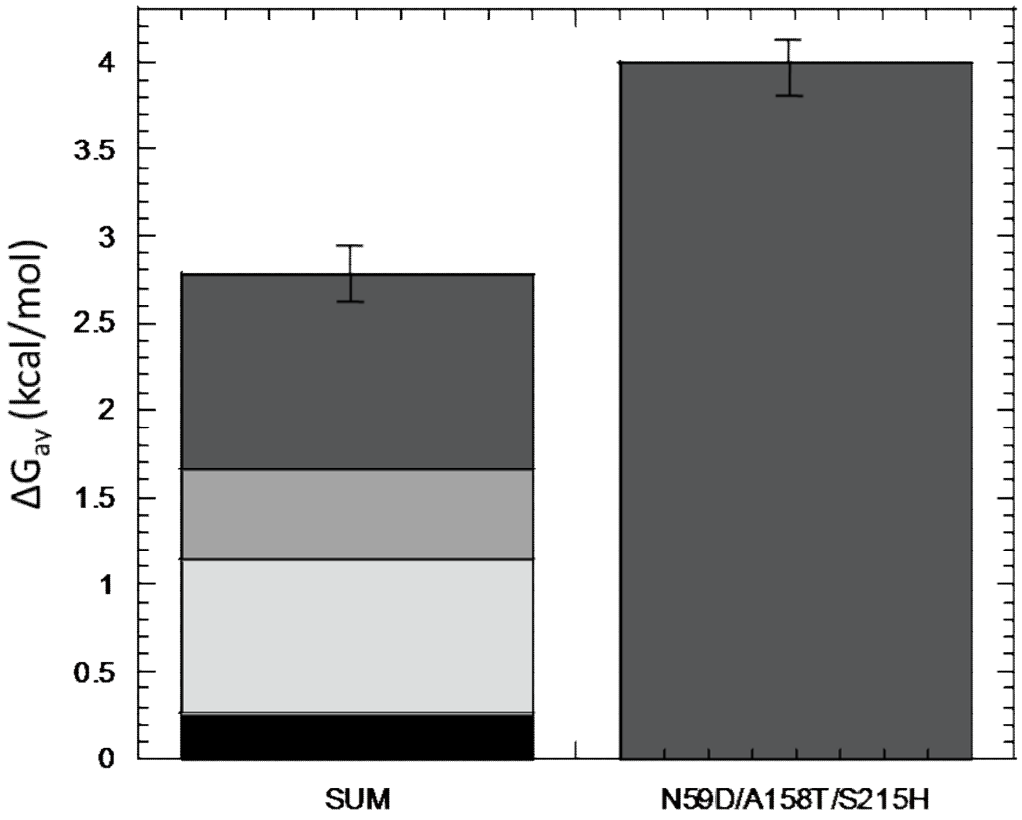

Figure 3-6. The sum of coupling free energy measured for the isolated interactions for TtPFK N59D/A158T/S215H compared to the total coupling free energy measured for TtPFK N59D/A158T/S215H at 25°C and pH 8. Dark grey is 22 Å interaction, grey is 30 Å interaction, white is 32 Å interaction and black is 45 Å interaction.

The coupling free energy for TtPFK N59D/A158T/S215H and BsPFK are 4.00 kcal/mol and 3.67 kcal/mol, respectively. The summary of coupling free energy for the isolated interactions in TtPFK N59D/A158T/S215H and BsPFK are 2.78 kcal/mol and 2.96 kcal/mol, respectively. The large discrepancy between 3.67 kcal/mol and 2.96 kcal/mol is due to PEP binding cooperativity in BsPFK. The coupling free energy for 4|1 control hybrid is BsPFK is 2.92 kcal/mol, which agrees well with the sum of coupling free energy measured for the isolated interactions. The discrepancy between 4.00 kcal/mol and 2.78 kcal/mol for still exists since there is no PEP binding cooperativity in TtPFK N59D/A158T/S215H.

Figure 3-7 shows the positions of D59, T158 and H215 in BsPFK structure relative to the four individual interactions. 32 Å interaction shows the strongest enhancement in coupling free energy after introducing these three substitutions. The residues colored in yellow are the three residues from one subunit; the residues colored in green are the three residues from the other subunit. T158 and H215 from one subunit are interacting with D59 from the other subunit as shown in the red box, and this D59 is missing in the 1:3 hybrid we construct. This may be the reason for the large discrepancy between the sum of the coupling free energy measured for the isolated interactions and the total coupling free energy in the native tetramer. The discrepancy is likely due to the mutated residues not all interacting within a single subunit.

Table 3-4. Coupling free energy for the isolated interactions in TtPFK, TtPFK N59D/A158T/S215H and BsPFK. BsPFK data is from Ortigosa et al., 2004.

Enzyme	TtPFK ΔGay (kcal/mol)	TtPFK N59D/A158T/S215H ΔGay (kcal/mol)	BsPFK ΔGay (kcal/mol)
22Å	0.84±0.03	1.12±0.04	1.48±0.15
30Å	0.32±0.01	0.52±0.01	0.49±0.11
32Å	0.19±0.01	0.88±0.04	0.82±0.12
45Å	0.05±0.01	0.26±0.01	0.17±0.20
Total	1.40±0.03	2.78±0.06	2.96±0.30
Tetramer	1.46±0.04	4.00±0.04	2.92±0.08

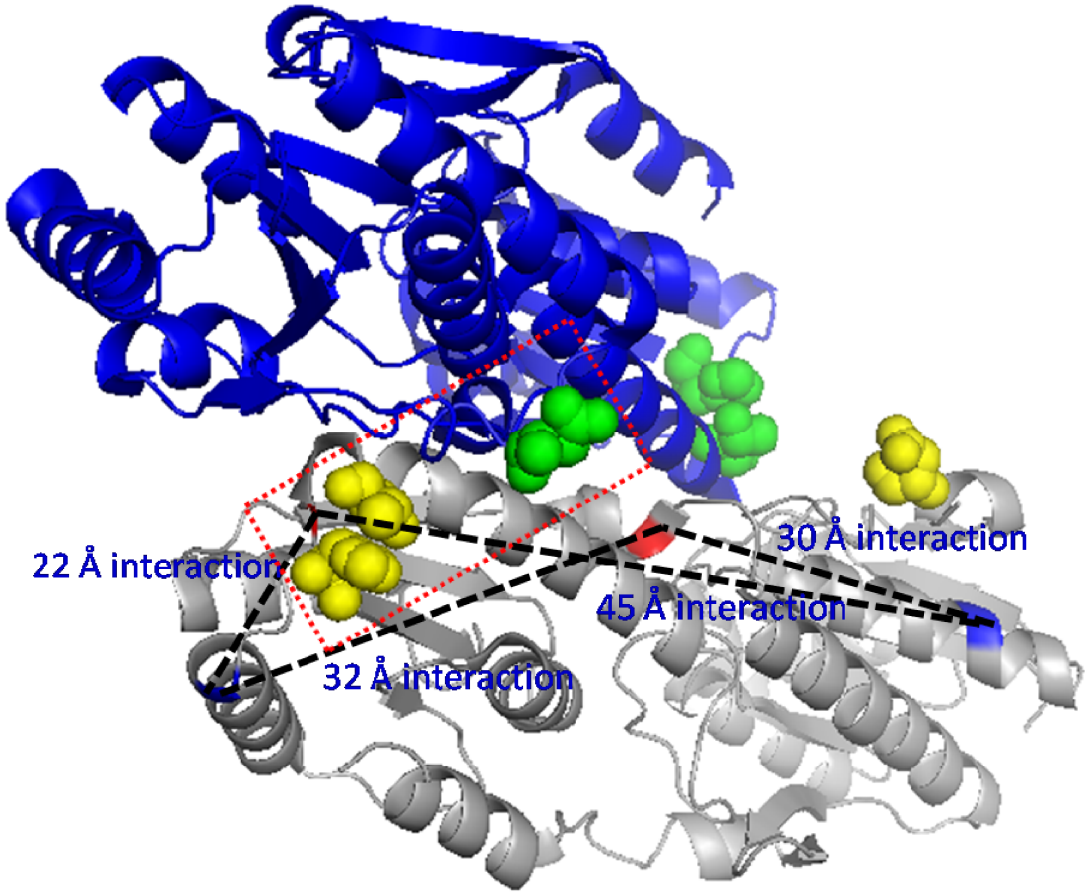

Figure 3-7. The positions of D59, T158 and H215 in BsPFK dimer structure. Active site residues are colored in red and allosteric site residues are colored in blue. D59, T158 and H215 from one subunit are colored in yellow; D59, T158 and H215 from the other subunit are colored in green. T158 and H215 from one subunit is interacting with D59 from the other subunit, as shown in the red box.

CHAPTER IV

IDENTIFICATION OF UNIQUE CONFORMATIONS AND REGIONS INVOLVED IN THE INHIBITION OF PHOSPHOFRUCTOKINASE FROM *THERMUS THERMOPHILUS*

Introduction

Researchers have been using the concerted (MWC) model (Monod et al., 1965) and the sequential (KNF) model (Koshland et al., 1966) to study allosteric regulation. In the two-state models, it is not usually expected that the enzyme binds substrate and inhibitor simultaneously. They only recognize binary complex, either substrate bound form or allosteric effector bound form, but not the ternary complex bound with both substrate and allosteric effector simultaneously. Thermodynamic linkage analysis model (Reinhart, 1983, 1988) provides another way to describe allosteric mechanism in free energy terms without assuming the nature of structural changes caused by ligand binding. There are four different ligation states that the enzyme can adopt, including the apo enzyme, enzyme bound with substrate, enzyme bound with allosteric effector, and enzyme bound with both substrate and allosteric effector simultaneously. Each ligation state is unique and can have different functional properties. This is in contrast to the two-state models, which only allow for the existence of either T-state or R-state, without the ternary complex because the enzyme can bind only one type of ligand, but not both.

When studying allosteric regulation in PFK, we need to consider all four species of the enzyme. The ternary complex with both substrate and activator bound is easy to achieve because positive cooperativity of the binding of these two ligands. However, the

ternary complex with both substrate and inhibitor is more difficult to achieve because of the antagonism of the binding of these two ligands. The tight binding for PEP and weaker coupling between Fru-6-P and PEP in TtPFK (PFK from *Thermus thermophilus*) suggests that the ternary complex with both Fru-6-P and PEP is easier to form compared to PFK from other organisms, which can be taken advantage of when studying allosteric regulation mechanisms.

As discussed in chapter I, fluorescence phasor is an easy and fast method to evaluate data obtained from frequency-domain measurement without the assumption of any exponential decay model. It allows a description of the system utilizing only the raw phase angle and modulation. The movement of the phasor point can be an indication of a conformational change of the protein. The aim of this chapter is to use fluorescence phasor plot to describe the four species, Apo-TtPFK, TtPFK-Fru-6-P, PEP-TtPFK, and PEP-TtPFK-Fru-6-P, involved in the allosteric coupling between Fru-6-P and PEP. If the ternary complex is a mixture of two binary complexes, the phasor point of the ternary complex will be on the line between the two binary complexes. If the ternary complex is a unique conformation, the phasor point of the ternary complex will be off the line between the two binary complexes as the position of the fluorescence reporter. We want to know whether the ternary complex exhibits a unique phasor value independent of whether it is formed by titrating the substrate followed by the inhibitor or *vice versa* and is also off the line between binary complex, in other words, whether we can show the presence of the four unique conformations that correspond to the different ligated states of the enzyme.

Fluorescence spectroscopic properties of intrinsic fluorophore of tryptophan are very sensitive to local environment within the protein. Tryptophan has been used as fluorescence probe to measure the dynamic properties and identify important residues for the allosteric regulation of PFKs (Riley-Lovingshimer et al., 2002; Pham and Reinhart, 2003; Riley-Lovingshimer and Reinhart, 2005; Fenton et al., 2003). There is no native tryptophan in TtPFK. To monitor the dynamic properties corresponding to ligand binding at different positions throughout the whole protein (Vivian and Callis, 2001), the mutagenesis strategy will be employed to locate the tryptophan at different positions in TtPFK without altering the kinetic and thermodynamic coupling parameters of the protein dramatically. We selected these positions: Y41, L69, F140, Y165, V197, Y226, A230, V243 and L313, since corresponding sites have been shown to be involved in allosteric communication in EcPFK and BsPFK (Cuijuan Tie and Stephanie Perez, unpublished data). We want to identify areas may be important for the propagation and transmission of allosteric information in TtPFK.

Materials and methods

Materials

All reagents were of analytical grade. Glycerol-3-phosphate dehydrogenase and creatine kinase were purchased from Roche (Indianapolis, IN). Phosphocreatine, Fru-6-P, PEP, aldolase, triose phosphate isomerase, and ATP were purchased from Sigma-Aldrich (St. Louis, MO). The coupling enzymes (glycerol-3-phosphate dehydrogenase, aldolase and triose phosphate isomerase) were in ammonium sulfate suspensions. They were dialyzed with three exchanges of 50 mM MOPS pH 8.0 buffer, which contains 100

mM KCl, 5 mM $MgCl_2$ and 0.1 mM EDTA before use. The mono Q anion exchange column used for fast performance liquid chromatography (FPLC) was purchased from GE Lifescience (Charlottesville, VA). Site-directed mutagenesis follows the instruction manual from Stratagene (La Jolla, CA). The template was pALTER-1 (Promega) with wild type TtPFK gene. Oligonucleotides for quikchange site-directed mutagenesis were purchased from Integrated DNA Technologies Inc (Coralville, IA). Plasmid purification kit was purchased from Qiagen (Hilden, Germany). XL1Blue cells used for transformation were purchase from Stratagene (La Jolla, CA). Plasmid sequencing to confirm the mutation introduced by quikchange site-directed mutagenesis is done with the BigDye kit of ABI (Foster City, CA) and Eton Bioscience (San Diego, CA).

Site-directed mutagenesis

Site-directed mutagenesis follows the instruction manual of QuikChange mutagenesis from Stratagene. The template was pALTER-1 plasmid with wild type TtPFK gene and tetracycline resistance. A pair of complementary primers was used to construct mutation in the wild type TtPFK gene in the plasmid. Table 4-1 lists all the oligonucleotides used in this chapter. Mutant strand synthesis reaction (thermal cycling) follows the instruction manual of quikchange site-directed mutagenesis system from Stratagene. After the PCR reaction the plasmids were transformed into competent XL1-Blue cells, colonies with tetracycline resistance were selected, and the plasmid was purified using a Qiagen kit and then sent to sequencing to confirm the mutated DNA bases.

Table 4-1. Oligonucleotides used in the quikchange site-directed mutagenesis.

	Oligonucleotides sequence
Y41W	5'CGGGATCCGCCGCGGCTGGGCCGGCATGATCC3'
L69W	5'CGGGGCGGGACGATCCTCTGGACGGCGAGGAGCCAGGAG3'
F165W	5'AGCCACGAGCGGGTCTGGTTCATAG3'
V197W	5'CGTCCCCGAGGAGCCCTGGGACCCCAAGGCCGTGG3'
Y226W	5'GGCCCCGCCGGGCCAGGCCCCCTCGGC3'
A230W	5'GCCTACCCCGGCGGGGCCTGGGGGCTTCTCGCCGCCATC3'
V243W	5'CGGGAGCACCTCCAGTGGGAGGCCCGGGTCACCGTC3'
L313W	5'GGACATCAACCGGGCCTGGTTGCGCCTATCGC3'

Protein expression and purification

The RL257 cells a PFK-1 and PFK-2 deficient strain (Lovingshimer et al., 2006) was grown at 37°C in LB (Luria-Bertani) media which contains 10 g/L tryptone, 5 g/L yeast extract, and 10 g/L sodium chloride with 15 µg/mL tetracycline until OD_{600} is 0.6. Then the cells were induced with 0.5mM IPTG and grow at 18°C for 24 hours. The cells are centrifuged in Beckman J6 centrifuge at 4,550 x g for 30 minutes at 4°C. The cell was stored in -80°C freezer for later use. The cell was resuspended in 20 mM pH 8 Tris-HCl buffer with 0.5 mM EDTA. The cells were lysed using Sonic Dismembrator Model 550 (Fisher Scientific).The program is 15 second sonication and 45 second delay to cool down and the total sonication time is 8 minutes. The lysate was centrifuged in Beckman J2-21 centrifuge at 22,500 x g for 30 min at 4°C. The supernatant was heated at a 70°C water bath for 15 minutes, cool on ice for 10 min and then centrifuged at 22,500 x g for 30 min at 4°C. The supernatant was applied to 35% ammonium sulfate precipitation and then centrifuged at 22,500 x g for another 30 min at 4°C. The protein pellet was resuspended in purification buffer A and then dialyzed to get rid of any residual ammonium sulfate in the protein solution with two each exchange of buffer, each 1 hour. The protein was then applied to mono Q anion exchange column. SDS-PAGE with 4% polyacrylamide stacking gel and 10% polyacrylamide resolving gel was used to check the purity of the protein. If there are multiple bands on the gel, proteins will be applied to another anion exchange column. Protein concentration was measured by pierce BCA assay (Smith et al., 1985).

Enzymatic activity assay

The activity of TtPFK enzyme was measured at 600 μL of EPPS-KOH buffer (pH 8, 50 mM EPPS, 100 mM KCl, 5 mM $MgCl_2$, 0.1 mM EDTA, 2 mM dithiothreitol), with 0.2 mM NADH, coupling enzymes (250 μg of aldolase, 50 μg of glycerol-3-phosphate dehydrogenase, 5 μg of triose phosphate isomerase) and 0.5mM MgATP. For maximal velocity assay, 3mM Fru-6-P was used. To measure the coupling between Fru-6-P and PEP, various concentration of Fru-6-P and PEP were used. All enzyme activity assays were measured by Beckman Series 600 spectrophotometer. The decrease in absorbance at 340nm was converted to enzyme rate.

Frequency-domain fluorescence measurement

Frequency-domain fluorescence measurement was done by ISS K2 multi-frequency fluorometer with 280nm Light Emitting Diode (LED). Different modulation frequencies (from 10MHz to 200MHz) were produced by Marconi 2022A Synthesizer. The emission polarizer was oriented at 35.3° (the magic angle) (Spencer and Weber, 1970; Weber, 1971, 1977 and 1978). Apo TtPFK was titrated with either Fru-6-P or PEP to form binary complex, EA and YE respectively. Then subsequently add PEP after Fru-6-P saturation, Fru-6-P after PEP saturation to form ternary complex YEA. The frequency dependent phase and modulation change at all four ligated state (apo enzyme, enzyme bound with Fru-6-P, enzyme bound with PEP and enzyme bound with both Fru-6-P and PEP simultaneously) is measured at 12 different frequencies (10MHz, 13MHz, 17MHz, 23MHz, 30MHz, 39MHz, 51MHz, 67MHz, 88MHz, 116MHz, 152MHz, and 200MHz). All measurements were done in 0.4cm× 1cm fluorescence cuvette. Low concentration of

EPPS buffer was used for all fluorescence measurement with EPPS-KOH buffer pH 8 (5 mM EPPS, 0.5 mM MgCl2, 10 mM KCl, and 0.01 mM EDTA. NATA (N-acetyl-tryptophanamide, phosphate buffer pH 7.0, Kodak) (Lackowicz and Gryczynski, 1991) with lifetime of 2.87ns was used to measure reference phase and modulation in all the measurement to avoid "color effect". For lifetime analysis, data were fit to Lorentzian model with combination of single exponential and continuous distribution (Alcala et al., 1987 a-b-c) because the decay of tryptophan emission in proteins is multi-exponential (Ghisaidoobe and Chung, 2014). All frequency domain measurements were corrected for blank contribution by measuring blank phase and modulation change at the same ligand concentration.

Data analysis

All data were fit using Kaleidagraph software (Synergy). The initial velocity data were fit to Hill equation (Hill, 1910):

$$v = \frac{V_{max}[A]^{n_H}}{K_{1/2}^{n_H} + [A]^{n_H}} \tag{4-1}$$

where v is the initial velocity, [A] is the concentration of Fru-6-P, V_{max} is the maximal velocity, n_H is the hill coefficient, and $K_{1/2}$ is the concentration of Fru-6-P when initial velocity is half maximal velocity.

Since $K_{1/2}$ increase with the increasing concentration of PEP, the $K_{1/2}$ data versus increasing concentration of PEP were fit to the following equation:

$$K_{1/2} = K_{ia}^{0}\left(\frac{K_{iy}^{0} + [Y]}{K_{iy}^{0} + Q_{ay}[Y]}\right) \tag{4-2}$$

where K_{ia}^{0} is the dissociation constant for Fru-6-P in the absence of PEP, K_{iy}^{0} is the dissociation constant for PEP in the absence of Fru-6-P, [Y] is the PEP concentration, Q_{ay} is the coupling constant between of PEP and Fru-6-P.

Blank subtraction

Data output from fluorometer is composite DC, composite phase delay, composite modulation, blank AC, blank DC, blank phase delay, blank modulation and reference modulation. The blank subtraction uses the raw data and generally follows the idea in Figure 4-1 (Reinhart et al., 1991). The figure is cited from Reinhart et al., 1991. The phase delay and modulation was calculated by subtracting the blank contribution using vector algebra, and then corrected relative to that of reference signal. The full names for the abbreviation are: $(AC)_C$ is composite AC, $(DC)_C$ is composite DC, M_C is composite modulation, $(AC)_B$ is blank AC, $(DC)_B$ is blank DC, M_B is blank modulation, S_x is x-coordinate of phasor difference, S_y is y-coordinate of phasor difference, Φ_C is composite phase delay, Φ_B is blank phase delay, AC_S is sample AC, DC_S is sample DC, M_S is sample modulation, Φ_S is sample phase delay, M_R is reference modulation, f is the frequency and τ_R is reference lifetime. The detailed equations used for the calculation are as follows.

(1). Calculating composite AC and blank AC

$(AC)_C = (DC)_C * M_C$

$(AC)_B = (DC)_B * M_B$

(2). Calculating x-coordinate and y-coordinate difference

$Sx = (AC)_C * \cos(\Phi_C) - (AC)_B * \cos(\Phi_B)$

$Sy = (AC)_C * \sin(\Phi_C) - (AC)_B * \sin(\Phi_B)$

(3). Calculating sample AC and sample DC

$AC_S = \text{sqrt}[(Sx)^2 + (Sy)^2]$

$DC_S = (DC)_C - (DC)_B$

(4). Calculating sample modulation and sample phase delay

$M_S = AC_S/DC_S$

$\Phi_S = \text{invtan}(Sy/Sx)$

(5). Calculating sample modulation and sample phase delay corrected for reference

$M = M_S/\{M_R[\text{sqrt}1+(2\pi * f * \tau_R)^2]\}$

$\Phi = \Phi_S + \text{invtan}(2\pi * \tau_R)$

The blank subtraction method was confirmed by using standard fluorophore to mimic background contamination. P-Terphenyl has a standard single exponential decay lifetime of 1.35ns in ethanol and POPOP (1, 4-bis (5-phenyloxazole-2-yl) benzene) has a standard single exponential decay lifetime of 1.05ns in ethanol. This method was applied to subtracting 5% p-terphenyl from mixture of 95% POPOP and 5% p-Terphenyl and subtracting 40% p-terphenyl from mixture of 60% POPOP and 40% p-Terphenyl. The phasor point of mixture of POPOP and p-terphenyl is inside the "universal circle". After blank subtraction, the phasor point lies on the "universal circle".

Structural analysis

All structural analysis was done by Pymol software.

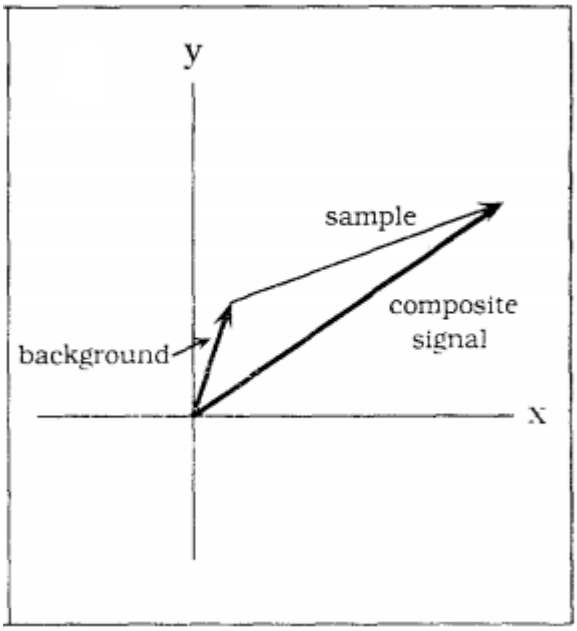

Figure 4-1. Vector representation of blank subtraction. Figure is from Reinhart et al., 1991.

Result

Tryptophan mutants characterization

The first step is to construct fluorescence probe that can be used to measure the dynamic properties of TtPFK. TtPFK contains no tryptophan and tryptophan mutants studied in this study are as follows: Y41W, L69W, F140W, F165W, V197W, Y226W, A230W, V243W, and L313W. Figure 4-2 shows the positions of the nine tryptophan mutants in BsPFK tetramer structure from different views. Figure 4-3 shows the positions of the nine tryptophan mutants in BsPFK monomer structure from different views. Generally these nine mutants cover most regions of the enzyme. Table 4-2 summarizes the distance of the nine tryptophan mutations to the nearest active site and allosteric site based on the reference BsPFK structure. A230W was removed from consideration because it is heat sensitive and very unstable. Table 4-3 summarizes the kinetic parameters of the eight tryptophan mutants. The dissociation constants for Fru-6-P and PEP and the coupling constant between Fru-6-P and PEP are all relatively unchanged in all the tryptophan mutants compared to wild type.

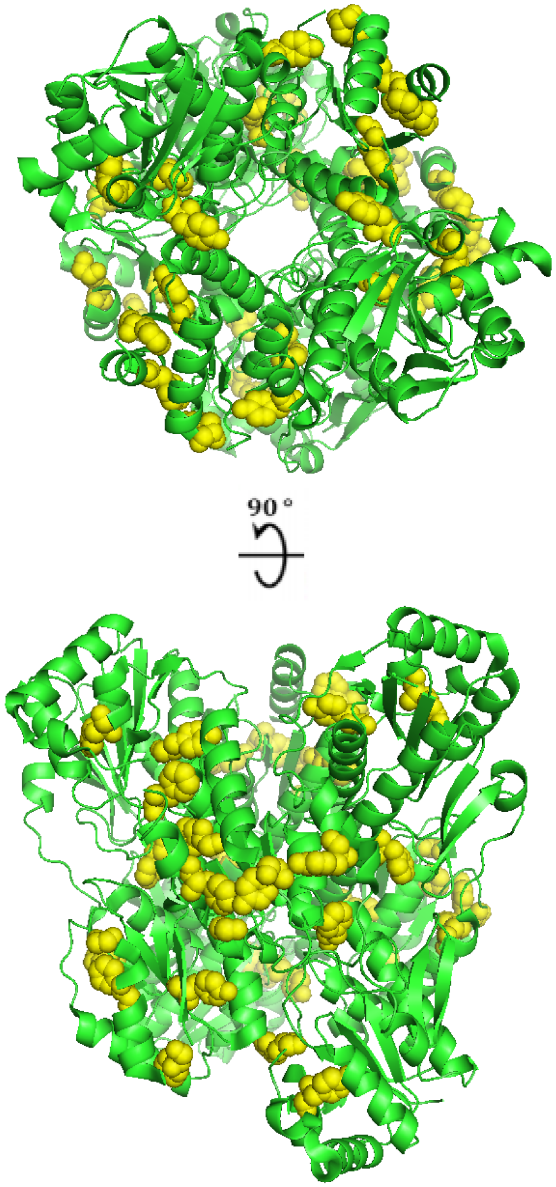

Figure 4-2. The positions of the nine tryptophan mutants in BsPFK tetramer structure from different views. Tryptophan residues are colored in yellow.

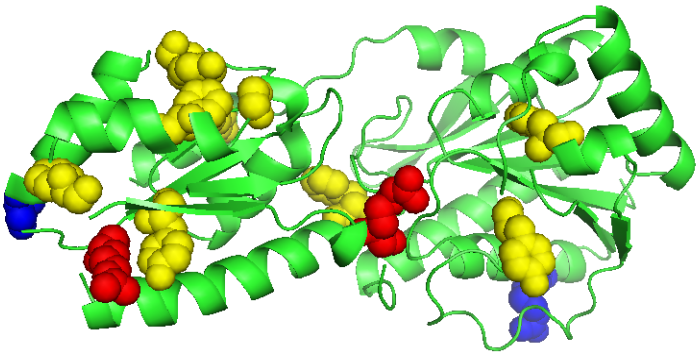

Figure 4-3. The positions of the nine tryptophan mutants in BsPFK monomer structure. Tryptophan residues are colored in yellow, active site residues are colored in red and allosteric site residues are colored in blue.

Table 4-2. The distance of the nine tryptophan mutations to the nearest active site and allosteric site.

Tryptophan position	Active site	Allosteric site
41	14.2Å	19.8Å
69	11.5Å	19.8Å
140	10.2Å	21.7Å
165	4.0Å	17.0Å
197	19.4Å	21.4Å
226	19.7Å	21.7Å
230	12.6Å	21.2Å
243	6.6Å	11.0Å
313	19.7Å	19.3Å

Table 4-3. Kinetic parameter of the eight tryptophan mutants at pH 8 and 25°C with [MgATP]=0.5 mM.

Enzyme	K°_{ia} (μM)	K°_{iy} (μM)	Q_{ay}
Wild type	27±2	1.6±0.2	0.070±0.005
Y41W	13±2	1.5±0.3	0.045±0.008
L69W	17±2	15±2	0.045±0.006
F140W	6.3±0.5	3.5±0.4	0.073±0.006
F165W	26±3	1.4±0.2	0.060±0.008
V197W	26±4	3.7±0.7	0.056±0.008
Y226W	15±4	2.2±0.7	0.028±0.008
V243W	28±3	1.5±0.2	0.071±0.008
L313W	14±3	1.2±0.1	0.067±0.002

Fluorescence lifetime analysis of L313W TtPFK

TtPFK contains no tryptophan, and the first tryptophan mutant examined was L313W because EcPFK has one native tryptophan at position 311 which has been used as fluorescence probe to measure the dynamic properties of EcPFK, and the corresponding residue in TtPFK is 313. The fluorescence intensity of L313W has a 25% decrease with the binding of PEP and 10% decrease with the binding of Fru-6-P. Figure 4-4 is the fluorescence phasor plot of Fru-6-P titration and PEP titration of L313W TtPFK at 12 different excitation frequencies logarithmically from 10 to 200 MHz. From right to left is low frequency to high frequency. Since the decay of tryptophan emission in proteins is very complex, not single exponential decay, so the phasor point is within the semi-circle. The fluorescence of residue 313 responds to PEP binding much more strongly than to Fru-6-P binding. Fluorescence lifetime parameters of L313W TtPFK at different ligand concentrations were measured. The data were fit best to Lorentzian model. Table 4-4 is the fluorescence lifetime analysis of L313W TtPFK at different Fru-6-P concentrations. Table 4-5 is the fluorescence lifetime analysis of L313W TtPFK at different PEP concentrations. The first component lifetime tau is described as the center of the distribution. The second component is the width of the distribution. The third component is fluorescence intensity contribution. The lifetime exhibits significant variation depending on the ligation states of the enzyme. In addition, the lifetime variations mimic the dynamic changes that results from the binding of the ligands. The lifetime of tryptophan 313 in TtPFK decreased approximately 0.03 ns with Fru-6-P bound relative to that of apo form. The lifetime of tryptophan 313 in TtPFK decreased

approximately 0.5 ns with PEP bound relative to that of apo form. Figure 4-5 is the phasor plot of TtPFK L313W and TtPFK F165W titrated with different ligands at 67 MHz. Red is Apo TtPFK, blue is Fru-6-P titration and purple is PEP titration to form binary complex; black is PEP titration after Fru-6-P saturation and green is Fru-6-P titration after PEP saturation to form ternary complex. The PEP titration in TtPFK L313W is curved, which may due to the unsymmetrical binding of PEP to the four subunits.

Fluorescence phasor plot of Y226W, Y41W, L69W and V197W TtPFK

Figure 4-6 is the fluorescence phasor plot of Y226W TtPFK titrated with different ligands. Apo TtPFK (red) was titrated with either Fru-6-P (blue) or PEP (purple) to form binary complex, EA and YE respectively. The subsequent addition of PEP after Fru-6-P saturation (black) and the addition of Fru-6-P after PEP saturation (green) form ternary complex YEA. The ternary complex is in the same position as the apo form and two binary complexes in the phasor plot. The fluorescence of this residue shows response to neither Fru-6-P binding nor PEP binding. The fluorescence of this residue shows response to neither F6P binding nor PEP binding. This residue cannot monitor the conformational change of neither F6P binding nor PEP binding, so only one enzyme conformation can be detected at this position.

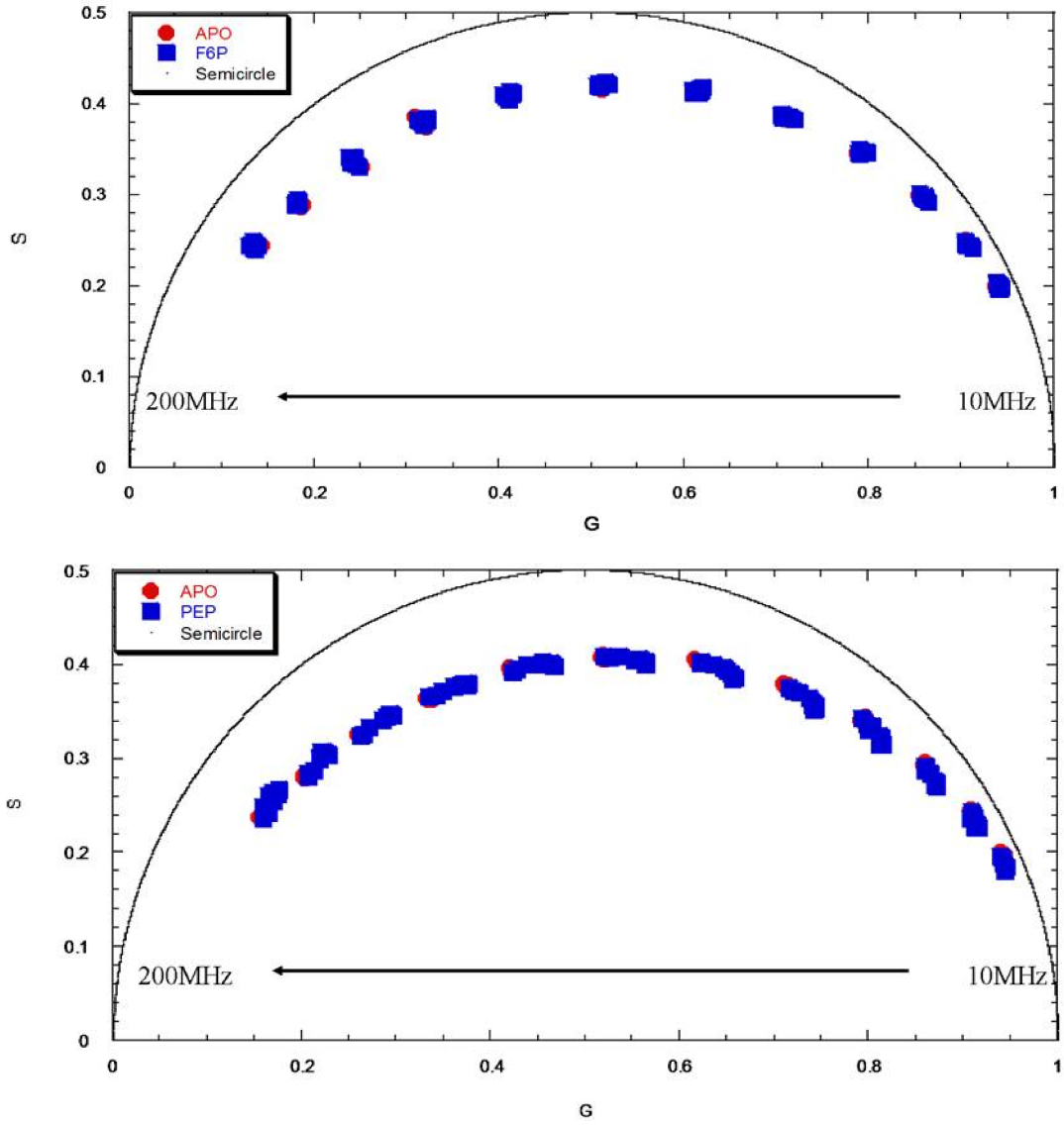

Figure 4-4. Fluorescence phasor plot of Fru-6-P titration and PEP titration of L313W TtPFK at different excitation frequencies. From right to left (10MHz, 13MHz, 17MHz, 23MHz, 30MHz, 39MHz, 51MHz, 67MHz, 88MHz, 116MHz, 152MHz, and 200MHz).

Table 4-4. Fluorescence lifetime analysis of L313W TtPFK at different Fru-6-P concentrations.

Fru-6-P (μM)	Tau(ns)	Width(ns)	Contributions	Chi square
0	2.981	2.620	0.9711	0.41
1	2.987	2.575	0.9734	3.20
2.15	2.979	2.585	0.9780	0.87
4.64	2.956	2.627	0.9819	0.91
10	3.017	2.504	0.9729	1.29
21.5	2.989	2.433	0.9758	0.68
46.4	2.948	2.454	0.9782	0.98
100	2.922	2.475	0.9805	0.70
215	2.942	2.418	0.9777	0.39
464	2.983	2.370	0.9734	0.58
1000	2.953	2.352	0.9745	0.46

Table 4-5. Fluorescence lifetime analysis of L313W TtPFK at different PEP concentrations.

PEP(μM)	Tau(ns)	Width(ns)	Contributions	Chi square
0	2.924	2.752	0.9544	0.91
1	2.993	2.594	0.9479	0.80
2.15	2.931	2.637	0.9497	0.71
4.64	2.778	2.682	0.9595	2.12
10	2.651	2.641	0.9603	0.60
21.5	2.572	2.696	0.9700	0.82
46.4	2.505	2.755	0.9707	0.45
100	2.432	2.855	0.9752	0.68
215	2.475	2.787	0.9675	0.24
464	2.439	2.875	0.9710	0.47
1000	2.408	2.904	0.9741	0.21

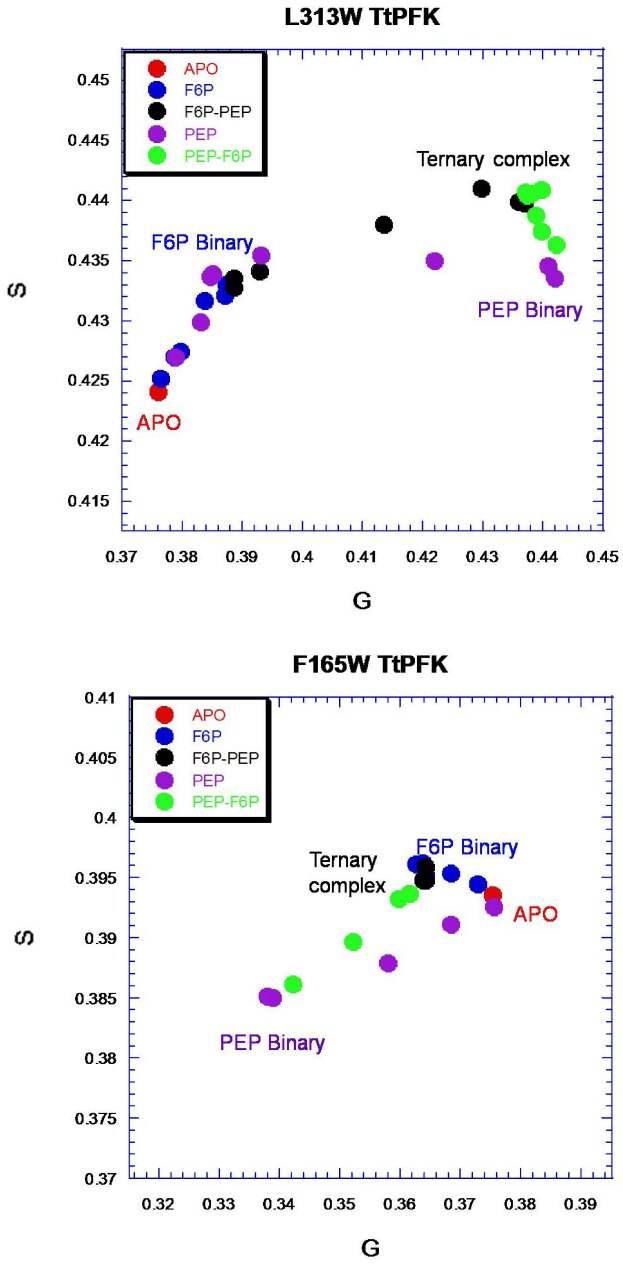

Figure 4-5. Phasor plot of L313W TtPFK and F165W TtPFK titrated with different ligands. Red is Apo TtPFK, blue is Fru-6-P titration and purple is PEP titration to form binary complex; black is PEP titration after Fru-6-P saturation and green is Fru-6-P titration after PEP saturation to form ternary complex.

Figure 4-7 is the fluorescence phasor plot of Y41W TtPFK titrated with different ligands. The fluorescence of this residue shows response to Fru-6-P binding but not PEP binding. PEP binary complex is at the same position as the apo. Either the titration of PEP on top of F6P or the titration of F6P on top of PEP produced the ternary complex does not vary much from the F6P binary complex. This residue can only monitor the conformational change of F6P binding, so only two enzyme conformations can be detected at this position.

Figure 4-8 is the fluorescence phasor plot of L69W TtPFK and V197W TtPFK titrated with different ligands. The fluorescence of these two residues shows response to PEP binding but not Fru-6-P binding. F6P binary complex is at the same position as the apo. Either the titration of PEP on top of F6P or the titration of F6P on top of PEP produced the ternary complex does not vary much from the PEP binary complex. These two residues can only monitor the conformational change of PEP binding, so only two enzyme conformations can be detected at these two positions.

Fluorescence phasor plot F140W, F165W, V243W and L313W TtPFK

Figure 4-9 is the fluorescence phasor plot of F140W TtPFK, F165W TtPFK titrated with different ligands. Figure 4-10 is the fluorescence phasor plot of V243W TtPFK and L313W TtPFK titrated with different ligands. Apo TtPFK (red) was titrated with either Fru-6-P (blue) or PEP (purple) to form binary complex, EA and YE respectively. The fluorescence of these four residues show response to both Fru-6-P binding and PEP binding. The phasor plot shows clearly the formation of these complexes. The subsequent addition of the inhibitor PEP after the Fru-6-P saturation (black) and the

addition of Fru-6-P after saturation with PEP (green) form the same ternary complex YEA. The titration of a second ligand to the binary complex, either EA or YE, produced the displacement of the phasor values to a common and unique phasor point in the plot and is also off the line between binary complexes, meaning the ternary complex is a unique conformation instead of a mixture of two binary complexes. These results suggest the presence of the four different conformations at these four positions, each of them characterized by a unique phasor value. We also have identified four residues that may be important for the propagation and transmission of allosteric inhibition information in TtPFK.

Discussion

Of the nine tryptophan mutants we studied in this chapter, one is removed from consideration because it is heat sensitive and very unstable; one responds to neither Fru-6-P binding nor PEP binding; one responds to Fru-6-P binding but not PEP binding; two respond to PEP binding but not Fru-6-P binding and four respond to both Fru-6-P binding and PEP binding.

Figure 4-11 shows the positions of all the 8 tryptophan mutants in BsPFK monomer structure from different views. Unique ternary complex can be detected at F140W, F165W, V243W and L313W. These four residues are in a region that can detect the conformational conflict between Fru-6-P binding and PEP binding.

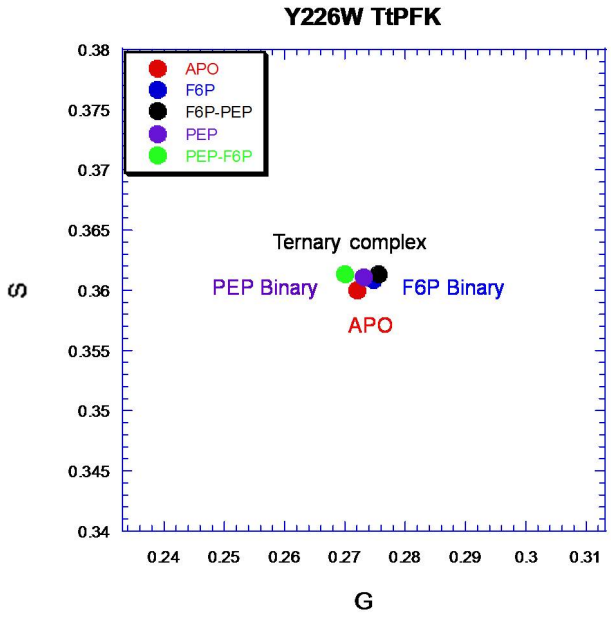

Figure 4-6. Fluorescence phasor plot of Y226W TtPFK, which shows no response to either Fru-6-P binding or PEP binding. Red is Apo TtPFK, blue is Fru-6-P titration and purple is PEP titration to form binary complex, EA and YE respectively; black is PEP titration after Fru-6-P saturation and green is Fru-6-P titration after PEP saturation to form ternary complex YEA.

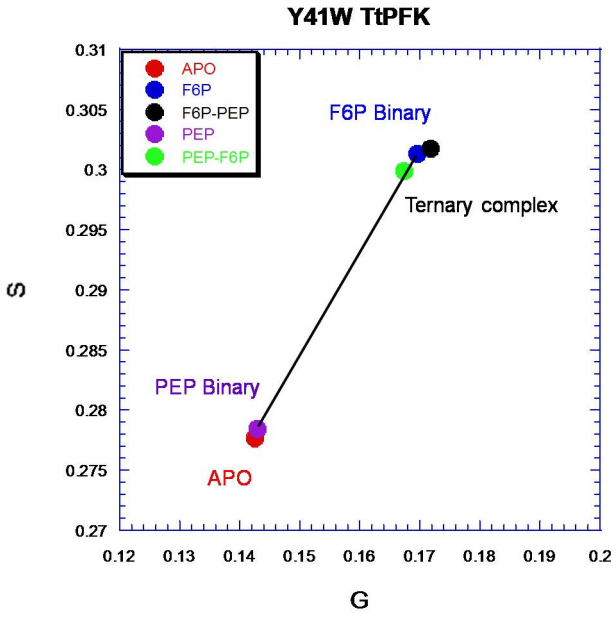

Figure 4-7. Fluorescence phasor plot of Y41W TtPFK, which shows response to Fru-6-P binding but not PEP binding. Red is Apo TtPFK, blue is Fru-6-P titration and purple is PEP titration to form binary complex, EA and YE respectively; black is PEP titration after Fru-6-P saturation and green is Fru-6-P titration after PEP saturation to form ternary complex YEA.

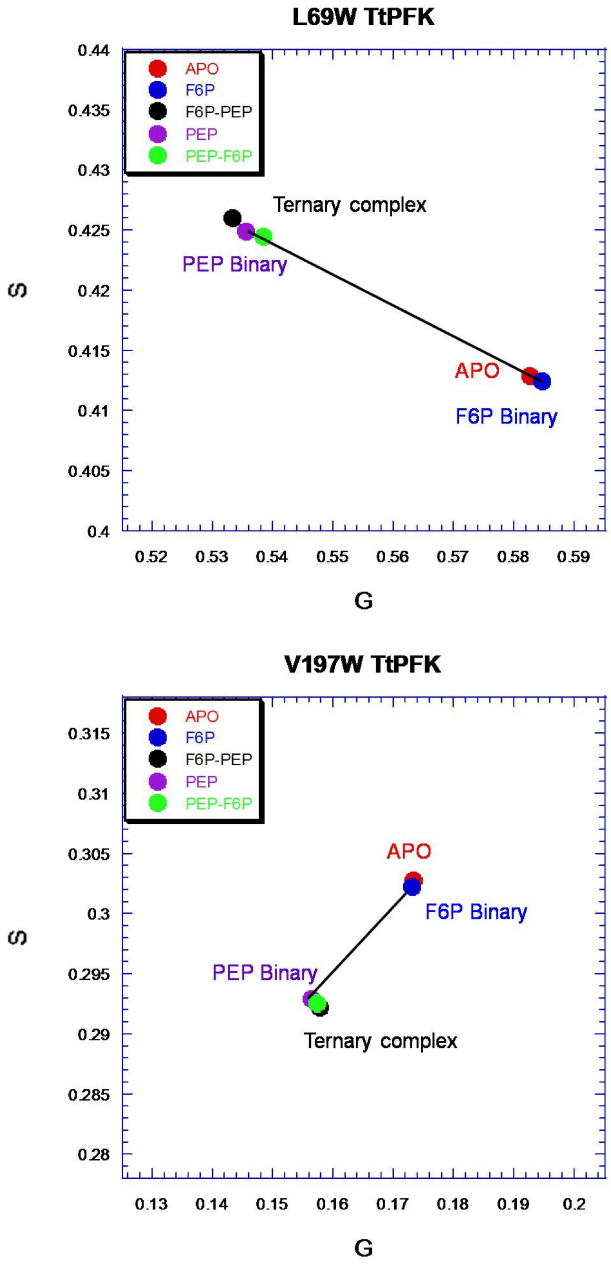

Figure 4-8. Fluorescence phasor plot of L69W TtPFK and V197W TtPFK, which shows response to PEP binding but not Fru-6-P binding. Red is Apo TtPFK, blue is Fru-6-P titration and purple is PEP titration to form binary complex, EA and YE respectively; black is PEP titration after Fru-6-P saturation and green is Fru-6-P titration after PEP saturation to form ternary complex YEA.

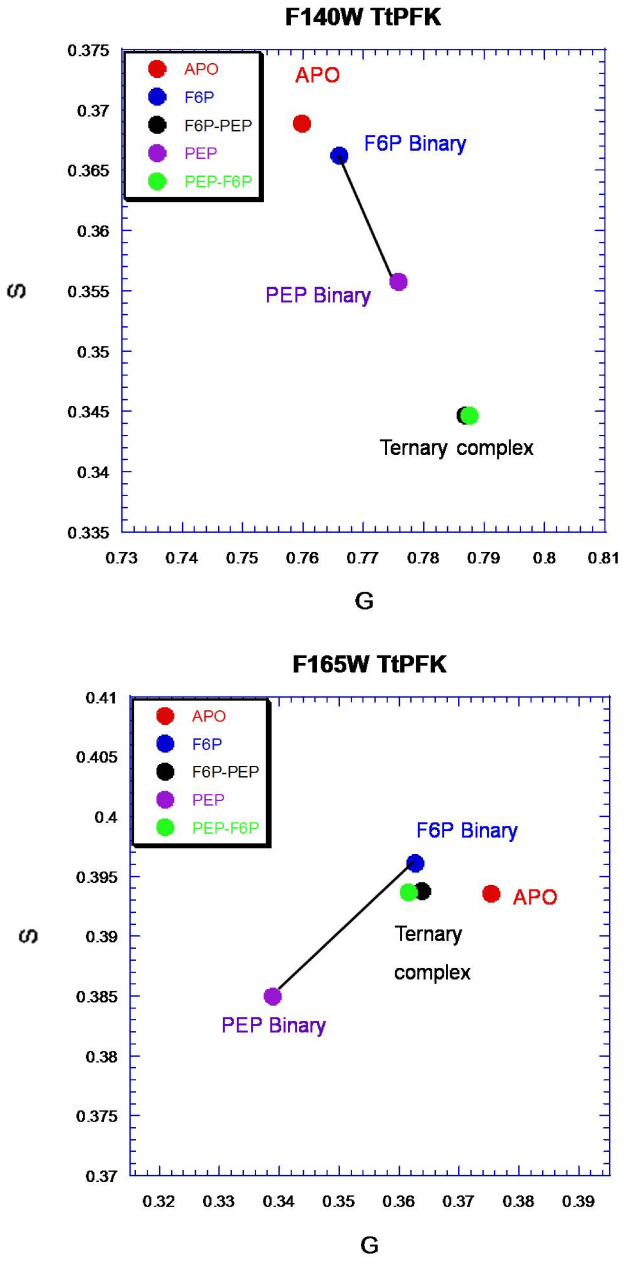

Figure 4-9. Fluorescence phasor plot of F140W TtPFK, F165W TtPFK, which shows response to both Fru-6-P binding and PEP binding. Red is Apo TtPFK, blue is Fru-6-P titration and purple is PEP titration to form binary complex, EA and YE respectively; black is PEP titration after Fru-6-P saturation and green is Fru-6-P titration after PEP saturation to form ternary complex YEA.

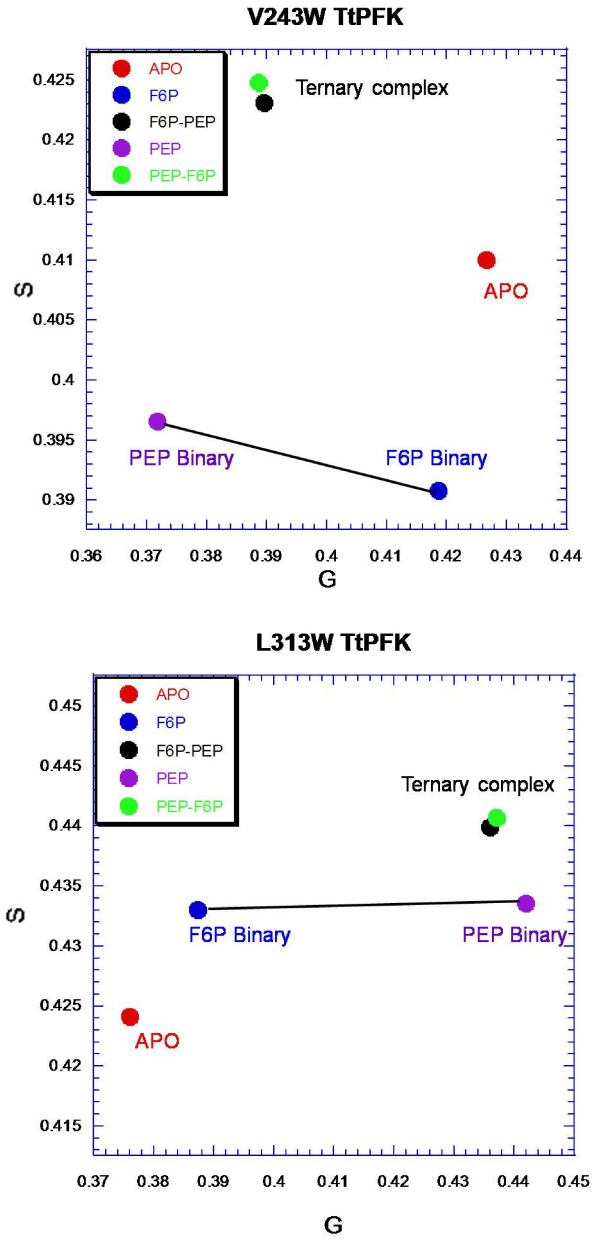

Figure 4-10. Fluorescence phasor plot of V243W TtPFK and L313W TtPFK, which shows response to both Fru-6-P binding and PEP binding. Red is Apo TtPFK, blue is Fru-6-P titration and purple is PEP titration to form binary complex, EA and YE respectively; black is PEP titration after Fru-6-P saturation and green is Fru-6-P titration after PEP saturation to form ternary complex YEA.

Y226W shows response to neither Fru-6-P binding nor PEP binding. Based on the reference BsPFK crystal structure, residue 226 is 19.7Å to the nearest active site and 21.7Å to the nearest allosteric site. This far away distance may be the reason it is responding to neither Fru-6-P binding nor PEP binding. Y41W shows response to Fru-6-P binding but not PEP binding. Residue 41 is 14.2Å to the nearest active site and 19.8Å to the nearest allosteric site. L69W show response to PEP binding but not Fru-6-P binding. Residue 69 is 11.5Å to the nearest active site and and 19.8Å to the nearest allosteric site. It is much closer to active site than allosteric site while it responds to PEP binding instead of Fru-6-P binding. V197W show response to PEP binding but not Fru-6-P binding. Residue 197 is 19.4Å to the nearest active site and and 21.4Å to the nearest allosteric site. It is about equal distance to active site and allosteric site but only responds to PEP binding. These two examples suggest that distance is not the only reason accounting for whether it is involved in ligand binding and allosteric communication or not.

F140W, F165W, V243W and L313W show response to both Fru-6-P binding and PEP binding. Figure 4-11 shows the position of F140W mutation in the BsPFK tetramer structure. Residue 140 is 10.2Å to the nearest active site and 21.7Å to the nearest allosteric site. It may play roles in the allosteric communication of 30Å interaction and 32Å interaction considering the close distance of residue 140 to active site R255.

Figure 4-12 shows the position of L313W mutation in the BsPFK tetramer structure. Residue 313 is 19.7Å to the nearest active site and 19.3Å to the nearest allosteric site. It

is relatively far away from the active site and allosteric site, but it is directly between sites that comprise the 32 Å interaction.

Figure 4-13 shows the positions of F165W and V243W mutations in the BsPFK tetramer structure and the zoom-in view of the position of F165W and V243W mutations with the active site and allosteric site. Residue 165 is 4.0Å to the nearest active site and 17.4Å to the nearest allosteric site. Residue 243 is 6.6Å to the nearest active site and 11.0Å to the nearest allosteric site. Both these two residues are very close to active site R163 and the 22Å interaction, which suggest they may play roles in the allosteric communication of the 22Å interaction.

Our results suggest that residues F140, L313, F165 and V243 maybe in an area important for the propagation and transmission of allosteric information in TtPFK. Previous work shows that residues Y164 and F240 are in a dynamic area important for the allosteric communication of the 22Å interaction in BsPFK (Stephanie Perez, unpublished data). These results suggest that residue Y164 in BsPFK (F165 in TtPFK) and F240 in BsPFK (V243 in TtPFK) may be involved in an interaction network common for BsPFK and TtPFK. For the future study we can combine the hybrid strategy discussed in chapter II and chapter II with the fluorescence phasor method to investigate the role of these residues in the potential individual interactions.

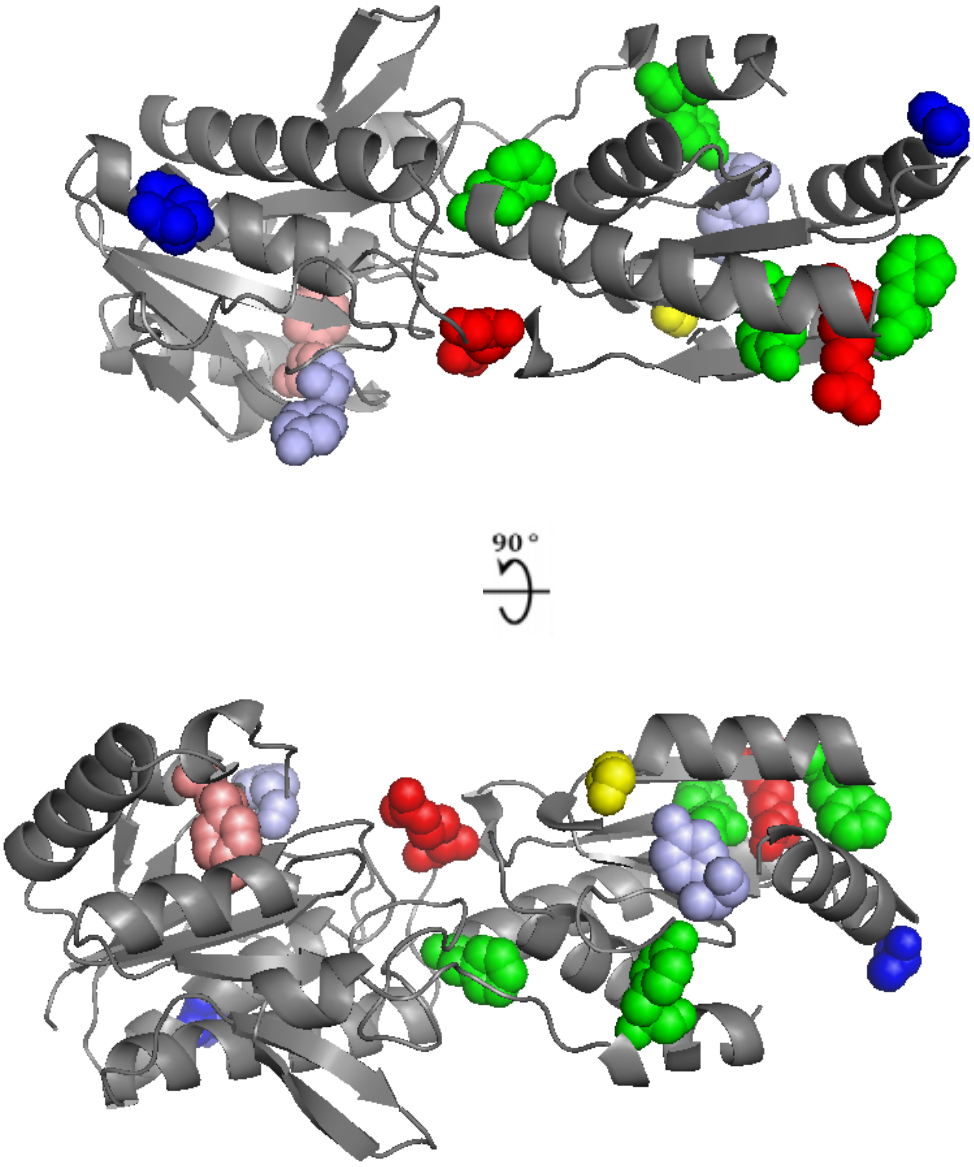

Figure 4-11. The positions of the 8 tryptophan mutants in BsPFK monomer structure from different views. Active site residues are colored in red, allosteric site residues are colored in blue, residue that responds to neither Fru-6-P binding nor PEP binding is colored in yellow (Y226W), residue that that responds to Fru-6-P binding is colored in light red (Y41W), residues that responds to PEP binding is colored in light blue (L69W and V197W) and residues that responds to both Fru-6-P and PEP binding are colored in green (F140W, F165W, V243W and L313W).

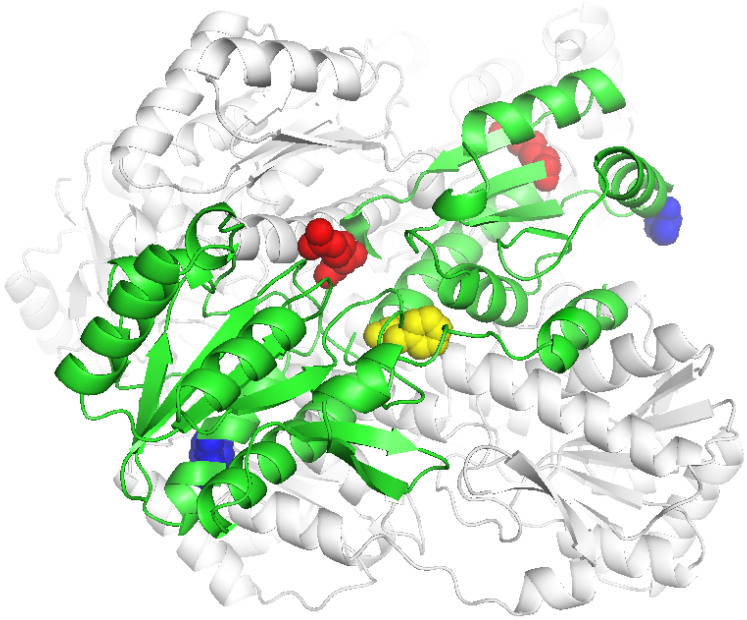

Figure 4-12. Position of F140W mutation in the BsPFK homotetramer with one subunit highlighted in green. Residue 140 is colored in yellow, active site residue is in red and allosteric site residue is in blue.

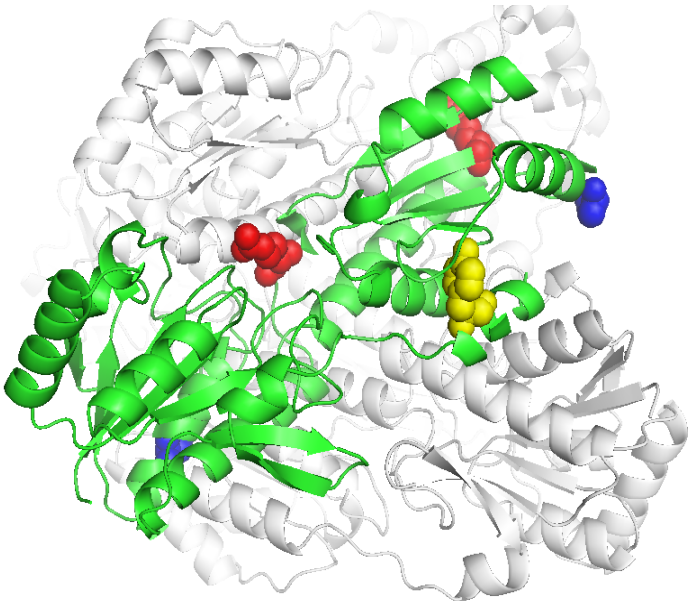

Figure 4-13. Position of L313W mutation in the BsPFK homotetramer with one subunit highlighted in green. Residue 313 is colored in yellow, active site residue is in red and allosteric site residue is in blue.

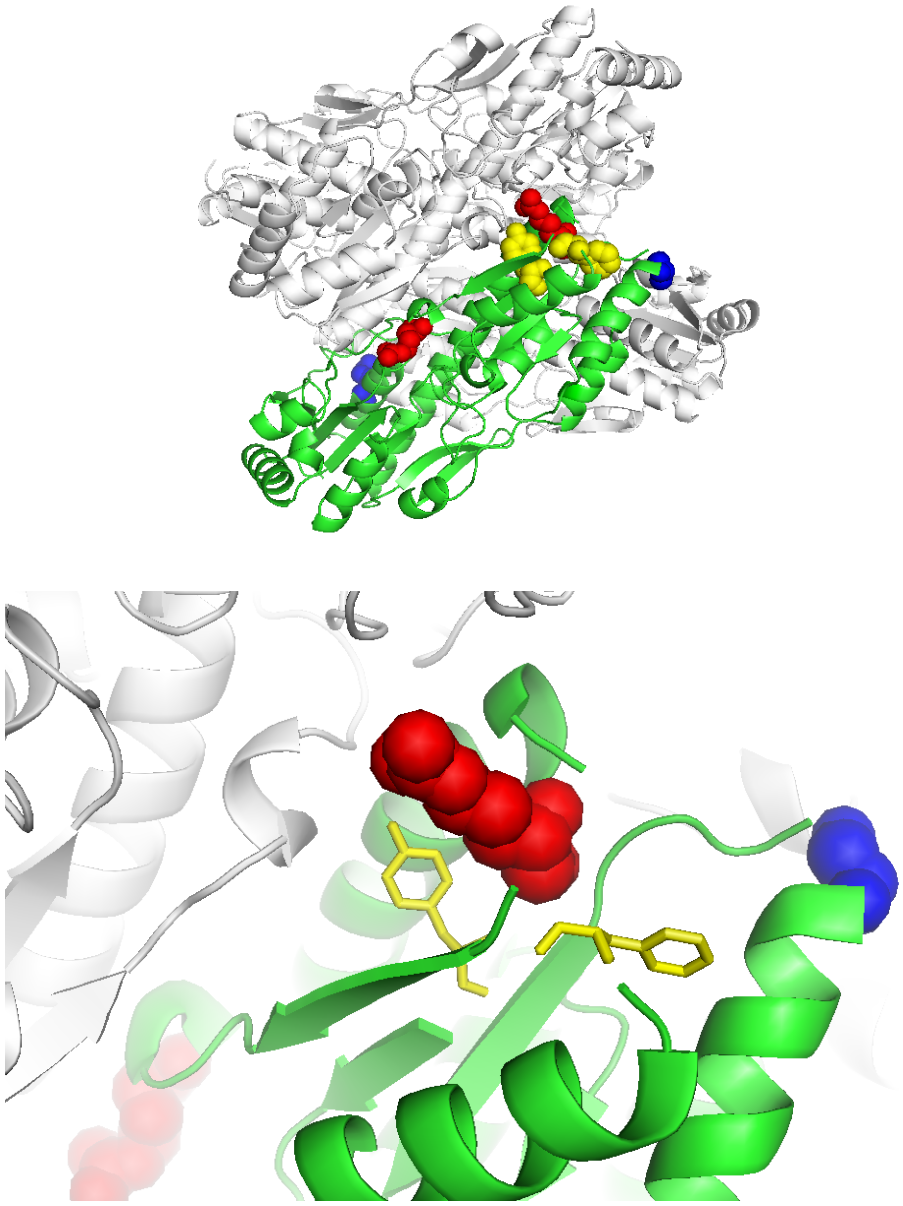

Figure 4-14. Position of F165W and V243W mutations in the BsPFK homotetramer with one subunit highlighted in green and the zoom-in view of the position of F165W and V243W mutations with the active site and allosteric site. Residue 165 and 243 is colored in yellow, active site residue is in red and allosteric site residue is in blue.

TtPFK is a very good model to study allosteric regulation in prokaryotes system. First, since we need to consider all the four species of the enzyme including the ternary complex when studying allosteric regulation, the much tighter binding for PEP and much weaker coupling between Fru-6-P and PEP in TtPFK suggests that the ternary complex with both Fru-6-P and PEP is easier to form compared to PFK from other organisms, which can be taken advantage of. Second, to use tryptophan as fluorescence probe to measure the dynamic properties and identify important residues for the allosteric regulation of PFK, we need to locate the tryptophan at different positions in PFK without altering the kinetic and thermodynamic coupling parameters of the protein dramatically. There is no native tryptophan in TtPFK, only one mutation is required to locate tryptophan at different positions of the protein instead of introducing two mutations to get tryptophan-shift mutant in BsPFK and EcPFK because they have native tryptophan at position 179 and 311 respectively.

Fluorescence phasor is a relatively new approach for the time-resolved studies on intrinsic protein fluorescence. It is a direct visual display of the raw data without any lifetime analysis model. The movement of the phasor point can be an indication of a conformational change of the protein. This method can be utilized with many protein studies to describe the overall excitation state decay process. Using fluorescence phasor to study protein dynamics coupled with placing the tryptophan fluorescence probe at different positions in the protein may be used as an alternative tool to map the dynamic properties of other proteins as well.

CHAPTER V

SUMMARY

PFK catalyzes the phosphorylation of fructose 6-phosphate in glycolysis pathway. PEP allosterically inhibits the binding of substrate Fru-6-P in TtPFK. TtPFK is homotetramer with four identical active sites and four identical allosteric sites. There are multiple homotropic and heterotropic allosteric interactions within the enzyme. The main goal of this study is to have a better understanding about the allosteric inhibition regulation in TtPFK. Crystal structures of overall secondary, tertiary and quaternary structures are generally conserved for bacteria source PFK, but the functional properties are dramatically different.

Four unique inhibition interactions have been successfully isolated in BsPFK and EcPFK. Chapter II applied the hybrid strategy to TtPFK and isolated the four individual inhibition interactions. The relative contribution of the four interactions in TtPFK is different from BsPFK and EcPFK. Each of the four interactions contribution to inhibition is unique and additive. The sum of the coupling free energy measured for the isolated interactions agrees well with the total coupling free energy measured for the control hybrid, which suggests that we can relate the coupling observed in the four isolated individual interactions to their corresponding interactions in the native tetramer. Further study can isolate the four individual activation interactions in TtPFK and see how the relative contribution of the four activation interactions compares to that of inhibition interactions.

The allosteric coupling between Fru-6-P and PEP in TtPFK is much weaker than BsPFK. N59D/A158T/S215H substitutions increase the coupling free energy of TtPFK by 2.4 kcal/mol. From the prospective of coupling free energy, entropy and enthalpy of inhibition and PEP binding affinity, TtPFK N59D/A158T/S215H behaves more like BsPFK than TtPFK. Chapter III applied the hybrid strategy to TtPFK N59D/A158T/S215H and isolated the four individual inhibition interactions. The substitutions can enhance all of the four heterotropic interactions, but to different extent. 32 Å interaction exhibits the biggest increase in coupling free energy and this big increase make it become the second biggest contribution in TtPFK N59D/A158T/S215H. The discrepancy between the sum of the coupling free energy in the isolated interactions and the total coupling free energy in the native tetramer is likely due to the mutated residues not all interacting within a single subunit. Further study can isolate each of the four individual interactions in each single substitution and see how these three substitutions act to enhance the coupling in TtPFK.

TtPFK has a smaller allosteric coupling between PEP and Fru-6-P compared to other prokaryotic PFKs which makes it easier to form ternary complex. Chapter IV used fluorescence phasor to describe the four species, Apo-TtPFK, TtPFK-Fru-6-P, PEP-TtPFK, and PEP-TtPFK-Fru-6-P, involved in the allosteric coupling between Fru-6-P and PEP. The titration of a second ligand to the binary complex produced the displacement of the phasor values to a common and unique phasor point and is also off the line between binary complexes. These results suggest the presence of the four different conformations at residues F140W, F165W, V243W and L313W, which is not

anticipated by the traditional two-state model. Residues F140, L313, F165 and V243 may be in an area important for the propagation and transmission of allosteric information in TtPFK. Further study can combine the hybrid strategy with the fluorescence phasor to investigate the role of these residues in the inhibition allosteric interaction in TtPFK.

REFERENCES

Ackers, G. K., Doyle, M. L., Myers, D., and Daugherty, M. a. (1992). Molecular code for cooperativity in hemoglobin. *Science*. *255*(5040), 54–63.

Alcala, J. R., Gratton, E., and Prendergast, F. G. (1987a). Interpretation of fluorescence decays in proteins using continuous lifetime distributions. *Biophysical Journal*, *51*(6), 925–936.

Alcala, J. R., Gratton, E., and Prendergast, F. G. (1987b). Resolvability of fluorescence lifetime distributions using phase fluorometry. *Biophysical Journal*, *51*(4), 587–596.

Babul, J. 1978. Phosphofructokinase from *Escherichia coli*. Purification and characterization of the nonallosteric isozyme. *Journal of Biological Chemistry*. 253:4350-4355.

Benigno C. Valdez, Brent A. French, Ezzat S. Younathan, and Chang, S. H. (1986). Site-directed Mutagenesis in *Bacillus stearothermophilus* Fructose-6-phosphate 1-Kinase. *Biochemical Journal*, (19), 131–135.

Blangy, D., Buc, H., and Monod, J. (1968). Kinetics of the allosteric interactions of phosphofructokinase from *Escherichia coli*. *Journal of Molecular Biology*, *31*(1), 13–35.

Bloxham, D. P., and Lardy, H. A. 1973. Phosphofructokinase. In The Enzymes, 3rd ed, Vol. 8. P. Boyer, editor. Academic Press, New York, NY.239-278.

Botts, J., and Morales, M. (1953). Analytical description of the effects of modifiers and of enzyme multivalency upon the steady state catalyzed reaction rate. *Transactions of the Faraday Society*, *49*(696), 696–707.

Braxton, B. L., Tlapak-Simmons, V. L., and Reinhart, G. D. (1994). Temperature-induced inversion of allosteric phenomena. *Journal of Biological Chemistry*, *269*(1), 47–50.

Byrnes, W. M., Hu, W., Younathan, E. S., and Chang, S. H. (1995). A chimeric bacterial phosphofructokinase exhibits cooperativity in the absence of heterotropic regulation. *Journal of Biological Chemistry*. 2170:3828-3835.

Cleland, W. W. 1963a. The kinetics of enzyme-catalyzed reactions with two ormore substrates or products. I. Nomenclature and rate equations. *Biochimica et Biophysica Acta*. 67:104-137.

Deville-Bonne, D., Le Bras, G., Teschner, W., and Garel, J. R. (1989). Ordered disruption of subunit interfaces during the stepwise reversible dissociation of *Escherichia coli* phosphofructokinase with KSCN. *Biochemistry*, *28*(4), 1917–1922.

Eroglu, B., and Powers-Lee, S. G. (2002). Unmasking a functional allosteric domain in an allosterically nonresponsive carbamoyl-phosphate synthetase. *Journal of Biological Chemistry*, *277*(47), 45466–45472.

Evans, P. R., G. W. Farrants, and P. J. Hudson. 1981. Phosphofructokinase: Structure and control. *Philosophical Transactions of the Royal Society B*. 293:53-62.

Evans, P. R., Farrants, G. W., and Lawrence, M. C. (1986). Crystallographic structure of allosterically inhibited phosphofructokinase at 7 Å resolution. *Journal of Molecular Biology*, *191*(4), 713–720.

Evans, P. R., and Hudson, P. J. 1979. Structure and control ofphosphofructokinase from *Bacillus stearothermophilus*. *Nature*. 279:500-504.

Fenton, A. W., and Reinhart, G. D. (2003). Mechanism of Substrate Inhibition in *Escherichia coli* Phosphofructokinase. *Biochemistry*, *42*(43), 12676–12681.

Fenton, A. W., Paricharttanakul, N. M., and Reinhart, G. D. (2003). Identification of substrate contact residues important for the allosteric regulation of phosphofructokinase from Eschericia coli. *Biochemistry*, *42*(21), 6453–6459.

Fenton, A. W., Paricharttanakul, N. M., and Reinhart, G. D. (2004). Disentangling the web of allosteric communication in a homotetramer: Heterotropic activation in phosphofructokinase from *Escherichia coli*. *Biochemistry*, *43*(44), 14104–14110.

Fenton, A. W., and Reinhart, G. D. (2002). Isolation of a single activating allosteric interaction in phosphofructokinase from *Escherichia coli*. *Biochemistry*, *41*(45), 13410–13416.

Fenton, A. W., and Reinhart, G. D. (2009). Disentangling the Web of Allosteric Communication in a Homotetramer: Heterotropic Inhibition in Phosphofructokinase from *Escherichia coli*. *Biochemistry*, *48*(51), 12323–12328.

Freiden, C. 1964. Treatment of enzyme kinetic data. I. The effects of modifierson the kinetic parameters of single substrate enzymes. *Journal of Biological Chemistry*. 239:3522-3531.

French, B. A., and Chang, S. H. (1987). Nucleotide sequence of the phosphofructokinase gene from *Bacillus stearothermophilus* and comparison with the homologous *Escherichia coli* gene. *Gene*, *54*(1), 65–71.

Ghisaidoobe, A. B. T., and Chung, S. J. (2014). Intrinsic tryptophan fluorescence in the detection and analysis of proteins: A focus on förster resonance energy transfer techniques. *International Journal of Molecular Sciences*, *15*(12), 22518–22538.

Gratton, E., Jameson, D. M., and Hall, R. D. (1984). The measurement and analysis of heterogeneous emissions by multifrequency phase and modulation fluorometry. *Applied Spectroscopy Reviews*. 20:55–106.

Gratton, E., Jameson, D. M., and Hall, R. D. (1984). Multifrequency phase and modulation. *Applied Spectroscopy Reviews*, *20*(1), 55–106.

Hill, A. V. 1910. The possible effects of the aggregation of the molecules of haemoglobin on its dissociation curves. *Journal of Physiology*. 40:iv-vii.

Jaenicke, R. (1991). Protein stability and molecular adaptation to extreme conditions. *European Journal of Biochemistry / FEBS*, *202*(3), 715–728.

James, N. G., Ross, J. A., Štefl, M., and Jameson, D. M. (2011). Applications of phasor plots to in vitro protein studies. *Analytical Biochemistry*, *410*(1), 70–76.

Johnson, J. L., Lasagna, M. D., and Reinhart, G. D. (2001). Influence of a sulfhydryl cross-link across the allosteric-site interface of *Escherichia coli* phosphofructokinase. *Protein Science*, *10*(11), 2186–2194.

Johnson, J. L., and Reinhart, G. D. (1992). MgATP and fructose 6-phosphate interactions with phosphofructokinase from *Escherichia coli*. *Biochemistry*. 31:11510–11518.

Johnson, J. L., and Reinhart, G. D. (1994a). Influence of MgADP on phosphofructokinase from *Escherichia coli*. Elucidation of coupling interactions with both substrates. *Biochemistry*, *33*(9), 2635–2643.

Johnson, J. L., and Reinhart, G. D. (1994b). Influence of substrates and MgADP on the time-resolved intrinsic fluorescence of phosphofructokinase from *Escherichia coli*. Correlation of tryptophan dynamics to coupling entropy. *Biochemistry*, *33*(9), 2644–2650.

Johnson, J. L., and Reinhart, G. D. (1997). Failure of a two-state model to describe the influence of phospho(enol)pyruvate on phosphofructokinase from *Escherichia coli*. *Biochemistry*, *36*(42), 12814–12822.

Kemp, R. G., and Foe, L. G. (1983). Allosteric regulatory properties of muscle phosphofructokinase. *Molecular and Cellular Biochemistry*, *57*, 147–154.

Kemp, R. G., and Gunasekera, D. (2002). Evolution of the allosteric ligand sites of mammalian phosphofructo-1-kinase. *Biochemistry*, *41*(30), 9426–9430.

Kimmel, J. L., and Reinhart, G. D. (2000). Reevaluation of the accepted allosteric mechanism of phosphofructokinase from *Bacillus stearothermophilus*. *Proceedings of the National Academy of Sciences of the United States of America*, *97*(8), 3844–3849.

Kimmel, J. L., and Reinhart, G. D. (2001). Isolation of an individual allosteric interaction in tetrameric phosphofructokinase from *Bacillus stearothermophilus*. *Biochemistry*, *40*(38), 11623–11629.

Kolartz, D., and Buc, H. 1982. Phosphofructokinase from *Escherichia coli*. *Methods Enzymol*. 90:60-70.

Koshland, D. E., Némethy, G., and Filmer, D. (1966). Comparison of experimental binding data and theoretical models in proteins containing subunits. *Biochemistry*, *5*(1), 365–385.

Lakowicz, J. R., and Gryczynski, I. 1991. Frequency domain fluorescence spectroscopy. In Topic of Fluorescence Spectroscopy, Vol 1. J. R. Lakowicz, editor. Plenum Press, New York, NY. 293-335.

Lau, F. T., and Fersht, A. R. (1989). Dissection of the effector-binding site and complementation studies of *Escherichia coli* phosphofructokinase using site-directed mutagenesis. *Biochemistry*, *28*(17), 6841–6847.

Lau, F. T., and Fersht, A. R. (1987). Conversion of allosteric inhibition to activation in phosphofructokinase by protein engineering. *Nature*. 326: 811-812.

Lau, F. T., Fersht, A. R., Hellinga, H. W., and Evans, P. R. (1987) Site-directed mutagenesis in the effector site of *Escherichia coli* phosphofructokinase, *Biochemistry*. 26:4143-4148.

Le Bras, G., Auzat, I., and Garel, J. R. (1995). Tetramer-dimer equilibrium of phosphofructokinase and formation of hybrid tetramers. *Biochemistry*, *34*(40), 13203–13210.

Lovingshimer, M. R., Siegele, D., and Reinhart, G. D. (2006). Construction of an inducible, pfkA and pfkB deficient strain of *Escherichia coli* for the expression and purification of phosphofructokinase from bacterial sources. *Protein Expression and Purification*, *46*(2), 475–482.

McGresham, M. S., Lovingshimer, M., and Reinhart, G. D. (2014). Allosteric regulation in phosphofructokinase from the extreme thermophile *Thermus thermophilus*. *Biochemistry*, *53*(1), 270–278.

McGresham, M. S., and Reinhart, G. D. (2015). Enhancing allosteric inhibition in *Thermus thermophilus* phosphofructokinase. *Biochemistry*, *54*(3), 952–958.

Monod, J., Wyman, J., and Changeux, J. P. (1965). On the Nature of Allosteric Transitions: a Plausible Model. *Journal of Molecular Biology*, *12*(1), 88–118.

Mosser, R., Reddy, M. C. M., Bruning, J. B., Sacchettini, J. C., and Reinhart, G. D. (2012). Structure of the apo form of *Bacillus stearothermophilus* phosphofructokinase. *Biochemistry*, *51*(3), 769–775.

Ortigosa, A. D., Kimmel, J. L., and Reinhart, G. D. (2004) Disentangling the web of allosteric communication in a homotetramer: heterotropic inhibition of phosphofructokinase from *Bacillus stearothermophilus*, *Biochemistry*. 43: 577-586.

Paricharttanakul, N. M., Ye, S., Menefee, A. L., Javid-Majd, F., Sacchettini, J. C., and Reinhart, G. D. (2005). Kinetic and structural characterization of phosphofructokinase from *Lactobacillus bulgaricus*. *Biochemistry*, *44*(46), 15280–15286.

Pawlyk, A. C., and Pettigrew, D. W. (2002). Transplanting allosteric control of enzyme activity by protein-protein interactions: coupling a regulatory site to the conserved catalytic core. *Proceedings of the National Academy of Sciences of the United States of America*, *99*(17), 11115–11120.

Perez, S. A., Illumination the heterotropic communication of the pair-wise interactions in phosphofructokinase from *Bacillus stearothermophilus*, Dissertation, Texas A&M University, College Station, TX.

Pham, A. S., and Reinhart, G. D. (2001). MgATP-dependent activation by phosphoenolpyruvate of the E187A mutant of *Escherichia coli* phosphofructokinase. *Biochemistry*, *40*(13), 4150–4158.

Pham, A. S., and Reinhart, G. D. (2001a). Pre-steady State Quantification of the Allosteric Influence of *Escherichia coli* Phosphofructokinase. *Journal of Biological Chemistry*, *276*(37), 34388–34395.

Pham, A. S., and Reinhart, G. D. (2001b). Pre-steady State Quantification of the Allosteric Influence of *Escherichia coli* Phosphofructokinase. *Journal of Biological Chemistry*, *276*(37), 34388–34395.

Plou, F. J., and Ballesteros, A. (1999). Stability and stabilization of biocatalysts. *Trends in Biotechnology*, *17*(8), 304–306.

Quinlan, R. J., and Reinhart, G. D. (2006). Effects of protein-ligand associations on the subunit interactions of phosphofructokinase from B. stearothermophilus. *Biochemistry*, *45*(38), 11333–11341.

Reinhart, G. D. (1983a). The determination of thermodynamic allosteric parameters of an enzyme undergoing steady-state turnover. *Archives of Biochemistry and Biophysics*, *224*(1), 389–401.

Reinhart, G. D. (1983b). Allosteric regulation of pig heart fumerase. *In* Biochemistry of Metabolic Processes. Lennon, D. L. F., Stratman, F. W., and Zahlten, R. N., editors. *Elsevier Science*, New York, NY. 273-284.

Reinhart, G. D. (1988). Linked-function origins of cooperativity in a symmetrical dimer. *Biophysical Chemistry*, *30*(2), 159–172.

Reinhart, G. D., Hartleip, S. B., and Symcox, M. M. (1989). Role of coupling entropy in establishing the nature and magnitude of allosteric response. *Proceedings of the National Academy of Sciences of the United States of America*, *86*(11), 4032–4036.

Reinhart, G. D., Marzola, P., Jameson, D. M., and Gratton, E. (1991). A method for on-line background subtraction in frequency domain fluorometry. *Journal of Fluorescence*, *1*(3), 153–162.

Riley-Lovingshimer, M. R., and Reinhart, G. D. (2001). Equilibrium binding studies of a tryptophan-shifted mutant of phosphofructokinase from *Bacillus stearothermophilus*. *Biochemistry*, *40*(9), 3002–3008.

Riley-Lovingshimer, M. R., and Reinhart, G. D. (2005). Examination of MgATP binding in a tryptophan-shift mutant of phosphofructokinase from *Bacillus stearothermophilus*. *Archives of Biochemistry and Biophysics*, *436*(1), 178–186.

Riley-Lovingshimer, M. R., Ronning, D. R., Sacchettini, J. C., and Reinhart, G. D. (2002). Reversible ligand-induced dissociation of a tryptophan-shift mutant of phosphofructokinase from *Bacillus stearothermophilus*. *Biochemistry*, *41*(43), 12967–12974.

Rypniewski, W. R., and Evans, P. R. (1989). Crystal structure of unliganded phosphofructokinase from *Escherichia coli*. *Journal of Molecular Biology*, *207*(4), 805–821.

Schirmer, T., and Evans, P. R. (1990). Structural basis of the allosteric behaviour of phosphofructokinase. *Nature*, *343*(6254), 140–145.

Shirakihara, Y., and Evans, P. R. (1988). Crystal structure of the complex of phosphofructokinase from *Escherichia coli* with its reaction products. *Journal of Molecular Biology*, *204*(4), 973–994.

Smith, P. K., Krohn, R. I., Hermanson, G. T., Mallia, A. K., Gartner, F. H., Provenzano, M. D., Fujioto, E.K., Goeke, N. M., Olson, B. J., and Klenk, D. C. (1985). Measurement of protein using bicinchoninic acid. *Analytical Biochemistry*, *150*(1), 76–85.

Shubina-McGresham, M. (2012) Characterization of the Allosteric Properties of *Thermus thermophilus*Phosphofructokinase and the Sources of Strong Inhibition Binding Affinity and Weak Inhibitory Response, Dissertation, Texas A&M University, College Station, TX.

Somero, G. N. (1978). Temperature Adaptation of Enzymes: Biological Optimization Through Structure-Function Compromises. *Annual Review of Ecology and Systematics*, *9*(1), 1–29.

Spencer, R. D. (1970). Influence of Brownian Rotations and Energy Transfer upon the Measurements of Fluorescence Lifetime. *The Journal of Chemical Physics*, *52*(4), 1654.

Štefl, M., James, N. G., Ross, J. A., and Jameson, D. M. (2011). Applications of phasors to in vitro time-resolved fluorescence measurements. *Analytical Biochemistry*, *410*(1), 62–69.

Symcox, M. M., and Reinhart, G. D. (1992). A steady-state kinetic method for the verification of the rapid-equilibrium assumption in allosteric enzymes. *Analytical Biochemistry*, *206*(2), 394–399.

Tie, C. (2008) Kinetics and Dynamics Study On the Allosteric Pathway of Phosphofructokinase from *Escherichia coli*, Dissertation, Texas A&M University, College Station, TX.

Tlapak-Simmons, V. L., and Reinhart, G. D. (1994). Comparison of the inhibition by phospho(enol)pyruvate and phosphoglycolate of phosphofructokinase from B. stearothermophilus. *Archives of Biochemistry and Biophysics*. 308:226-230.

Tlapak-Simmons, V. L., and Reinhart, G. D. (1998). Obfuscation of allosteric structure-function relationships by enthalpy-entropy compensation. *Biophysical Journal*, *75*(2), 1010–1015.

Uyeda, K. 1979. Phosphofructokinase. *Advances in Enzymology and Related Areas of Molecular Biology*. 48:193-244.

Vivian, J. T., and Callis, P. R. (2001). Mechanisms of tryptophan fluorescence shifts in proteins. *Biophysical Journal*, *80*(5), 2093–2109.

Wagner, B. D., James, D. R., and Ware, W. R. (1987). Fluorescence lifetime distributions in homotryptophan derivatives. *Chemical Physics Letters*, *138*(2-3), 181–184.

Wang, X., and Kemp, R. G. (1999). Identification of residues of *Escherichia coli* phosphofructokinase that contribute to nucleotide binding and specificity. *Biochemistry*, *38*(14), 4313–4318.

Weber, G.1971. Theory of fluorescence depolarization by anisotropic Brownian rotations. Discontinuous distribution approach. *Journal of Chemical Physics*. 55: 2399-2407.

Weber, G. 1972. Ligand binding and internal equilibriumin proteins. *Biochemistry.* 11: 864-878.

Weber, G. 1975. Energetics of ligand binding to proteins. *Advances in Protein Chemistry*. 29: 1-83.

Weber, G. (1977). Theory of differential phase fluorometry: Detection of anisotropic molecular rotations. *The Journal of Chemical Physics*, *66*(9), 4081.

Weber, G. 1978. Limited rotational motion: recognition by differential phase fluorometer. *Acta Physica Polonica.* A54: 859-865.

Wyman, J. 1964. Linked functions and reciprocal effects in hemoglobin: A second look. *Advances in Protein Chemistry*. 19:223-286.

Wyman, J. (1967). Allosteric linkage. *Journal of the American Chemical Society*, *407*(1), 2202–2218.

Xu, J., Oshima, T., and Yoshida, M. (1990). Tetramer-dimer conversion of phosphofructokinase from *Thermus thermophilus* induced by its allosteric effectors. *Journal of Molecular Biology*, *215*(4), 597–606.

Yoshida, M. (1972) Allosteric nature of thermostable phosphofructokinase from an extreme thermophilic bacterium, *Biochemistry*. 11: 1087-1093.

Yoshida, M., Oshima, T., and Imahori, K. (1971) The thermostable allosteric enzyme: phosphofructokinase from an extreme thermophile, *Biochemical and Biophysical Research Communications*. 43: 36-39.